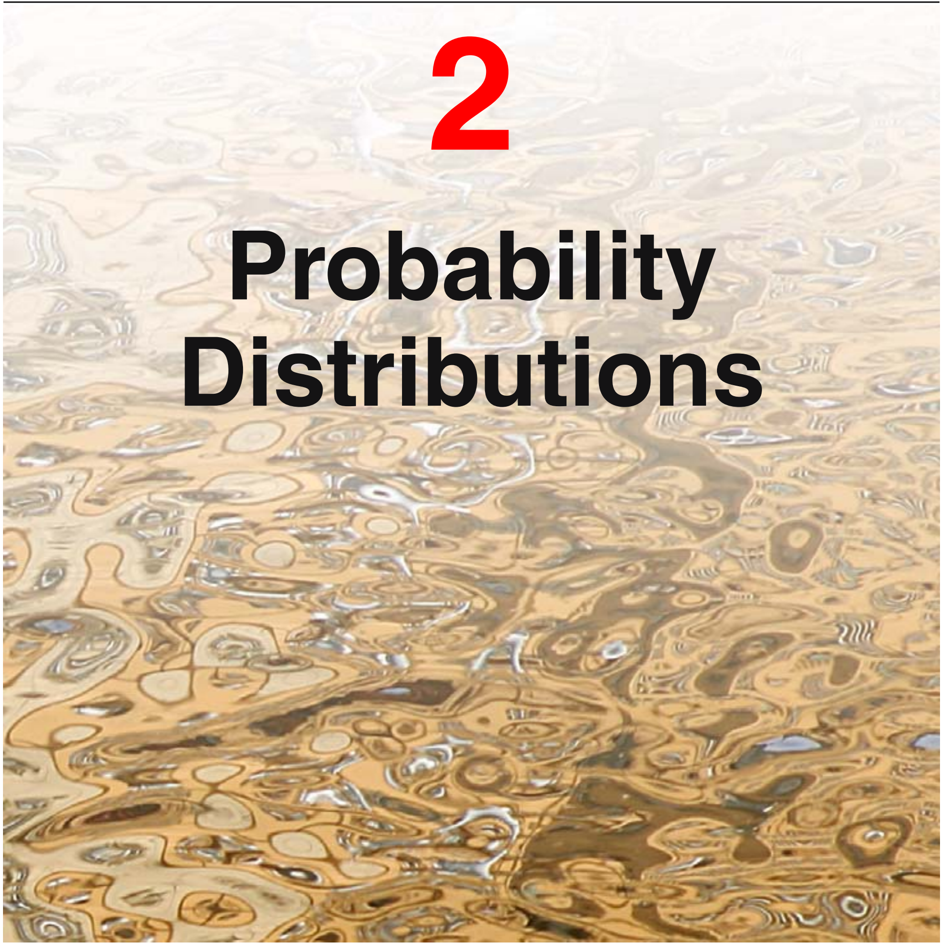

2 Probability Distributions

In Chapter 1, we emphasized the central role played by probability theory in the solution of pattern recognition problems. We turn now to an exploration of some particular examples of probability distributions and their properties. As well as being of great interest in their own right, these distributions can form building blocks for more complex models and will be used extensively throughout the book. The distributions introduced in this chapter will also serve another important purpose, namely to provide us with the opportunity to discuss some key statistical concepts, such as Bayesian inference, in the context of simple models before we encounter them in more complex situations in later chapters.

One role for the distributions discussed in this chapter is to model the probability distribution $p(\mathbf{x})$ of a random variable $\mathbf{x}$, given a finite set $\mathbf{x}_1, \ldots, \mathbf{x}_N$ of observations. This problem is known as *density estimation*. For the purposes of this chapter, we shall assume that the data points are independent and identically distributed. It should be emphasized that the problem of density estimation is fundamentally ill-posed, because there are infinitely many probability distributions that could have given rise to the observed finite data set. Indeed, any distribution $p(\mathbf{x})$ that is nonzero at each of the data points $\mathbf{x}_1, \ldots, \mathbf{x}_N$ is a potential candidate. The issue of choosing an appropriate distribution relates to the problem of model selection that has already been encountered in the context of polynomial curve fitting in Chapter 1 and that is a central issue in pattern recognition.

We begin by considering the binomial and multinomial distributions for discrete random variables and the Gaussian distribution for continuous random variables. These are specific examples of *parametric* distributions, so-called because they are governed by a small number of adaptive parameters, such as the mean and variance in the case of a Gaussian for example. To apply such models to the problem of density estimation, we need a procedure for determining suitable values for the parameters, given an observed data set. In a frequentist treatment, we choose specific values for the parameters by optimizing some criterion, such as the likelihood function. By contrast, in a Bayesian treatment we introduce prior distributions over the parameters and then use Bayes' theorem to compute the corresponding posterior distribution given the observed data.

We shall see that an important role is played by *conjugate* priors, that lead to posterior distributions having the same functional form as the prior, and that therefore lead to a greatly simplified Bayesian analysis. For example, the conjugate prior for the parameters of the multinomial distribution is called the *Dirichlet* distribution, while the conjugate prior for the mean of a Gaussian is another Gaussian. All of these distributions are examples of the *exponential family* of distributions, which possess a number of important properties, and which will be discussed in some detail.

One limitation of the parametric approach is that it assumes a specific functional form for the distribution, which may turn out to be inappropriate for a particular application. An alternative approach is given by *nonparametric* density estimation methods in which the form of the distribution typically depends on the size of the data set. Such models still contain parameters, but these control the model complexity rather than the form of the distribution. We end this chapter by considering three nonparametric methods based respectively on histograms, nearest-neighbours, and kernels.

2.1. Binary Variables

We begin by considering a single binary random variable $x \in \{0, 1\}$. For example, x might describe the outcome of flipping a coin, with $x = 1$ representing 'heads', and $x = 0$ representing 'tails'. We can imagine that this is a damaged coin so that the probability of landing heads is not necessarily the same as that of landing tails. The probability of $x = 1$ will be denoted by the parameter μ so that

$$p(x = 1|\mu) = \mu \tag{2.1}$$

where $0 \leqslant \mu \leqslant 1$, from which it follows that $p(x=0|\mu) = 1-\mu$. The probability distribution over x can therefore be written in the form

$$\mathrm{Bern}(x|\mu) = \mu^x(1-\mu)^{1-x} \tag{2.2}$$

Exercise 2.1

which is known as the *Bernoulli* distribution. It is easily verified that this distribution is normalized and that it has mean and variance given by

$$\begin{aligned} \mathbb{E}[x] &= \mu && (2.3)\\ \mathrm{var}[x] &= \mu(1-\mu). && (2.4) \end{aligned}$$

Now suppose we have a data set $\mathcal{D} = \{x_1, \ldots, x_N\}$ of observed values of x. We can construct the likelihood function, which is a function of μ, on the assumption that the observations are drawn independently from $p(x|\mu)$, so that

$$p(\mathcal{D}|\mu) = \prod_{n=1}^{N} p(x_n|\mu) = \prod_{n=1}^{N} \mu^{x_n}(1-\mu)^{1-x_n}. \tag{2.5}$$

In a frequentist setting, we can estimate a value for μ by maximizing the likelihood function, or equivalently by maximizing the logarithm of the likelihood. In the case of the Bernoulli distribution, the log likelihood function is given by

$$\ln p(\mathcal{D}|\mu) = \sum_{n=1}^{N} \ln p(x_n|\mu) = \sum_{n=1}^{N} \{x_n \ln \mu + (1-x_n)\ln(1-\mu)\}. \tag{2.6}$$

At this point, it is worth noting that the log likelihood function depends on the N observations x_n only through their sum $\sum_n x_n$. This sum provides an example of a *sufficient statistic* for the data under this distribution, and we shall study the important role of sufficient statistics in some detail. If we set the derivative of $\ln p(\mathcal{D}|\mu)$ with respect to μ equal to zero, we obtain the maximum likelihood estimator

Section 2.4

$$\mu_{\mathrm{ML}} = \frac{1}{N}\sum_{n=1}^{N} x_n \tag{2.7}$$

Jacob Bernoulli
1654–1705

Jacob Bernoulli, also known as Jacques or James Bernoulli, was a Swiss mathematician and was the first of many in the Bernoulli family to pursue a career in science and mathematics. Although compelled to study philosophy and theology against his will by his parents, he travelled extensively after graduating in order to meet with many of the leading scientists of his time, including Boyle and Hooke in England. When he returned to Switzerland, he taught mechanics and became Professor of Mathematics at Basel in 1687. Unfortunately, rivalry between Jacob and his younger brother Johann turned an initially productive collaboration into a bitter and public dispute. Jacob's most significant contributions to mathematics appeared in *The Art of Conjecture* published in 1713, eight years after his death, which deals with topics in probability theory including what has become known as the Bernoulli distribution.

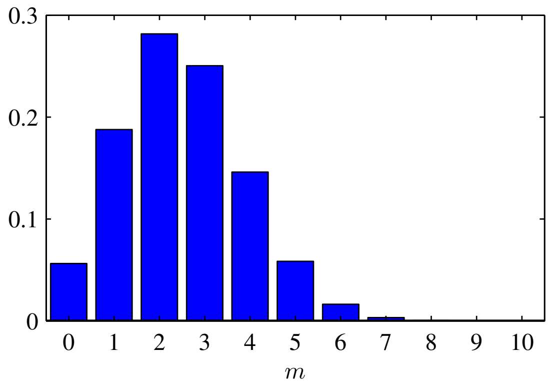

Figure 2.1 Histogram plot of the binomial distribution (2.9) as a function of m for $N = 10$ and $\mu = 0.25$.

which is also known as the *sample mean*. If we denote the number of observations of $x = 1$ (heads) within this data set by m, then we can write (2.7) in the form

$$\mu_{\mathrm{ML}} = \frac{m}{N} \tag{2.8}$$

so that the probability of landing heads is given, in this maximum likelihood framework, by the fraction of observations of heads in the data set.

Now suppose we flip a coin, say, 3 times and happen to observe 3 heads. Then $N = m = 3$ and $\mu_{\mathrm{ML}} = 1$. In this case, the maximum likelihood result would predict that all future observations should give heads. Common sense tells us that this is unreasonable, and in fact this is an extreme example of the over-fitting associated with maximum likelihood. We shall see shortly how to arrive at more sensible conclusions through the introduction of a prior distribution over μ.

We can also work out the distribution of the number m of observations of $x = 1$, given that the data set has size N. This is called the *binomial* distribution, and from (2.5) we see that it is proportional to $\mu^m(1-\mu)^{N-m}$. In order to obtain the normalization coefficient we note that out of N coin flips, we have to add up all of the possible ways of obtaining m heads, so that the binomial distribution can be written

$$\mathrm{Bin}(m|N,\mu) = \binom{N}{m}\mu^m(1-\mu)^{N-m} \tag{2.9}$$

where

$$\binom{N}{m} \equiv \frac{N!}{(N-m)!m!} \tag{2.10}$$

Exercise 2.3

is the number of ways of choosing m objects out of a total of N identical objects. Figure 2.1 shows a plot of the binomial distribution for $N = 10$ and $\mu = 0.25$.

The mean and variance of the binomial distribution can be found by using the result of Exercise 1.10, which shows that for independent events the mean of the sum is the sum of the means, and the variance of the sum is the sum of the variances. Because $m = x_1 + \ldots + x_N$, and for each observation the mean and variance are given by (2.3) and (2.4), respectively, we have

$$\mathbb{E}[m] \equiv \sum_{m=0}^{N} m\mathrm{Bin}(m|N,\mu) = N\mu \tag{2.11}$$

$$\mathrm{var}[m] \equiv \sum_{m=0}^{N} (m - \mathbb{E}[m])^2 \,\mathrm{Bin}(m|N,\mu) = N\mu(1-\mu). \tag{2.12}$$

Exercise 2.4 These results can also be proved directly using calculus.

2.1.1 The beta distribution

We have seen in (2.8) that the maximum likelihood setting for the parameter μ in the Bernoulli distribution, and hence in the binomial distribution, is given by the fraction of the observations in the data set having $x = 1$. As we have already noted, this can give severely over-fitted results for small data sets. In order to develop a Bayesian treatment for this problem, we need to introduce a prior distribution $p(\mu)$ over the parameter μ. Here we consider a form of prior distribution that has a simple interpretation as well as some useful analytical properties. To motivate this prior, we note that the likelihood function takes the form of the product of factors of the form $\mu^x(1-\mu)^{1-x}$. If we choose a prior to be proportional to powers of μ and $(1-\mu)$, then the posterior distribution, which is proportional to the product of the prior and the likelihood function, will have the same functional form as the prior. This property is called *conjugacy* and we will see several examples of it later in this chapter. We therefore choose a prior, called the *beta* distribution, given by

$$\mathrm{Beta}(\mu|a,b) = \frac{\Gamma(a+b)}{\Gamma(a)\Gamma(b)}\mu^{a-1}(1-\mu)^{b-1} \tag{2.13}$$

where $\Gamma(x)$ is the gamma function defined by (1.141), and the coefficient in (2.13) ensures that the beta distribution is normalized, so that *Exercise 2.5*

$$\int_0^1 \mathrm{Beta}(\mu|a,b)\,\mathrm{d}\mu = 1. \tag{2.14}$$

Exercise 2.6 The mean and variance of the beta distribution are given by

$$\mathbb{E}[\mu] = \frac{a}{a+b} \tag{2.15}$$

$$\mathrm{var}[\mu] = \frac{ab}{(a+b)^2(a+b+1)}. \tag{2.16}$$

The parameters a and b are often called *hyperparameters* because they control the distribution of the parameter μ. Figure 2.2 shows plots of the beta distribution for various values of the hyperparameters.

The posterior distribution of μ is now obtained by multiplying the beta prior (2.13) by the binomial likelihood function (2.9) and normalizing. Keeping only the factors that depend on μ, we see that this posterior distribution has the form

$$p(\mu|m,l,a,b) \propto \mu^{m+a-1}(1-\mu)^{l+b-1} \tag{2.17}$$

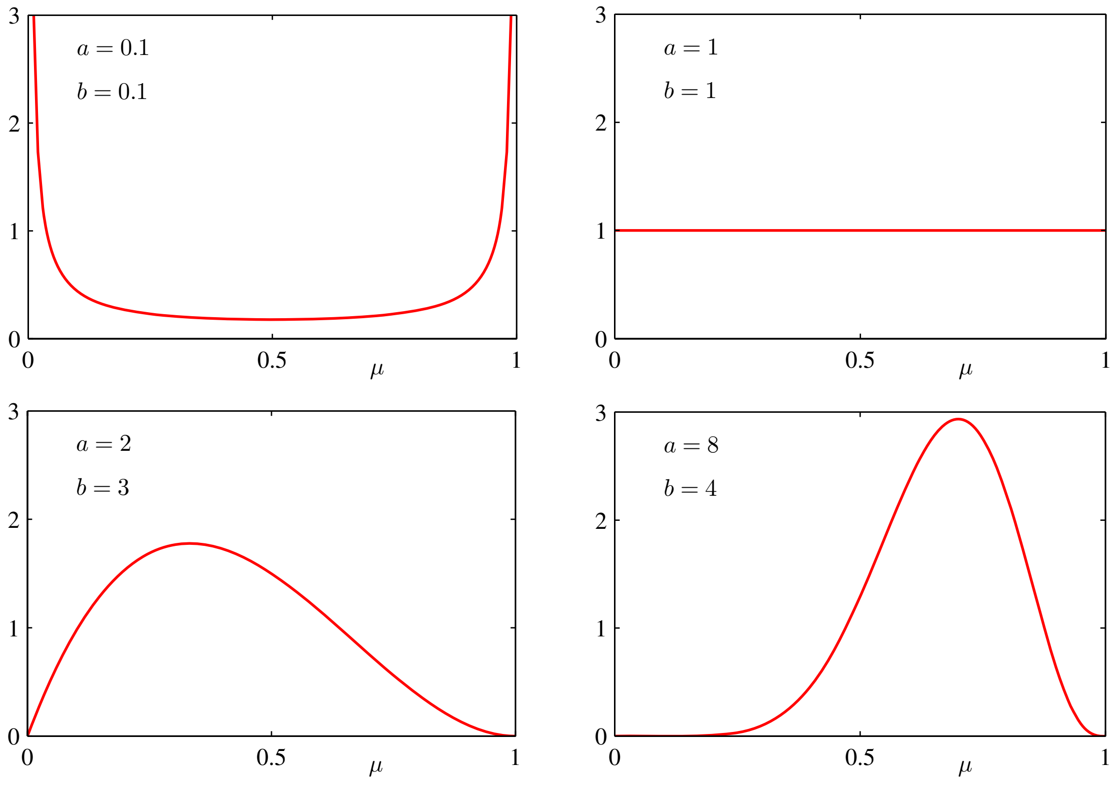

Figure 2.2 Plots of the beta distribution $\mathrm{Beta}(\mu|a, b)$ given by (2.13) as a function of μ for various values of the hyperparameters a and b.

where $l = N - m$, and therefore corresponds to the number of 'tails' in the coin example. We see that (2.17) has the same functional dependence on μ as the prior distribution, reflecting the conjugacy properties of the prior with respect to the likelihood function. Indeed, it is simply another beta distribution, and its normalization coefficient can therefore be obtained by comparison with (2.13) to give

$$p(\mu|m, l, a, b) = \frac{\Gamma(m + a + l + b)}{\Gamma(m + a)\Gamma(l + b)}\mu^{m+a-1}(1 - \mu)^{l+b-1}. \tag{2.18}$$

We see that the effect of observing a data set of m observations of $x = 1$ and l observations of $x = 0$ has been to increase the value of a by m, and the value of b by l, in going from the prior distribution to the posterior distribution. This allows us to provide a simple interpretation of the hyperparameters a and b in the prior as an *effective number of observations* of $x = 1$ and $x = 0$, respectively. Note that a and b need not be integers. Furthermore, the posterior distribution can act as the prior if we subsequently observe additional data. To see this, we can imagine taking observations one at a time and after each observation updating the current posterior

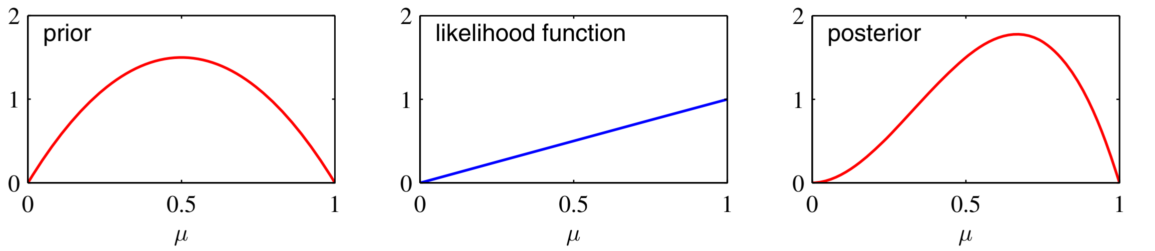

Figure 2.3 Illustration of one step of sequential Bayesian inference. The prior is given by a beta distribution with parameters $a = 2$, $b = 2$, and the likelihood function, given by (2.9) with $N = m = 1$, corresponds to a single observation of $x = 1$, so that the posterior is given by a beta distribution with parameters $a = 3$, $b = 2$.

distribution by multiplying by the likelihood function for the new observation and then normalizing to obtain the new, revised posterior distribution. At each stage, the posterior is a beta distribution with some total number of (prior and actual) observed values for $x = 1$ and $x = 0$ given by the parameters a and b. Incorporation of an additional observation of $x = 1$ simply corresponds to incrementing the value of a by 1, whereas for an observation of $x = 0$ we increment b by 1. Figure 2.3 illustrates one step in this process.

We see that this *sequential* approach to learning arises naturally when we adopt a Bayesian viewpoint. It is independent of the choice of prior and of the likelihood function and depends only on the assumption of i.i.d. data. Sequential methods make use of observations one at a time, or in small batches, and then discard them before the next observations are used. They can be used, for example, in real-time learning scenarios where a steady stream of data is arriving, and predictions must be made before all of the data is seen. Because they do not require the whole data set to be stored or loaded into memory, sequential methods are also useful for large data sets. Maximum likelihood methods can also be cast into a sequential framework.

Section 2.3.5

If our goal is to predict, as best we can, the outcome of the next trial, then we must evaluate the predictive distribution of x, given the observed data set $\mathcal{D}$. From the sum and product rules of probability, this takes the form

$$p(x = 1|\mathcal{D}) = \int_0^1 p(x = 1|\mu)p(\mu|\mathcal{D})\,\mathrm{d}\mu = \int_0^1 \mu p(\mu|\mathcal{D})\,\mathrm{d}\mu = \mathbb{E}[\mu|\mathcal{D}]. \tag{2.19}$$

Using the result (2.18) for the posterior distribution $p(\mu|\mathcal{D})$, together with the result (2.15) for the mean of the beta distribution, we obtain

$$p(x = 1|\mathcal{D}) = \frac{m + a}{m + a + l + b} \tag{2.20}$$

which has a simple interpretation as the total fraction of observations (both real observations and fictitious prior observations) that correspond to $x = 1$. Note that in the limit of an infinitely large data set $m, l \to \infty$ the result (2.20) reduces to the maximum likelihood result (2.8). As we shall see, it is a very general property that the Bayesian and maximum likelihood results will agree in the limit of an infinitely large data set. For a finite data set, the posterior mean for μ always lies between the prior mean and the maximum likelihood estimate for μ corresponding to the relative frequencies of events given by (2.7).

Exercise 2.7

From Figure 2.2, we see that as the number of observations increases, so the posterior distribution becomes more sharply peaked. This can also be seen from the result (2.16) for the variance of the beta distribution, in which we see that the variance goes to zero for $a \to \infty$ or $b \to \infty$. In fact, we might wonder whether it is a general property of Bayesian learning that, as we observe more and more data, the uncertainty represented by the posterior distribution will steadily decrease.

To address this, we can take a frequentist view of Bayesian learning and show that, on average, such a property does indeed hold. Consider a general Bayesian inference problem for a parameter $\boldsymbol{\theta}$ for which we have observed a data set $\mathcal{D}$, described by the joint distribution $p(\boldsymbol{\theta}, \mathcal{D})$. The following result

Exercise 2.8

$$\mathbb{E}_{\boldsymbol{\theta}}[\boldsymbol{\theta}] = \mathbb{E}_{\mathcal{D}}\left[\mathbb{E}_{\boldsymbol{\theta}}[\boldsymbol{\theta}|\mathcal{D}]\right] \tag{2.21}$$

where

$$\mathbb{E}_{\boldsymbol{\theta}}[\boldsymbol{\theta}] \equiv \int p(\boldsymbol{\theta})\boldsymbol{\theta}\,\mathrm{d}\boldsymbol{\theta} \tag{2.22}$$

$$\mathbb{E}_{\mathcal{D}}[\mathbb{E}_{\boldsymbol{\theta}}[\boldsymbol{\theta}|\mathcal{D}]] \equiv \int\left\{\int \boldsymbol{\theta} p(\boldsymbol{\theta}|\mathcal{D})\,\mathrm{d}\boldsymbol{\theta}\right\} p(\mathcal{D})\,\mathrm{d}\mathcal{D} \tag{2.23}$$

says that the posterior mean of $\boldsymbol{\theta}$, averaged over the distribution generating the data, is equal to the prior mean of $\boldsymbol{\theta}$. Similarly, we can show that

$$\mathrm{var}_{\boldsymbol{\theta}}[\boldsymbol{\theta}] = \mathbb{E}_{\mathcal{D}}\left[\mathrm{var}_{\boldsymbol{\theta}}[\boldsymbol{\theta}|\mathcal{D}]\right] + \mathrm{var}_{\mathcal{D}}\left[\mathbb{E}_{\boldsymbol{\theta}}[\boldsymbol{\theta}|\mathcal{D}]\right]. \tag{2.24}$$

The term on the left-hand side of (2.24) is the prior variance of $\boldsymbol{\theta}$. On the right-hand side, the first term is the average posterior variance of $\boldsymbol{\theta}$, and the second term measures the variance in the posterior mean of $\boldsymbol{\theta}$. Because this variance is a positive quantity, this result shows that, on average, the posterior variance of $\boldsymbol{\theta}$ is smaller than the prior variance. The reduction in variance is greater if the variance in the posterior mean is greater. Note, however, that this result only holds on average, and that for a particular observed data set it is possible for the posterior variance to be larger than the prior variance.

2.2. Multinomial Variables

Binary variables can be used to describe quantities that can take one of two possible values. Often, however, we encounter discrete variables that can take on one of K possible mutually exclusive states. Although there are various alternative ways to express such variables, we shall see shortly that a particularly convenient representation is the 1-of-K scheme in which the variable is represented by a K-dimensional vector $\mathbf{x}$ in which one of the elements x_k equals 1, and all remaining elements equal

0. So, for instance if we have a variable that can take $K = 6$ states and a particular observation of the variable happens to correspond to the state where $x_3 = 1$, then $\mathbf{x}$ will be represented by

$$\mathbf{x} = (0, 0, 1, 0, 0, 0)^{\mathrm{T}}. \tag{2.25}$$

Note that such vectors satisfy $\sum_{k=1}^{K} x_k = 1$. If we denote the probability of $x_k = 1$ by the parameter μ_k, then the distribution of $\mathbf{x}$ is given

$$p(\mathbf{x}|\boldsymbol{\mu}) = \prod_{k=1}^{K} \mu_k^{x_k} \tag{2.26}$$

where $\boldsymbol{\mu} = (\mu_1, \ldots, \mu_K)^{\mathrm{T}}$, and the parameters μ_k are constrained to satisfy $\mu_k \geqslant 0$ and $\sum_k \mu_k = 1$, because they represent probabilities. The distribution (2.26) can be regarded as a generalization of the Bernoulli distribution to more than two outcomes. It is easily seen that the distribution is normalized

$$\sum_{\mathbf{x}} p(\mathbf{x}|\boldsymbol{\mu}) = \sum_{k=1}^{K} \mu_k = 1 \tag{2.27}$$

and that

$$\mathbb{E}[\mathbf{x}|\boldsymbol{\mu}] = \sum_{\mathbf{x}} p(\mathbf{x}|\boldsymbol{\mu})\mathbf{x} = (\mu_1, \ldots, \mu_M)^{\mathrm{T}} = \boldsymbol{\mu}. \tag{2.28}$$

Now consider a data set $\mathcal{D}$ of N independent observations $\mathbf{x}_1, \ldots, \mathbf{x}_N$. The corresponding likelihood function takes the form

$$p(\mathcal{D}|\boldsymbol{\mu}) = \prod_{n=1}^{N} \prod_{k=1}^{K} \mu_k^{x_{nk}} = \prod_{k=1}^{K} \mu_k^{(\sum_n x_{nk})} = \prod_{k=1}^{K} \mu_k^{m_k}. \tag{2.29}$$

We see that the likelihood function depends on the N data points only through the K quantities

$$m_k = \sum_n x_{nk} \tag{2.30}$$

which represent the number of observations of $x_k = 1$. These are called the *sufficient statistics* for this distribution.

Section 2.4

In order to find the maximum likelihood solution for $\boldsymbol{\mu}$, we need to maximize $\ln p(\mathcal{D}|\boldsymbol{\mu})$ with respect to μ_k taking account of the constraint that the μ_k must sum to one. This can be achieved using a Lagrange multiplier λ and maximizing

Appendix E

$$\sum_{k=1}^{K} m_k \ln \mu_k + \lambda \left(\sum_{k=1}^{K} \mu_k - 1 \right). \tag{2.31}$$

Setting the derivative of (2.31) with respect to μ_k to zero, we obtain

$$\mu_k = -m_k/\lambda. \tag{2.32}$$

We can solve for the Lagrange multiplier λ by substituting (2.32) into the constraint $\sum_k \mu_k = 1$ to give $\lambda = -N$. Thus we obtain the maximum likelihood solution in the form

$$\mu_k^{\mathrm{ML}} = \frac{m_k}{N} \tag{2.33}$$

which is the fraction of the N observations for which $x_k = 1$.

We can consider the joint distribution of the quantities $m_1, \ldots, m_K$, conditioned on the parameters $\boldsymbol{\mu}$ and on the total number N of observations. From (2.29) this takes the form

$$\mathrm{Mult}(m_1, m_2, \ldots, m_K | \boldsymbol{\mu}, N) = \binom{N}{m_1 m_2 \ldots m_K} \prod_{k=1}^{K} \mu_k^{m_k} \tag{2.34}$$

which is known as the *multinomial* distribution. The normalization coefficient is the number of ways of partitioning N objects into K groups of size $m_1, \ldots, m_K$ and is given by

$$\binom{N}{m_1 m_2 \ldots m_K} = \frac{N!}{m_1! m_2! \ldots m_K!}. \tag{2.35}$$

Note that the variables m_k are subject to the constraint

$$\sum_{k=1}^{K} m_k = N. \tag{2.36}$$

2.2.1 The Dirichlet distribution

We now introduce a family of prior distributions for the parameters $\{\mu_k\}$ of the multinomial distribution (2.34). By inspection of the form of the multinomial distribution, we see that the conjugate prior is given by

$$p(\boldsymbol{\mu}|\boldsymbol{\alpha}) \propto \prod_{k=1}^{K} \mu_k^{\alpha_k - 1} \tag{2.37}$$

where $0 \leqslant \mu_k \leqslant 1$ and $\sum_k \mu_k = 1$. Here $\alpha_1, \ldots, \alpha_K$ are the parameters of the distribution, and $\boldsymbol{\alpha}$ denotes $(\alpha_1, \ldots, \alpha_K)^{\mathrm{T}}$. Note that, because of the summation constraint, the distribution over the space of the $\{\mu_k\}$ is confined to a *simplex* of dimensionality $K - 1$, as illustrated for $K = 3$ in Figure 2.4.

Exercise 2.9

The normalized form for this distribution is by

$$\mathrm{Dir}(\boldsymbol{\mu}|\boldsymbol{\alpha}) = \frac{\Gamma(\alpha_0)}{\Gamma(\alpha_1) \cdots \Gamma(\alpha_K)} \prod_{k=1}^{K} \mu_k^{\alpha_k - 1} \tag{2.38}$$

which is called the *Dirichlet* distribution. Here $\Gamma(x)$ is the gamma function defined by (1.141) while

$$\alpha_0 = \sum_{k=1}^{K} \alpha_k. \tag{2.39}$$

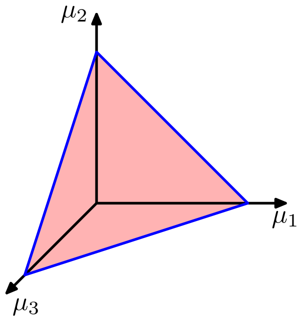

Figure 2.4 The Dirichlet distribution over three variables μ_1, μ_2, μ_3 is confined to a simplex (a bounded linear manifold) of the form shown, as a consequence of the constraints $0 \leqslant \mu_k \leqslant 1$ and $\sum_k \mu_k = 1$.

Plots of the Dirichlet distribution over the simplex, for various settings of the parameters α_k, are shown in Figure 2.5.

Multiplying the prior (2.38) by the likelihood function (2.34), we obtain the posterior distribution for the parameters $\{\mu_k\}$ in the form

$$p(\boldsymbol{\mu}|\mathcal{D}, \boldsymbol{\alpha}) \propto p(\mathcal{D}|\boldsymbol{\mu})p(\boldsymbol{\mu}|\boldsymbol{\alpha}) \propto \prod_{k=1}^{K} \mu_k^{\alpha_k + m_k - 1}. \tag{2.40}$$

We see that the posterior distribution again takes the form of a Dirichlet distribution, confirming that the Dirichlet is indeed a conjugate prior for the multinomial. This allows us to determine the normalization coefficient by comparison with (2.38) so that

$$\begin{aligned} p(\boldsymbol{\mu}|\mathcal{D}, \boldsymbol{\alpha}) &= \mathrm{Dir}(\boldsymbol{\mu}|\boldsymbol{\alpha} + \mathbf{m}) \\ &= \frac{\Gamma(\alpha_0 + N)}{\Gamma(\alpha_1 + m_1) \cdots \Gamma(\alpha_K + m_K)} \prod_{k=1}^{K} \mu_k^{\alpha_k + m_k - 1} \end{aligned} \tag{2.41}$$

where we have denoted $\mathbf{m} = (m_1, \ldots, m_K)^{\mathrm{T}}$. As for the case of the binomial distribution with its beta prior, we can interpret the parameters α_k of the Dirichlet prior as an effective number of observations of $x_k = 1$.

Note that two-state quantities can either be represented as binary variables and

Lejeune Dirichlet
1805–1859

Johann Peter Gustav Lejeune Dirichlet was a modest and reserved mathematician who made contributions in number theory, mechanics, and astronomy, and who gave the first rigorous analysis of Fourier series. His family originated from Richelet in Belgium, and the name Lejeune Dirichlet comes from 'le jeune de Richelet' (the young person from Richelet). Dirichlet's first paper, which was published in 1825, brought him instant fame. It concerned Fermat's last theorem, which claims that there are no positive integer solutions to $x^n + y^n = z^n$ for $n > 2$. Dirichlet gave a partial proof for the case $n = 5$, which was sent to Legendre for review and who in turn completed the proof. Later, Dirichlet gave a complete proof for $n = 14$, although a full proof of Fermat's last theorem for arbitrary n had to wait until the work of Andrew Wiles in the closing years of the 20th century.

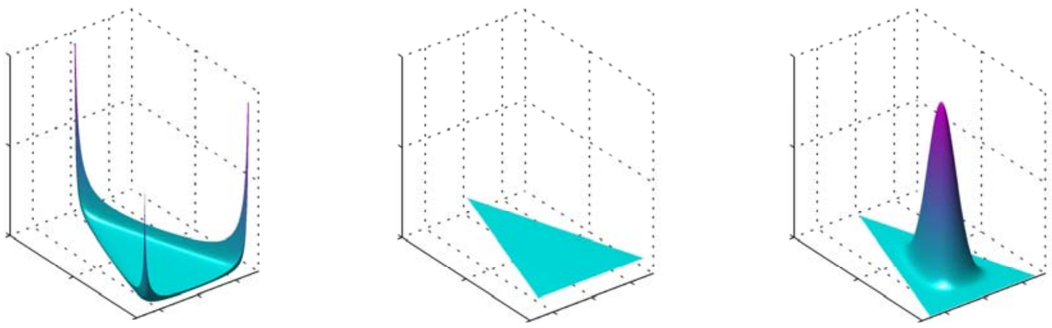

Figure 2.5 Plots of the Dirichlet distribution over three variables, where the two horizontal axes are coordinates in the plane of the simplex and the vertical axis corresponds to the value of the density. Here $\{\alpha_k\} = 0.1$ on the left plot, $\{\alpha_k\} = 1$ in the centre plot, and $\{\alpha_k\} = 10$ in the right plot.

modelled using the binomial distribution (2.9) or as 1-of-2 variables and modelled using the multinomial distribution (2.34) with $K = 2$.

2.3. The Gaussian Distribution

The Gaussian, also known as the normal distribution, is a widely used model for the distribution of continuous variables. In the case of a single variable x, the Gaussian distribution can be written in the form

$$\mathcal{N}(x|\mu, \sigma^2) = \frac{1}{(2\pi\sigma^2)^{1/2}} \exp\left\{-\frac{1}{2\sigma^2}(x-\mu)^2\right\} \tag{2.42}$$

where μ is the mean and σ^2 is the variance. For a D-dimensional vector $\mathbf{x}$, the multivariate Gaussian distribution takes the form

$$\mathcal{N}(\mathbf{x}|\boldsymbol{\mu}, \boldsymbol{\Sigma}) = \frac{1}{(2\pi)^{D/2}} \frac{1}{|\boldsymbol{\Sigma}|^{1/2}} \exp\left\{-\frac{1}{2}(\mathbf{x}-\boldsymbol{\mu})^{\mathrm{T}}\boldsymbol{\Sigma}^{-1}(\mathbf{x}-\boldsymbol{\mu})\right\} \tag{2.43}$$

where $\boldsymbol{\mu}$ is a D-dimensional mean vector, $\boldsymbol{\Sigma}$ is a $D \times D$ covariance matrix, and $|\boldsymbol{\Sigma}|$ denotes the determinant of $\boldsymbol{\Sigma}$.

The Gaussian distribution arises in many different contexts and can be motivated from a variety of different perspectives. For example, we have already seen that for a single real variable, the distribution that maximizes the entropy is the Gaussian. This property applies also to the multivariate Gaussian.

Section 1.6

Exercise 2.14

Another situation in which the Gaussian distribution arises is when we consider the sum of multiple random variables. The *central limit theorem* (due to Laplace) tells us that, subject to certain mild conditions, the sum of a set of random variables, which is of course itself a random variable, has a distribution that becomes increasingly Gaussian as the number of terms in the sum increases (Walker, 1969). We can

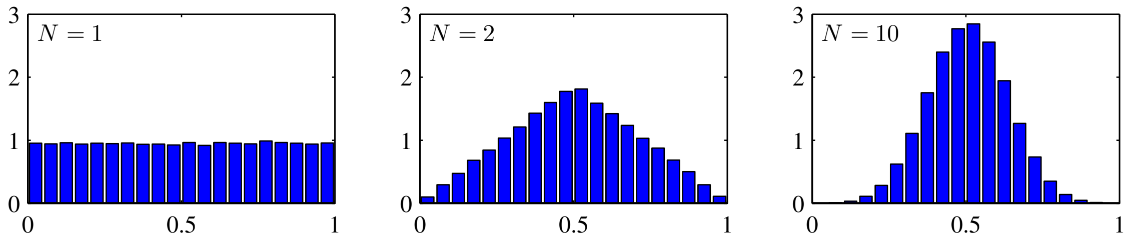

Figure 2.6 Histogram plots of the mean of N uniformly distributed numbers for various values of N. We observe that as N increases, the distribution tends towards a Gaussian.

illustrate this by considering N variables $x_1, \ldots, x_N$ each of which has a uniform distribution over the interval $[0, 1]$ and then considering the distribution of the mean $(x_1 + \cdots + x_N)/N$. For large N, this distribution tends to a Gaussian, as illustrated in Figure 2.6. In practice, the convergence to a Gaussian as N increases can be very rapid. One consequence of this result is that the binomial distribution (2.9), which is a distribution over m defined by the sum of N observations of the random binary variable x, will tend to a Gaussian as $N \to \infty$ (see Figure 2.1 for the case of $N = 10$).

The Gaussian distribution has many important analytical properties, and we shall consider several of these in detail. As a result, this section will be rather more technically involved than some of the earlier sections, and will require familiarity with various matrix identities. *Appendix C* However, we strongly encourage the reader to become proficient in manipulating Gaussian distributions using the techniques presented here as this will prove invaluable in understanding the more complex models presented in later chapters.

We begin by considering the geometrical form of the Gaussian distribution. The

Carl Friedrich Gauss
1777–1855

It is said that when Gauss went to elementary school at age 7, his teacher Büttner, trying to keep the class occupied, asked the pupils to sum the integers from 1 to 100. To the teacher's amazement, Gauss arrived at the answer in a matter of moments by noting that the sum can be represented as 50 pairs ($1 + 100$, $2 + 99$, etc.) each of which added to 101, giving the answer 5,050. It is now believed that the problem which was actually set was of the same form but somewhat harder in that the sequence had a larger starting value and a larger increment. Gauss was a German mathematician and scientist with a reputation for being a hard-working perfectionist. One of his many contributions was to show that least squares can be derived under the assumption of normally distributed errors. He also created an early formulation of non-Euclidean geometry (a self-consistent geometrical theory that violates the axioms of Euclid) but was reluctant to discuss it openly for fear that his reputation might suffer if it were seen that he believed in such a geometry. At one point, Gauss was asked to conduct a geodetic survey of the state of Hanover, which led to his formulation of the normal distribution, now also known as the Gaussian. After his death, a study of his diaries revealed that he had discovered several important mathematical results years or even decades before they were published by others.

functional dependence of the Gaussian on $\mathbf{x}$ is through the quadratic form

$$\Delta^2 = (\mathbf{x}-\boldsymbol{\mu})^{\mathrm{T}}\boldsymbol{\Sigma}^{-1}(\mathbf{x}-\boldsymbol{\mu}) \tag{2.44}$$

which appears in the exponent. The quantity Δ is called the *Mahalanobis distance* from $\boldsymbol{\mu}$ to $\mathbf{x}$ and reduces to the Euclidean distance when $\boldsymbol{\Sigma}$ is the identity matrix. The Gaussian distribution will be constant on surfaces in $\mathbf{x}$-space for which this quadratic form is constant.

First of all, we note that the matrix $\boldsymbol{\Sigma}$ can be taken to be symmetric, without loss of generality, because any antisymmetric component would disappear from the exponent. Now consider the eigenvector equation for the covariance matrix

Exercise 2.17

$$\boldsymbol{\Sigma}\mathbf{u}_i = \lambda_i \mathbf{u}_i \tag{2.45}$$

where $i = 1, \ldots, D$. Because $\boldsymbol{\Sigma}$ is a real, symmetric matrix its eigenvalues will be real, and its eigenvectors can be chosen to form an orthonormal set, so that

Exercise 2.18

$$\mathbf{u}_i^{\mathrm{T}}\mathbf{u}_j = I_{ij} \tag{2.46}$$

where I_{ij} is the i, j element of the identity matrix and satisfies

$$I_{ij} = \begin{cases} 1, & \text{if } i = j \\ 0, & \text{otherwise.} \end{cases} \tag{2.47}$$

The covariance matrix $\boldsymbol{\Sigma}$ can be expressed as an expansion in terms of its eigenvectors in the form

Exercise 2.19

$$\boldsymbol{\Sigma} = \sum_{i=1}^{D} \lambda_i \mathbf{u}_i \mathbf{u}_i^{\mathrm{T}} \tag{2.48}$$

and similarly the inverse covariance matrix $\boldsymbol{\Sigma}^{-1}$ can be expressed as

$$\boldsymbol{\Sigma}^{-1} = \sum_{i=1}^{D} \frac{1}{\lambda_i} \mathbf{u}_i \mathbf{u}_i^{\mathrm{T}}. \tag{2.49}$$

Substituting (2.49) into (2.44), the quadratic form becomes

$$\Delta^2 = \sum_{i=1}^{D} \frac{y_i^2}{\lambda_i} \tag{2.50}$$

where we have defined

$$y_i = \mathbf{u}_i^{\mathrm{T}}(\mathbf{x}-\boldsymbol{\mu}). \tag{2.51}$$

We can interpret $\{y_i\}$ as a new coordinate system defined by the orthonormal vectors $\mathbf{u}_i$ that are shifted and rotated with respect to the original x_i coordinates. Forming the vector $\mathbf{y} = (y_1, \ldots, y_D)^{\mathrm{T}}$, we have

$$\mathbf{y} = \mathbf{U}(\mathbf{x}-\boldsymbol{\mu}) \tag{2.52}$$

Figure 2.7 The red curve shows the elliptical surface of constant probability density for a Gaussian in a two-dimensional space $\mathbf{x} = (x_1, x_2)$ on which the density is $\exp(-1/2)$ of its value at $\mathbf{x} = \boldsymbol{\mu}$. The major axes of the ellipse are defined by the eigenvectors $\mathbf{u}_i$ of the covariance matrix, with corresponding eigenvalues λ_i.

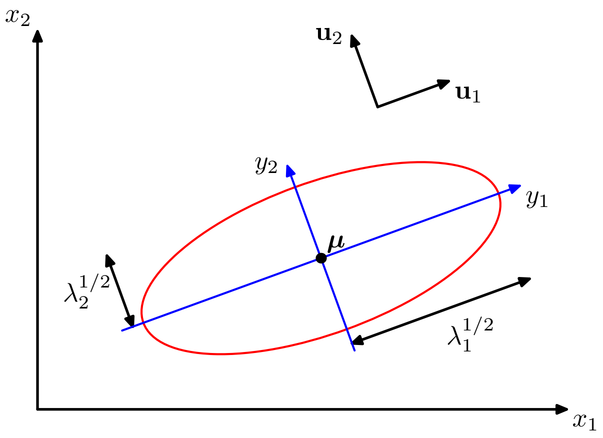

Appendix C

where $\mathbf{U}$ is a matrix whose rows are given by $\mathbf{u}_i^{\mathrm{T}}$. From (2.46) it follows that $\mathbf{U}$ is an *orthogonal* matrix, i.e., it satisfies $\mathbf{U}\mathbf{U}^{\mathrm{T}} = \mathbf{I}$, and hence also $\mathbf{U}^{\mathrm{T}}\mathbf{U} = \mathbf{I}$, where $\mathbf{I}$ is the identity matrix.

The quadratic form, and hence the Gaussian density, will be constant on surfaces for which (2.51) is constant. If all of the eigenvalues λ_i are positive, then these surfaces represent ellipsoids, with their centres at $\boldsymbol{\mu}$ and their axes oriented along $\mathbf{u}_i$, and with scaling factors in the directions of the axes given by $\lambda_i^{1/2}$, as illustrated in Figure 2.7.

For the Gaussian distribution to be well defined, it is necessary for all of the eigenvalues λ_i of the covariance matrix to be strictly positive, otherwise the distribution cannot be properly normalized. A matrix whose eigenvalues are strictly positive is said to be *positive definite*. In Chapter 12, we will encounter Gaussian distributions for which one or more of the eigenvalues are zero, in which case the distribution is singular and is confined to a subspace of lower dimensionality. If all of the eigenvalues are nonnegative, then the covariance matrix is said to be *positive semidefinite*.

Now consider the form of the Gaussian distribution in the new coordinate system defined by the y_i. In going from the $\mathbf{x}$ to the $\mathbf{y}$ coordinate system, we have a Jacobian matrix $\mathbf{J}$ with elements given by

$$J_{ij} = \frac{\partial x_i}{\partial y_j} = U_{ji} \tag{2.53}$$

where U_{ji} are the elements of the matrix $\mathbf{U}^{\mathrm{T}}$. Using the orthonormality property of the matrix $\mathbf{U}$, we see that the square of the determinant of the Jacobian matrix is

$$|\mathbf{J}|^2 = \left|\mathbf{U}^{\mathrm{T}}\right|^2 = \left|\mathbf{U}^{\mathrm{T}}\right| |\mathbf{U}| = \left|\mathbf{U}^{\mathrm{T}}\mathbf{U}\right| = |\mathbf{I}| = 1 \tag{2.54}$$

and hence $|\mathbf{J}| = 1$. Also, the determinant $|\boldsymbol{\Sigma}|$ of the covariance matrix can be written as the product of its eigenvalues, and hence

$$|\boldsymbol{\Sigma}|^{1/2} = \prod_{j=1}^{D} \lambda_j^{1/2}. \tag{2.55}$$

Thus in the y_j coordinate system, the Gaussian distribution takes the form

$$p(\mathbf{y}) = p(\mathbf{x})|\mathbf{J}| = \prod_{j=1}^{D} \frac{1}{(2\pi\lambda_j)^{1/2}} \exp\left\{-\frac{y_j^2}{2\lambda_j}\right\} \tag{2.56}$$

which is the product of D independent univariate Gaussian distributions. The eigenvectors therefore define a new set of shifted and rotated coordinates with respect to which the joint probability distribution factorizes into a product of independent distributions. The integral of the distribution in the $\mathbf{y}$ coordinate system is then

$$\int p(\mathbf{y})\,\mathrm{d}\mathbf{y} = \prod_{j=1}^{D} \int_{-\infty}^{\infty} \frac{1}{(2\pi\lambda_j)^{1/2}} \exp\left\{-\frac{y_j^2}{2\lambda_j}\right\} \mathrm{d}y_j = 1 \tag{2.57}$$

where we have used the result (1.48) for the normalization of the univariate Gaussian. This confirms that the multivariate Gaussian (2.43) is indeed normalized.

We now look at the moments of the Gaussian distribution and thereby provide an interpretation of the parameters $\boldsymbol{\mu}$ and $\boldsymbol{\Sigma}$. The expectation of $\mathbf{x}$ under the Gaussian distribution is given by

$$\begin{aligned}\mathbb{E}[\mathbf{x}] &= \frac{1}{(2\pi)^{D/2}} \frac{1}{|\boldsymbol{\Sigma}|^{1/2}} \int \exp\left\{-\frac{1}{2}(\mathbf{x}-\boldsymbol{\mu})^{\mathrm{T}}\boldsymbol{\Sigma}^{-1}(\mathbf{x}-\boldsymbol{\mu})\right\} \mathbf{x}\,\mathrm{d}\mathbf{x} \\ &= \frac{1}{(2\pi)^{D/2}} \frac{1}{|\boldsymbol{\Sigma}|^{1/2}} \int \exp\left\{-\frac{1}{2}\mathbf{z}^{\mathrm{T}}\boldsymbol{\Sigma}^{-1}\mathbf{z}\right\} (\mathbf{z}+\boldsymbol{\mu})\,\mathrm{d}\mathbf{z}\end{aligned} \tag{2.58}$$

where we have changed variables using $\mathbf{z} = \mathbf{x} - \boldsymbol{\mu}$. We now note that the exponent is an even function of the components of $\mathbf{z}$ and, because the integrals over these are taken over the range $(-\infty, \infty)$, the term in $\mathbf{z}$ in the factor $(\mathbf{z} + \boldsymbol{\mu})$ will vanish by symmetry. Thus

$$\mathbb{E}[\mathbf{x}] = \boldsymbol{\mu} \tag{2.59}$$

and so we refer to $\boldsymbol{\mu}$ as the mean of the Gaussian distribution.

We now consider second order moments of the Gaussian. In the univariate case, we considered the second order moment given by $\mathbb{E}[x^2]$. For the multivariate Gaussian, there are D^2 second order moments given by $\mathbb{E}[x_i x_j]$, which we can group together to form the matrix $\mathbb{E}[\mathbf{x}\mathbf{x}^{\mathrm{T}}]$. This matrix can be written as

$$\begin{aligned}\mathbb{E}[\mathbf{x}\mathbf{x}^{\mathrm{T}}] &= \frac{1}{(2\pi)^{D/2}} \frac{1}{|\boldsymbol{\Sigma}|^{1/2}} \int \exp\left\{-\frac{1}{2}(\mathbf{x}-\boldsymbol{\mu})^{\mathrm{T}}\boldsymbol{\Sigma}^{-1}(\mathbf{x}-\boldsymbol{\mu})\right\} \mathbf{x}\mathbf{x}^{\mathrm{T}}\,\mathrm{d}\mathbf{x} \\ &= \frac{1}{(2\pi)^{D/2}} \frac{1}{|\boldsymbol{\Sigma}|^{1/2}} \int \exp\left\{-\frac{1}{2}\mathbf{z}^{\mathrm{T}}\boldsymbol{\Sigma}^{-1}\mathbf{z}\right\} (\mathbf{z}+\boldsymbol{\mu})(\mathbf{z}+\boldsymbol{\mu})^{\mathrm{T}}\,\mathrm{d}\mathbf{z}\end{aligned}$$

where again we have changed variables using $\mathbf{z} = \mathbf{x} - \boldsymbol{\mu}$. Note that the cross-terms involving $\boldsymbol{\mu}\mathbf{z}^{\mathrm{T}}$ and $\boldsymbol{\mu}^{\mathrm{T}}\mathbf{z}$ will again vanish by symmetry. The term $\boldsymbol{\mu}\boldsymbol{\mu}^{\mathrm{T}}$ is constant and can be taken outside the integral, which itself is unity because the Gaussian distribution is normalized. Consider the term involving $\mathbf{z}\mathbf{z}^{\mathrm{T}}$. Again, we can make use of the eigenvector expansion of the covariance matrix given by (2.45), together with the completeness of the set of eigenvectors, to write

$$\mathbf{z} = \sum_{j=1}^{D} y_j \mathbf{u}_j \tag{2.60}$$

where $y_j = \mathbf{u}_j^{\mathrm{T}}\mathbf{z}$, which gives

$$\begin{aligned} &\frac{1}{(2\pi)^{D/2}} \frac{1}{|\boldsymbol{\Sigma}|^{1/2}} \int \exp\left\{-\frac{1}{2}\mathbf{z}^{\mathrm{T}}\boldsymbol{\Sigma}^{-1}\mathbf{z}\right\} \mathbf{z}\mathbf{z}^{\mathrm{T}}\,\mathrm{d}\mathbf{z} \\ &= \frac{1}{(2\pi)^{D/2}} \frac{1}{|\boldsymbol{\Sigma}|^{1/2}} \sum_{i=1}^{D}\sum_{j=1}^{D} \mathbf{u}_i\mathbf{u}_j^{\mathrm{T}} \int \exp\left\{-\sum_{k=1}^{D}\frac{y_k^2}{2\lambda_k}\right\} y_i y_j\,\mathrm{d}\mathbf{y} \\ &= \sum_{i=1}^{D} \mathbf{u}_i\mathbf{u}_i^{\mathrm{T}}\lambda_i = \boldsymbol{\Sigma} \end{aligned} \tag{2.61}$$

where we have made use of the eigenvector equation (2.45), together with the fact that the integral on the right-hand side of the middle line vanishes by symmetry unless $i = j$, and in the final line we have made use of the results (1.50) and (2.55), together with (2.48). Thus we have

$$\mathbb{E}[\mathbf{x}\mathbf{x}^{\mathrm{T}}] = \boldsymbol{\mu}\boldsymbol{\mu}^{\mathrm{T}} + \boldsymbol{\Sigma}. \tag{2.62}$$

For single random variables, we subtracted the mean before taking second moments in order to define a variance. Similarly, in the multivariate case it is again convenient to subtract off the mean, giving rise to the *covariance* of a random vector $\mathbf{x}$ defined by

$$\mathrm{cov}[\mathbf{x}] = \mathbb{E}\left[(\mathbf{x} - \mathbb{E}[\mathbf{x}])(\mathbf{x} - \mathbb{E}[\mathbf{x}])^{\mathrm{T}}\right]. \tag{2.63}$$

For the specific case of a Gaussian distribution, we can make use of $\mathbb{E}[\mathbf{x}] = \boldsymbol{\mu}$, together with the result (2.62), to give

$$\mathrm{cov}[\mathbf{x}] = \boldsymbol{\Sigma}. \tag{2.64}$$

Because the parameter matrix $\boldsymbol{\Sigma}$ governs the covariance of $\mathbf{x}$ under the Gaussian distribution, it is called the covariance matrix.

Although the Gaussian distribution (2.43) is widely used as a density model, it suffers from some significant limitations. Consider the number of free parameters in the distribution. A general symmetric covariance matrix $\boldsymbol{\Sigma}$ will have $D(D+1)/2$ independent parameters, and there are another D independent parameters in $\boldsymbol{\mu}$, giving $D(D+3)/2$ parameters in total. For large D, the total number of parameters

Exercise 2.21

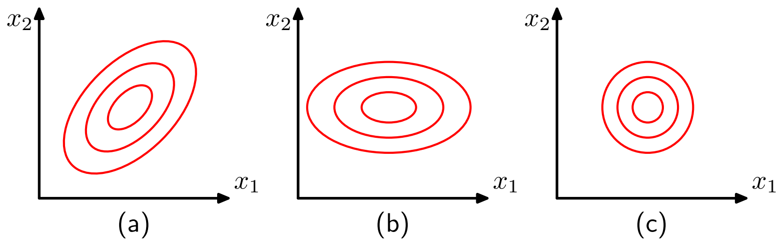

Figure 2.8 Contours of constant probability density for a Gaussian distribution in two dimensions in which the covariance matrix is (a) of general form, (b) diagonal, in which the elliptical contours are aligned with the coordinate axes, and (c) proportional to the identity matrix, in which the contours are concentric circles.

therefore grows quadratically with D, and the computational task of manipulating and inverting large matrices can become prohibitive. One way to address this problem is to use restricted forms of the covariance matrix. If we consider covariance matrices that are *diagonal*, so that $\mathbf{\Sigma} = \mathrm{diag}(\sigma_i^2)$, we then have a total of $2D$ independent parameters in the density model. The corresponding contours of constant density are given by axis-aligned ellipsoids. We could further restrict the covariance matrix to be proportional to the identity matrix, $\mathbf{\Sigma} = \sigma^2\mathbf{I}$, known as an *isotropic* covariance, giving $D + 1$ independent parameters in the model and spherical surfaces of constant density. The three possibilities of general, diagonal, and isotropic covariance matrices are illustrated in Figure 2.8. Unfortunately, whereas such approaches limit the number of degrees of freedom in the distribution and make inversion of the covariance matrix a much faster operation, they also greatly restrict the form of the probability density and limit its ability to capture interesting correlations in the data.

A further limitation of the Gaussian distribution is that it is intrinsically unimodal (i.e., has a single maximum) and so is unable to provide a good approximation to multimodal distributions. Thus the Gaussian distribution can be both too flexible, in the sense of having too many parameters, while also being too limited in the range of distributions that it can adequately represent. We will see later that the introduction of *latent* variables, also called *hidden* variables or *unobserved* variables, allows both of these problems to be addressed. In particular, a rich family of multimodal distributions is obtained by introducing discrete latent variables leading to mixtures of Gaussians, as discussed in Section 2.3.9. Similarly, the introduction of continuous latent variables, as described in Chapter 12, leads to models in which the number of free parameters can be controlled independently of the dimensionality D of the data space while still allowing the model to capture the dominant correlations in the data set. Indeed, these two approaches can be combined and further extended to derive a very rich set of hierarchical models that can be adapted to a broad range of practical applications. For instance, the Gaussian version of the *Markov random field*, which is widely used as a probabilistic model of images, is a Gaussian distribution over the joint space of pixel intensities but rendered tractable through the imposition of considerable structure reflecting the spatial organization of the pixels. Similarly, the *linear dynamical system*, used to model time series data for applications such as tracking, is also a joint Gaussian distribution over a potentially large number of observed and latent variables and again is tractable due to the structure imposed on the distribution. A powerful framework for expressing the form and properties of

Section 8.3

Section 13.3

such complex distributions is that of probabilistic graphical models, which will form the subject of Chapter 8.

2.3.1 Conditional Gaussian distributions

An important property of the multivariate Gaussian distribution is that if two sets of variables are jointly Gaussian, then the conditional distribution of one set conditioned on the other is again Gaussian. Similarly, the marginal distribution of either set is also Gaussian.

Consider first the case of conditional distributions. Suppose $\mathbf{x}$ is a D-dimensional vector with Gaussian distribution $\mathcal{N}(\mathbf{x}|\boldsymbol{\mu}, \boldsymbol{\Sigma})$ and that we partition $\mathbf{x}$ into two disjoint subsets $\mathbf{x}_a$ and $\mathbf{x}_b$. Without loss of generality, we can take $\mathbf{x}_a$ to form the first M components of $\mathbf{x}$, with $\mathbf{x}_b$ comprising the remaining $D - M$ components, so that

$$\mathbf{x} = \begin{pmatrix} \mathbf{x}_a \\ \mathbf{x}_b \end{pmatrix}. \tag{2.65}$$

We also define corresponding partitions of the mean vector $\boldsymbol{\mu}$ given by

$$\boldsymbol{\mu} = \begin{pmatrix} \boldsymbol{\mu}_a \\ \boldsymbol{\mu}_b \end{pmatrix} \tag{2.66}$$

and of the covariance matrix $\boldsymbol{\Sigma}$ given by

$$\boldsymbol{\Sigma} = \begin{pmatrix} \boldsymbol{\Sigma}_{aa} & \boldsymbol{\Sigma}_{ab} \\ \boldsymbol{\Sigma}_{ba} & \boldsymbol{\Sigma}_{bb} \end{pmatrix}. \tag{2.67}$$

Note that the symmetry $\boldsymbol{\Sigma}^{\mathrm{T}} = \boldsymbol{\Sigma}$ of the covariance matrix implies that $\boldsymbol{\Sigma}_{aa}$ and $\boldsymbol{\Sigma}_{bb}$ are symmetric, while $\boldsymbol{\Sigma}_{ba} = \boldsymbol{\Sigma}_{ab}^{\mathrm{T}}$.

In many situations, it will be convenient to work with the inverse of the covariance matrix

$$\boldsymbol{\Lambda} \equiv \boldsymbol{\Sigma}^{-1} \tag{2.68}$$

which is known as the *precision matrix*. In fact, we shall see that some properties of Gaussian distributions are most naturally expressed in terms of the covariance, whereas others take a simpler form when viewed in terms of the precision. We therefore also introduce the partitioned form of the precision matrix

$$\boldsymbol{\Lambda} = \begin{pmatrix} \boldsymbol{\Lambda}_{aa} & \boldsymbol{\Lambda}_{ab} \\ \boldsymbol{\Lambda}_{ba} & \boldsymbol{\Lambda}_{bb} \end{pmatrix} \tag{2.69}$$

Exercise 2.22

corresponding to the partitioning (2.65) of the vector $\mathbf{x}$. Because the inverse of a symmetric matrix is also symmetric, we see that $\boldsymbol{\Lambda}_{aa}$ and $\boldsymbol{\Lambda}_{bb}$ are symmetric, while $\boldsymbol{\Lambda}_{ab}^{\mathrm{T}} = \boldsymbol{\Lambda}_{ba}$. It should be stressed at this point that, for instance, $\boldsymbol{\Lambda}_{aa}$ is not simply given by the inverse of $\boldsymbol{\Sigma}_{aa}$. In fact, we shall shortly examine the relation between the inverse of a partitioned matrix and the inverses of its partitions.

Let us begin by finding an expression for the conditional distribution $p(\mathbf{x}_a|\mathbf{x}_b)$. From the product rule of probability, we see that this conditional distribution can be evaluated from the joint distribution $p(\mathbf{x}) = p(\mathbf{x}_a, \mathbf{x}_b)$ simply by fixing $\mathbf{x}_b$ to the observed value and normalizing the resulting expression to obtain a valid probability distribution over $\mathbf{x}_a$. Instead of performing this normalization explicitly, we can obtain the solution more efficiently by considering the quadratic form in the exponent of the Gaussian distribution given by (2.44) and then reinstating the normalization coefficient at the end of the calculation. If we make use of the partitioning (2.65), (2.66), and (2.69), we obtain

$$\begin{aligned} -\frac{1}{2}(\mathbf{x}-\boldsymbol{\mu})^{\mathrm{T}}\boldsymbol{\Sigma}^{-1}(\mathbf{x}-\boldsymbol{\mu}) = \\ -\frac{1}{2}(\mathbf{x}_a-\boldsymbol{\mu}_a)^{\mathrm{T}}\boldsymbol{\Lambda}_{aa}(\mathbf{x}_a-\boldsymbol{\mu}_a) - \frac{1}{2}(\mathbf{x}_a-\boldsymbol{\mu}_a)^{\mathrm{T}}\boldsymbol{\Lambda}_{ab}(\mathbf{x}_b-\boldsymbol{\mu}_b) \\ -\frac{1}{2}(\mathbf{x}_b-\boldsymbol{\mu}_b)^{\mathrm{T}}\boldsymbol{\Lambda}_{ba}(\mathbf{x}_a-\boldsymbol{\mu}_a) - \frac{1}{2}(\mathbf{x}_b-\boldsymbol{\mu}_b)^{\mathrm{T}}\boldsymbol{\Lambda}_{bb}(\mathbf{x}_b-\boldsymbol{\mu}_b). \end{aligned} \tag{2.70}$$

We see that as a function of $\mathbf{x}_a$, this is again a quadratic form, and hence the corresponding conditional distribution $p(\mathbf{x}_a|\mathbf{x}_b)$ will be Gaussian. Because this distribution is completely characterized by its mean and its covariance, our goal will be to identify expressions for the mean and covariance of $p(\mathbf{x}_a|\mathbf{x}_b)$ by inspection of (2.70).

This is an example of a rather common operation associated with Gaussian distributions, sometimes called 'completing the square', in which we are given a quadratic form defining the exponent terms in a Gaussian distribution, and we need to determine the corresponding mean and covariance. Such problems can be solved straightforwardly by noting that the exponent in a general Gaussian distribution $\mathcal{N}(\mathbf{x}|\boldsymbol{\mu}, \boldsymbol{\Sigma})$ can be written

$$-\frac{1}{2}(\mathbf{x}-\boldsymbol{\mu})^{\mathrm{T}}\boldsymbol{\Sigma}^{-1}(\mathbf{x}-\boldsymbol{\mu}) = -\frac{1}{2}\mathbf{x}^{\mathrm{T}}\boldsymbol{\Sigma}^{-1}\mathbf{x} + \mathbf{x}^{\mathrm{T}}\boldsymbol{\Sigma}^{-1}\boldsymbol{\mu} + \text{const} \tag{2.71}$$

where 'const' denotes terms which are independent of $\mathbf{x}$, and we have made use of the symmetry of $\boldsymbol{\Sigma}$. Thus if we take our general quadratic form and express it in the form given by the right-hand side of (2.71), then we can immediately equate the matrix of coefficients entering the second order term in $\mathbf{x}$ to the inverse covariance matrix $\boldsymbol{\Sigma}^{-1}$ and the coefficient of the linear term in $\mathbf{x}$ to $\boldsymbol{\Sigma}^{-1}\boldsymbol{\mu}$, from which we can obtain $\boldsymbol{\mu}$.

Now let us apply this procedure to the conditional Gaussian distribution $p(\mathbf{x}_a|\mathbf{x}_b)$ for which the quadratic form in the exponent is given by (2.70). We will denote the mean and covariance of this distribution by $\boldsymbol{\mu}_{a|b}$ and $\boldsymbol{\Sigma}_{a|b}$, respectively. Consider the functional dependence of (2.70) on $\mathbf{x}_a$ in which $\mathbf{x}_b$ is regarded as a constant. If we pick out all terms that are second order in $\mathbf{x}_a$, we have

$$-\frac{1}{2}\mathbf{x}_a^{\mathrm{T}}\boldsymbol{\Lambda}_{aa}\mathbf{x}_a \tag{2.72}$$

from which we can immediately conclude that the covariance (inverse precision) of $p(\mathbf{x}_a|\mathbf{x}_b)$ is given by

$$\boldsymbol{\Sigma}_{a|b} = \boldsymbol{\Lambda}_{aa}^{-1}. \tag{2.73}$$

Now consider all of the terms in (2.70) that are linear in $\mathbf{x}_a$

$$\mathbf{x}_a^{\mathrm{T}} \left\{ \boldsymbol{\Lambda}_{aa}\boldsymbol{\mu}_a - \boldsymbol{\Lambda}_{ab}(\mathbf{x}_b - \boldsymbol{\mu}_b) \right\} \tag{2.74}$$

where we have used $\boldsymbol{\Lambda}_{ba}^{\mathrm{T}} = \boldsymbol{\Lambda}_{ab}$. From our discussion of the general form (2.71), the coefficient of $\mathbf{x}_a$ in this expression must equal $\boldsymbol{\Sigma}_{a|b}^{-1}\boldsymbol{\mu}_{a|b}$ and hence

$$\begin{aligned} \boldsymbol{\mu}_{a|b} &= \boldsymbol{\Sigma}_{a|b} \left\{ \boldsymbol{\Lambda}_{aa}\boldsymbol{\mu}_a - \boldsymbol{\Lambda}_{ab}(\mathbf{x}_b - \boldsymbol{\mu}_b) \right\} \\ &= \boldsymbol{\mu}_a - \boldsymbol{\Lambda}_{aa}^{-1}\boldsymbol{\Lambda}_{ab}(\mathbf{x}_b - \boldsymbol{\mu}_b) \end{aligned} \tag{2.75}$$

where we have made use of (2.73).

The results (2.73) and (2.75) are expressed in terms of the partitioned precision matrix of the original joint distribution $p(\mathbf{x}_a, \mathbf{x}_b)$. We can also express these results in terms of the corresponding partitioned covariance matrix. To do this, we make use of the following identity for the inverse of a partitioned matrix

Exercise 2.24

$$\begin{pmatrix} \mathbf{A} & \mathbf{B} \\ \mathbf{C} & \mathbf{D} \end{pmatrix}^{-1} = \begin{pmatrix} \mathbf{M} & -\mathbf{M}\mathbf{B}\mathbf{D}^{-1} \\ -\mathbf{D}^{-1}\mathbf{C}\mathbf{M} & \mathbf{D}^{-1} + \mathbf{D}^{-1}\mathbf{C}\mathbf{M}\mathbf{B}\mathbf{D}^{-1} \end{pmatrix} \tag{2.76}$$

where we have defined

$$\mathbf{M} = (\mathbf{A} - \mathbf{B}\mathbf{D}^{-1}\mathbf{C})^{-1}. \tag{2.77}$$

The quantity $\mathbf{M}^{-1}$ is known as the *Schur complement* of the matrix on the left-hand side of (2.76) with respect to the submatrix $\mathbf{D}$. Using the definition

$$\begin{pmatrix} \boldsymbol{\Sigma}_{aa} & \boldsymbol{\Sigma}_{ab} \\ \boldsymbol{\Sigma}_{ba} & \boldsymbol{\Sigma}_{bb} \end{pmatrix}^{-1} = \begin{pmatrix} \boldsymbol{\Lambda}_{aa} & \boldsymbol{\Lambda}_{ab} \\ \boldsymbol{\Lambda}_{ba} & \boldsymbol{\Lambda}_{bb} \end{pmatrix} \tag{2.78}$$

and making use of (2.76), we have

$$\boldsymbol{\Lambda}_{aa} = (\boldsymbol{\Sigma}_{aa} - \boldsymbol{\Sigma}_{ab}\boldsymbol{\Sigma}_{bb}^{-1}\boldsymbol{\Sigma}_{ba})^{-1} \tag{2.79}$$

$$\boldsymbol{\Lambda}_{ab} = -(\boldsymbol{\Sigma}_{aa} - \boldsymbol{\Sigma}_{ab}\boldsymbol{\Sigma}_{bb}^{-1}\boldsymbol{\Sigma}_{ba})^{-1}\boldsymbol{\Sigma}_{ab}\boldsymbol{\Sigma}_{bb}^{-1}. \tag{2.80}$$

From these we obtain the following expressions for the mean and covariance of the conditional distribution $p(\mathbf{x}_a|\mathbf{x}_b)$

$$\boldsymbol{\mu}_{a|b} = \boldsymbol{\mu}_a + \boldsymbol{\Sigma}_{ab}\boldsymbol{\Sigma}_{bb}^{-1}(\mathbf{x}_b - \boldsymbol{\mu}_b) \tag{2.81}$$

$$\boldsymbol{\Sigma}_{a|b} = \boldsymbol{\Sigma}_{aa} - \boldsymbol{\Sigma}_{ab}\boldsymbol{\Sigma}_{bb}^{-1}\boldsymbol{\Sigma}_{ba}. \tag{2.82}$$

Comparing (2.73) and (2.82), we see that the conditional distribution $p(\mathbf{x}_a|\mathbf{x}_b)$ takes a simpler form when expressed in terms of the partitioned precision matrix than when it is expressed in terms of the partitioned covariance matrix. Note that the mean of the conditional distribution $p(\mathbf{x}_a|\mathbf{x}_b)$, given by (2.81), is a linear function of $\mathbf{x}_b$ and that the covariance, given by (2.82), is independent of $\mathbf{x}_a$. This represents an example of a *linear-Gaussian* model.

Section 8.1.4

2.3.2 Marginal Gaussian distributions

We have seen that if a joint distribution $p(\mathbf{x}_a, \mathbf{x}_b)$ is Gaussian, then the conditional distribution $p(\mathbf{x}_a|\mathbf{x}_b)$ will again be Gaussian. Now we turn to a discussion of the marginal distribution given by

$$p(\mathbf{x}_a) = \int p(\mathbf{x}_a, \mathbf{x}_b)\,\mathrm{d}\mathbf{x}_b \tag{2.83}$$

which, as we shall see, is also Gaussian. Once again, our strategy for evaluating this distribution efficiently will be to focus on the quadratic form in the exponent of the joint distribution and thereby to identify the mean and covariance of the marginal distribution $p(\mathbf{x}_a)$.

The quadratic form for the joint distribution can be expressed, using the partitioned precision matrix, in the form (2.70). Because our goal is to integrate out $\mathbf{x}_b$, this is most easily achieved by first considering the terms involving $\mathbf{x}_b$ and then completing the square in order to facilitate integration. Picking out just those terms that involve $\mathbf{x}_b$, we have

$$-\frac{1}{2}\mathbf{x}_b^{\mathrm{T}}\mathbf{\Lambda}_{bb}\mathbf{x}_b + \mathbf{x}_b^{T}\mathbf{m} = -\frac{1}{2}(\mathbf{x}_b - \mathbf{\Lambda}_{bb}^{-1}\mathbf{m})^{\mathrm{T}}\mathbf{\Lambda}_{bb}(\mathbf{x}_b - \mathbf{\Lambda}_{bb}^{-1}\mathbf{m}) + \frac{1}{2}\mathbf{m}^{\mathrm{T}}\mathbf{\Lambda}_{bb}^{-1}\mathbf{m} \tag{2.84}$$

where we have defined

$$\mathbf{m} = \mathbf{\Lambda}_{bb}\boldsymbol{\mu}_b - \mathbf{\Lambda}_{ba}(\mathbf{x}_a - \boldsymbol{\mu}_a). \tag{2.85}$$

We see that the dependence on $\mathbf{x}_b$ has been cast into the standard quadratic form of a Gaussian distribution corresponding to the first term on the right-hand side of (2.84), plus a term that does not depend on $\mathbf{x}_b$ (but that does depend on $\mathbf{x}_a$). Thus, when we take the exponential of this quadratic form, we see that the integration over $\mathbf{x}_b$ required by (2.83) will take the form

$$\int \exp\left\{-\frac{1}{2}(\mathbf{x}_b - \mathbf{\Lambda}_{bb}^{-1}\mathbf{m})^{\mathrm{T}}\mathbf{\Lambda}_{bb}(\mathbf{x}_b - \mathbf{\Lambda}_{bb}^{-1}\mathbf{m})\right\}\mathrm{d}\mathbf{x}_b. \tag{2.86}$$

This integration is easily performed by noting that it is the integral over an unnormalized Gaussian, and so the result will be the reciprocal of the normalization coefficient. We know from the form of the normalized Gaussian given by (2.43), that this coefficient is independent of the mean and depends only on the determinant of the covariance matrix. Thus, by completing the square with respect to $\mathbf{x}_b$, we can integrate out $\mathbf{x}_b$ and the only term remaining from the contributions on the left-hand side of (2.84) that depends on $\mathbf{x}_a$ is the last term on the right-hand side of (2.84) in which $\mathbf{m}$ is given by (2.85). Combining this term with the remaining terms from

(2.70) that depend on $\mathbf{x}_a$, we obtain

$$\begin{aligned}
&\frac{1}{2}\left[\boldsymbol{\Lambda}_{bb}\boldsymbol{\mu}_b - \boldsymbol{\Lambda}_{ba}(\mathbf{x}_a - \boldsymbol{\mu}_a)\right]^{\mathrm{T}} \boldsymbol{\Lambda}_{bb}^{-1}\left[\boldsymbol{\Lambda}_{bb}\boldsymbol{\mu}_b - \boldsymbol{\Lambda}_{ba}(\mathbf{x}_a - \boldsymbol{\mu}_a)\right] \\
&\qquad -\frac{1}{2}\mathbf{x}_a^{\mathrm{T}}\boldsymbol{\Lambda}_{aa}\mathbf{x}_a + \mathbf{x}_a^{\mathrm{T}}(\boldsymbol{\Lambda}_{aa}\boldsymbol{\mu}_a + \boldsymbol{\Lambda}_{ab}\boldsymbol{\mu}_b) + \text{const} \\
&= -\frac{1}{2}\mathbf{x}_a^{\mathrm{T}}(\boldsymbol{\Lambda}_{aa} - \boldsymbol{\Lambda}_{ab}\boldsymbol{\Lambda}_{bb}^{-1}\boldsymbol{\Lambda}_{ba})\mathbf{x}_a \\
&\qquad +\mathbf{x}_a^{\mathrm{T}}(\boldsymbol{\Lambda}_{aa} - \boldsymbol{\Lambda}_{ab}\boldsymbol{\Lambda}_{bb}^{-1}\boldsymbol{\Lambda}_{ba})^{-1}\boldsymbol{\mu}_a + \text{const}
\end{aligned} \tag{2.87}$$

where 'const' denotes quantities independent of $\mathbf{x}_a$. Again, by comparison with (2.71), we see that the covariance of the marginal distribution of $p(\mathbf{x}_a)$ is given by

$$\boldsymbol{\Sigma}_a = (\boldsymbol{\Lambda}_{aa} - \boldsymbol{\Lambda}_{ab}\boldsymbol{\Lambda}_{bb}^{-1}\boldsymbol{\Lambda}_{ba})^{-1}. \tag{2.88}$$

Similarly, the mean is given by

$$\boldsymbol{\Sigma}_a(\boldsymbol{\Lambda}_{aa} - \boldsymbol{\Lambda}_{ab}\boldsymbol{\Lambda}_{bb}^{-1}\boldsymbol{\Lambda}_{ba})\boldsymbol{\mu}_a = \boldsymbol{\mu}_a \tag{2.89}$$

where we have used (2.88). The covariance in (2.88) is expressed in terms of the partitioned precision matrix given by (2.69). We can rewrite this in terms of the corresponding partitioning of the covariance matrix given by (2.67), as we did for the conditional distribution. These partitioned matrices are related by

$$\begin{pmatrix} \boldsymbol{\Lambda}_{aa} & \boldsymbol{\Lambda}_{ab} \\ \boldsymbol{\Lambda}_{ba} & \boldsymbol{\Lambda}_{bb} \end{pmatrix}^{-1} = \begin{pmatrix} \boldsymbol{\Sigma}_{aa} & \boldsymbol{\Sigma}_{ab} \\ \boldsymbol{\Sigma}_{ba} & \boldsymbol{\Sigma}_{bb} \end{pmatrix} \tag{2.90}$$

Making use of (2.76), we then have

$$\left(\boldsymbol{\Lambda}_{aa} - \boldsymbol{\Lambda}_{ab}\boldsymbol{\Lambda}_{bb}^{-1}\boldsymbol{\Lambda}_{ba}\right)^{-1} = \boldsymbol{\Sigma}_{aa}. \tag{2.91}$$

Thus we obtain the intuitively satisfying result that the marginal distribution $p(\mathbf{x}_a)$ has mean and covariance given by

$$\mathbb{E}[\mathbf{x}_a] = \boldsymbol{\mu}_a \tag{2.92}$$
$$\operatorname{cov}[\mathbf{x}_a] = \boldsymbol{\Sigma}_{aa}. \tag{2.93}$$

We see that for a marginal distribution, the mean and covariance are most simply expressed in terms of the partitioned covariance matrix, in contrast to the conditional distribution for which the partitioned precision matrix gives rise to simpler expressions.

Our results for the marginal and conditional distributions of a partitioned Gaussian are summarized below.

Partitioned Gaussians

Given a joint Gaussian distribution $\mathcal{N}(\mathbf{x}|\boldsymbol{\mu}, \boldsymbol{\Sigma})$ with $\boldsymbol{\Lambda} \equiv \boldsymbol{\Sigma}^{-1}$ and

$$\mathbf{x} = \begin{pmatrix} \mathbf{x}_a \\ \mathbf{x}_b \end{pmatrix}, \quad \boldsymbol{\mu} = \begin{pmatrix} \boldsymbol{\mu}_a \\ \boldsymbol{\mu}_b \end{pmatrix} \tag{2.94}$$

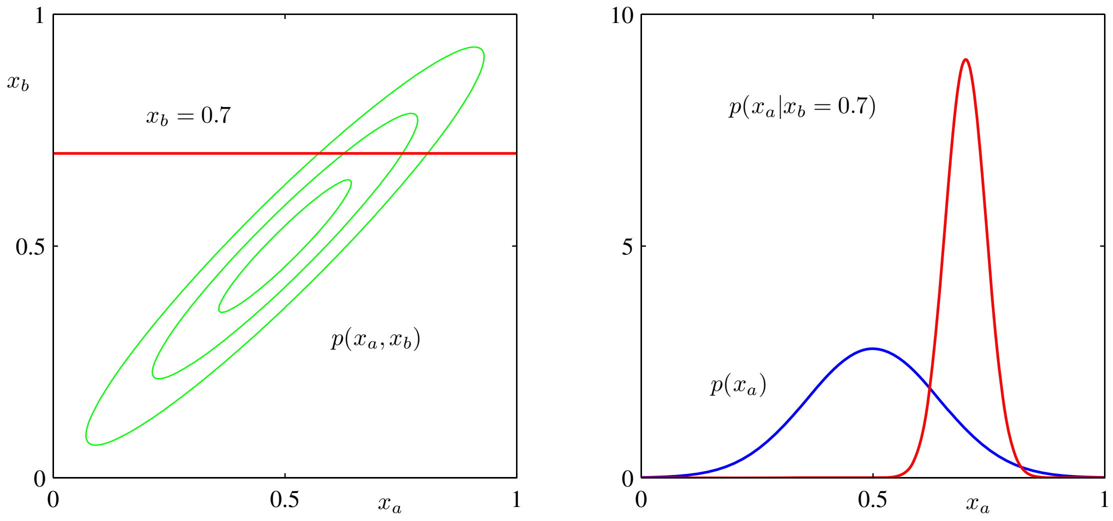

Figure 2.9 The plot on the left shows the contours of a Gaussian distribution $p(x_a, x_b)$ over two variables, and the plot on the right shows the marginal distribution $p(x_a)$ (blue curve) and the conditional distribution $p(x_a|x_b)$ for $x_b = 0.7$ (red curve).

$$\boldsymbol{\Sigma} = \begin{pmatrix} \boldsymbol{\Sigma}_{aa} & \boldsymbol{\Sigma}_{ab} \\ \boldsymbol{\Sigma}_{ba} & \boldsymbol{\Sigma}_{bb} \end{pmatrix}, \qquad \boldsymbol{\Lambda} = \begin{pmatrix} \boldsymbol{\Lambda}_{aa} & \boldsymbol{\Lambda}_{ab} \\ \boldsymbol{\Lambda}_{ba} & \boldsymbol{\Lambda}_{bb} \end{pmatrix}. \tag{2.95}$$

Conditional distribution:

$$p(\mathbf{x}_a|\mathbf{x}_b) = \mathcal{N}(\mathbf{x}|\boldsymbol{\mu}_{a|b}, \boldsymbol{\Lambda}_{aa}^{-1}) \tag{2.96}$$

$$\boldsymbol{\mu}_{a|b} = \boldsymbol{\mu}_a - \boldsymbol{\Lambda}_{aa}^{-1}\boldsymbol{\Lambda}_{ab}(\mathbf{x}_b - \boldsymbol{\mu}_b). \tag{2.97}$$

Marginal distribution:

$$p(\mathbf{x}_a) = \mathcal{N}(\mathbf{x}_a|\boldsymbol{\mu}_a, \boldsymbol{\Sigma}_{aa}). \tag{2.98}$$

We illustrate the idea of conditional and marginal distributions associated with a multivariate Gaussian using an example involving two variables in Figure 2.9.

2.3.3 Bayes' theorem for Gaussian variables

In Sections 2.3.1 and 2.3.2, we considered a Gaussian $p(\mathbf{x})$ in which we partitioned the vector $\mathbf{x}$ into two subvectors $\mathbf{x} = (\mathbf{x}_a, \mathbf{x}_b)$ and then found expressions for the conditional distribution $p(\mathbf{x}_a|\mathbf{x}_b)$ and the marginal distribution $p(\mathbf{x}_a)$. We noted that the mean of the conditional distribution $p(\mathbf{x}_a|\mathbf{x}_b)$ was a linear function of $\mathbf{x}_b$. Here we shall suppose that we are given a Gaussian marginal distribution $p(\mathbf{x})$ and a Gaussian conditional distribution $p(\mathbf{y}|\mathbf{x})$ in which $p(\mathbf{y}|\mathbf{x})$ has a mean that is a linear function of $\mathbf{x}$, and a covariance which is independent of $\mathbf{x}$. This is an example of a *linear Gaussian model* (Roweis and Ghahramani, 1999), which we shall study in greater generality in Section 8.1.4. We wish to find the marginal distribution $p(\mathbf{y})$ and the conditional distribution $p(\mathbf{x}|\mathbf{y})$. This is a problem that will arise frequently in subsequent chapters, and it will prove convenient to derive the general results here.

We shall take the marginal and conditional distributions to be

$$\begin{aligned} p(\mathbf{x}) &= \mathcal{N}\left(\mathbf{x}|\boldsymbol{\mu}, \boldsymbol{\Lambda}^{-1}\right) && (2.99)\\ p(\mathbf{y}|\mathbf{x}) &= \mathcal{N}\left(\mathbf{y}|\mathbf{A}\mathbf{x}+\mathbf{b}, \mathbf{L}^{-1}\right) && (2.100)\end{aligned}$$

where $\boldsymbol{\mu}$, $\mathbf{A}$, and $\mathbf{b}$ are parameters governing the means, and $\boldsymbol{\Lambda}$ and $\mathbf{L}$ are precision matrices. If $\mathbf{x}$ has dimensionality M and $\mathbf{y}$ has dimensionality D, then the matrix $\mathbf{A}$ has size $D \times M$.

First we find an expression for the joint distribution over $\mathbf{x}$ and $\mathbf{y}$. To do this, we define

$$\mathbf{z} = \begin{pmatrix} \mathbf{x} \\ \mathbf{y} \end{pmatrix} \tag{2.101}$$

and then consider the log of the joint distribution

$$\begin{aligned} \ln p(\mathbf{z}) &= \ln p(\mathbf{x}) + \ln p(\mathbf{y}|\mathbf{x}) \\ &= -\frac{1}{2}(\mathbf{x}-\boldsymbol{\mu})^{\mathrm{T}}\boldsymbol{\Lambda}(\mathbf{x}-\boldsymbol{\mu}) \\ &\quad -\frac{1}{2}(\mathbf{y}-\mathbf{A}\mathbf{x}-\mathbf{b})^{\mathrm{T}}\mathbf{L}(\mathbf{y}-\mathbf{A}\mathbf{x}-\mathbf{b}) + \text{const} && (2.102)\end{aligned}$$

where 'const' denotes terms independent of $\mathbf{x}$ and $\mathbf{y}$. As before, we see that this is a quadratic function of the components of $\mathbf{z}$, and hence $p(\mathbf{z})$ is Gaussian distribution. To find the precision of this Gaussian, we consider the second order terms in (2.102), which can be written as

$$\begin{aligned} &-\frac{1}{2}\mathbf{x}^{\mathrm{T}}(\boldsymbol{\Lambda}+\mathbf{A}^{\mathrm{T}}\mathbf{L}\mathbf{A})\mathbf{x} - \frac{1}{2}\mathbf{y}^{\mathrm{T}}\mathbf{L}\mathbf{y} + \frac{1}{2}\mathbf{y}^{\mathrm{T}}\mathbf{L}\mathbf{A}\mathbf{x} + \frac{1}{2}\mathbf{x}^{\mathrm{T}}\mathbf{A}^{\mathrm{T}}\mathbf{L}\mathbf{y} \\ &= -\frac{1}{2}\begin{pmatrix} \mathbf{x} \\ \mathbf{y} \end{pmatrix}^{\mathrm{T}} \begin{pmatrix} \boldsymbol{\Lambda}+\mathbf{A}^{\mathrm{T}}\mathbf{L}\mathbf{A} & -\mathbf{A}^{\mathrm{T}}\mathbf{L} \\ -\mathbf{L}\mathbf{A} & \mathbf{L} \end{pmatrix} \begin{pmatrix} \mathbf{x} \\ \mathbf{y} \end{pmatrix} = -\frac{1}{2}\mathbf{z}^{\mathrm{T}}\mathbf{R}\mathbf{z} && (2.103)\end{aligned}$$

and so the Gaussian distribution over $\mathbf{z}$ has precision (inverse covariance) matrix given by

$$\mathbf{R} = \begin{pmatrix} \boldsymbol{\Lambda}+\mathbf{A}^{\mathrm{T}}\mathbf{L}\mathbf{A} & -\mathbf{A}^{\mathrm{T}}\mathbf{L} \\ -\mathbf{L}\mathbf{A} & \mathbf{L} \end{pmatrix}. \tag{2.104}$$

Exercise 2.29

The covariance matrix is found by taking the inverse of the precision, which can be done using the matrix inversion formula (2.76) to give

$$\operatorname{cov}[\mathbf{z}] = \mathbf{R}^{-1} = \begin{pmatrix} \boldsymbol{\Lambda}^{-1} & \boldsymbol{\Lambda}^{-1}\mathbf{A}^{\mathrm{T}} \\ \mathbf{A}\boldsymbol{\Lambda}^{-1} & \mathbf{L}^{-1}+\mathbf{A}\boldsymbol{\Lambda}^{-1}\mathbf{A}^{\mathrm{T}} \end{pmatrix}. \tag{2.105}$$

Similarly, we can find the mean of the Gaussian distribution over $\mathbf{z}$ by identifying the linear terms in (2.102), which are given by

$$\mathbf{x}^{\mathrm{T}}\boldsymbol{\Lambda}\boldsymbol{\mu} - \mathbf{x}^{\mathrm{T}}\mathbf{A}^{\mathrm{T}}\mathbf{L}\mathbf{b} + \mathbf{y}^{\mathrm{T}}\mathbf{L}\mathbf{b} = \begin{pmatrix} \mathbf{x} \\ \mathbf{y} \end{pmatrix}^{\mathrm{T}} \begin{pmatrix} \boldsymbol{\Lambda}\boldsymbol{\mu} - \mathbf{A}^{\mathrm{T}}\mathbf{L}\mathbf{b} \\ \mathbf{L}\mathbf{b} \end{pmatrix}. \tag{2.106}$$

Using our earlier result (2.71) obtained by completing the square over the quadratic form of a multivariate Gaussian, we find that the mean of $\mathbf{z}$ is given by

$$\mathbb{E}[\mathbf{z}] = \mathbf{R}^{-1} \begin{pmatrix} \boldsymbol{\Lambda}\boldsymbol{\mu} - \mathbf{A}^{\mathrm{T}}\mathbf{L}\mathbf{b} \\ \mathbf{L}\mathbf{b} \end{pmatrix}. \tag{2.107}$$

Exercise 2.30

Making use of (2.105), we then obtain

$$\mathbb{E}[\mathbf{z}] = \begin{pmatrix} \boldsymbol{\mu} \\ \mathbf{A}\boldsymbol{\mu} + \mathbf{b} \end{pmatrix}. \tag{2.108}$$

Section 2.3

Next we find an expression for the marginal distribution $p(\mathbf{y})$ in which we have marginalized over $\mathbf{x}$. Recall that the marginal distribution over a subset of the components of a Gaussian random vector takes a particularly simple form when expressed in terms of the partitioned covariance matrix. Specifically, its mean and covariance are given by (2.92) and (2.93), respectively. Making use of (2.105) and (2.108) we see that the mean and covariance of the marginal distribution $p(\mathbf{y})$ are given by

$$\begin{aligned} \mathbb{E}[\mathbf{y}] &= \mathbf{A}\boldsymbol{\mu} + \mathbf{b} & (2.109) \\ \operatorname{cov}[\mathbf{y}] &= \mathbf{L}^{-1} + \mathbf{A}\boldsymbol{\Lambda}^{-1}\mathbf{A}^{\mathrm{T}}. & (2.110) \end{aligned}$$

A special case of this result is when $\mathbf{A} = \mathbf{I}$, in which case it reduces to the convolution of two Gaussians, for which we see that the mean of the convolution is the sum of the mean of the two Gaussians, and the covariance of the convolution is the sum of their covariances.

Section 2.3

Finally, we seek an expression for the conditional $p(\mathbf{x}|\mathbf{y})$. Recall that the results for the conditional distribution are most easily expressed in terms of the partitioned precision matrix, using (2.73) and (2.75). Applying these results to (2.105) and (2.108) we see that the conditional distribution $p(\mathbf{x}|\mathbf{y})$ has mean and covariance given by

$$\begin{aligned} \mathbb{E}[\mathbf{x}|\mathbf{y}] &= (\boldsymbol{\Lambda} + \mathbf{A}^{\mathrm{T}}\mathbf{L}\mathbf{A})^{-1}\left\{\mathbf{A}^{\mathrm{T}}\mathbf{L}(\mathbf{y} - \mathbf{b}) + \boldsymbol{\Lambda}\boldsymbol{\mu}\right\} & (2.111) \\ \operatorname{cov}[\mathbf{x}|\mathbf{y}] &= (\boldsymbol{\Lambda} + \mathbf{A}^{\mathrm{T}}\mathbf{L}\mathbf{A})^{-1}. & (2.112) \end{aligned}$$

The evaluation of this conditional can be seen as an example of Bayes' theorem. We can interpret the distribution $p(\mathbf{x})$ as a prior distribution over $\mathbf{x}$. If the variable $\mathbf{y}$ is observed, then the conditional distribution $p(\mathbf{x}|\mathbf{y})$ represents the corresponding posterior distribution over $\mathbf{x}$. Having found the marginal and conditional distributions, we effectively expressed the joint distribution $p(\mathbf{z}) = p(\mathbf{x})p(\mathbf{y}|\mathbf{x})$ in the form $p(\mathbf{x}|\mathbf{y})p(\mathbf{y})$. These results are summarized below.

Marginal and Conditional Gaussians

Given a marginal Gaussian distribution for $\mathbf{x}$ and a conditional Gaussian distribution for $\mathbf{y}$ given $\mathbf{x}$ in the form

$$p(\mathbf{x}) = \mathcal{N}(\mathbf{x}|\boldsymbol{\mu}, \boldsymbol{\Lambda}^{-1}) \tag{2.113}$$
$$p(\mathbf{y}|\mathbf{x}) = \mathcal{N}(\mathbf{y}|\mathbf{A}\mathbf{x}+\mathbf{b}, \mathbf{L}^{-1}) \tag{2.114}$$

the marginal distribution of $\mathbf{y}$ and the conditional distribution of $\mathbf{x}$ given $\mathbf{y}$ are given by

$$p(\mathbf{y}) = \mathcal{N}(\mathbf{y}|\mathbf{A}\boldsymbol{\mu}+\mathbf{b}, \mathbf{L}^{-1}+\mathbf{A}\boldsymbol{\Lambda}^{-1}\mathbf{A}^{\mathrm{T}}) \tag{2.115}$$
$$p(\mathbf{x}|\mathbf{y}) = \mathcal{N}(\mathbf{x}|\boldsymbol{\Sigma}\{\mathbf{A}^{\mathrm{T}}\mathbf{L}(\mathbf{y}-\mathbf{b})+\boldsymbol{\Lambda}\boldsymbol{\mu}\}, \boldsymbol{\Sigma}) \tag{2.116}$$

where

$$\boldsymbol{\Sigma} = (\boldsymbol{\Lambda}+\mathbf{A}^{\mathrm{T}}\mathbf{L}\mathbf{A})^{-1}. \tag{2.117}$$

2.3.4 Maximum likelihood for the Gaussian

Given a data set $\mathbf{X} = (\mathbf{x}_1, \ldots, \mathbf{x}_N)^{\mathrm{T}}$ in which the observations $\{\mathbf{x}_n\}$ are assumed to be drawn independently from a multivariate Gaussian distribution, we can estimate the parameters of the distribution by maximum likelihood. The log likelihood function is given by

$$\ln p(\mathbf{X}|\boldsymbol{\mu}, \boldsymbol{\Sigma}) = -\frac{ND}{2}\ln(2\pi) - \frac{N}{2}\ln|\boldsymbol{\Sigma}| - \frac{1}{2}\sum_{n=1}^{N}(\mathbf{x}_n-\boldsymbol{\mu})^{\mathrm{T}}\boldsymbol{\Sigma}^{-1}(\mathbf{x}_n-\boldsymbol{\mu}). \tag{2.118}$$

By simple rearrangement, we see that the likelihood function depends on the data set only through the two quantities

$$\sum_{n=1}^{N}\mathbf{x}_n, \qquad \sum_{n=1}^{N}\mathbf{x}_n\mathbf{x}_n^{\mathrm{T}}. \tag{2.119}$$

Appendix C

These are known as the *sufficient statistics* for the Gaussian distribution. Using (C.19), the derivative of the log likelihood with respect to $\boldsymbol{\mu}$ is given by

$$\frac{\partial}{\partial \boldsymbol{\mu}}\ln p(\mathbf{X}|\boldsymbol{\mu}, \boldsymbol{\Sigma}) = \sum_{n=1}^{N}\boldsymbol{\Sigma}^{-1}(\mathbf{x}_n-\boldsymbol{\mu}) \tag{2.120}$$

and setting this derivative to zero, we obtain the solution for the maximum likelihood estimate of the mean given by

$$\boldsymbol{\mu}_{\mathrm{ML}} = \frac{1}{N}\sum_{n=1}^{N}\mathbf{x}_n \tag{2.121}$$

which is the mean of the observed set of data points. The maximization of (2.118) with respect to $\boldsymbol{\Sigma}$ is rather more involved. The simplest approach is to ignore the symmetry constraint and show that the resulting solution is symmetric as required. *Exercise 2.34* Alternative derivations of this result, which impose the symmetry and positive definiteness constraints explicitly, can be found in Magnus and Neudecker (1999). The result is as expected and takes the form

$$\boldsymbol{\Sigma}_{\mathrm{ML}} = \frac{1}{N}\sum_{n=1}^{N}(\mathbf{x}_n - \boldsymbol{\mu}_{\mathrm{ML}})(\mathbf{x}_n - \boldsymbol{\mu}_{\mathrm{ML}})^{\mathrm{T}} \tag{2.122}$$

which involves $\boldsymbol{\mu}_{\mathrm{ML}}$ because this is the result of a joint maximization with respect to $\boldsymbol{\mu}$ and $\boldsymbol{\Sigma}$. Note that the solution (2.121) for $\boldsymbol{\mu}_{\mathrm{ML}}$ does not depend on $\boldsymbol{\Sigma}_{\mathrm{ML}}$, and so we can first evaluate $\boldsymbol{\mu}_{\mathrm{ML}}$ and then use this to evaluate $\boldsymbol{\Sigma}_{\mathrm{ML}}$.

If we evaluate the expectations of the maximum likelihood solutions under the true distribution, we obtain the following results *Exercise 2.35*

$$\mathbb{E}[\boldsymbol{\mu}_{\mathrm{ML}}] = \boldsymbol{\mu} \tag{2.123}$$

$$\mathbb{E}[\boldsymbol{\Sigma}_{\mathrm{ML}}] = \frac{N-1}{N}\boldsymbol{\Sigma}. \tag{2.124}$$

We see that the expectation of the maximum likelihood estimate for the mean is equal to the true mean. However, the maximum likelihood estimate for the covariance has an expectation that is less than the true value, and hence it is biased. We can correct this bias by defining a different estimator $\widetilde{\boldsymbol{\Sigma}}$ given by

$$\widetilde{\boldsymbol{\Sigma}} = \frac{1}{N-1}\sum_{n=1}^{N}(\mathbf{x}_n - \boldsymbol{\mu}_{\mathrm{ML}})(\mathbf{x}_n - \boldsymbol{\mu}_{\mathrm{ML}})^{\mathrm{T}}. \tag{2.125}$$

Clearly from (2.122) and (2.124), the expectation of $\widetilde{\boldsymbol{\Sigma}}$ is equal to $\boldsymbol{\Sigma}$.

2.3.5 Sequential estimation

Our discussion of the maximum likelihood solution for the parameters of a Gaussian distribution provides a convenient opportunity to give a more general discussion of the topic of sequential estimation for maximum likelihood. Sequential methods allow data points to be processed one at a time and then discarded and are important for on-line applications, and also where large data sets are involved so that batch processing of all data points at once is infeasible.

Consider the result (2.121) for the maximum likelihood estimator of the mean $\boldsymbol{\mu}_{\mathrm{ML}}$, which we will denote by $\boldsymbol{\mu}_{\mathrm{ML}}^{(N)}$ when it is based on N observations. If we

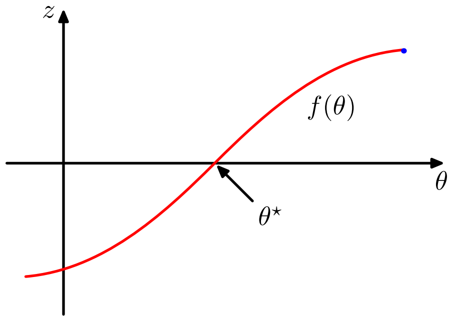

Figure 2.10 A schematic illustration of two correlated random variables z and θ, together with the regression function $f(\theta)$ given by the conditional expectation $\mathbb{E}[z|\theta]$. The Robbins-Monro algorithm provides a general sequential procedure for finding the root $\theta^\star$ of such functions.

dissect out the contribution from the final data point $\mathbf{x}_N$, we obtain

$$\begin{aligned}
\boldsymbol{\mu}_{\mathrm{ML}}^{(N)} &= \frac{1}{N}\sum_{n=1}^{N}\mathbf{x}_n \\
&= \frac{1}{N}\mathbf{x}_N + \frac{1}{N}\sum_{n=1}^{N-1}\mathbf{x}_n \\
&= \frac{1}{N}\mathbf{x}_N + \frac{N-1}{N}\boldsymbol{\mu}_{\mathrm{ML}}^{(N-1)} \\
&= \boldsymbol{\mu}_{\mathrm{ML}}^{(N-1)} + \frac{1}{N}(\mathbf{x}_N - \boldsymbol{\mu}_{\mathrm{ML}}^{(N-1)}).
\end{aligned} \tag{2.126}$$

This result has a nice interpretation, as follows. After observing $N-1$ data points we have estimated $\boldsymbol{\mu}$ by $\boldsymbol{\mu}_{\mathrm{ML}}^{(N-1)}$. We now observe data point $\mathbf{x}_N$, and we obtain our revised estimate $\boldsymbol{\mu}_{\mathrm{ML}}^{(N)}$ by moving the old estimate a small amount, proportional to $1/N$, in the direction of the 'error signal' $(\mathbf{x}_N - \boldsymbol{\mu}_{\mathrm{ML}}^{(N-1)})$. Note that, as N increases, so the contribution from successive data points gets smaller.

The result (2.126) will clearly give the same answer as the batch result (2.121) because the two formulae are equivalent. However, we will not always be able to derive a sequential algorithm by this route, and so we seek a more general formulation of sequential learning, which leads us to the *Robbins-Monro* algorithm. Consider a pair of random variables θ and z governed by a joint distribution $p(z, \theta)$. The conditional expectation of z given θ defines a deterministic function $f(\theta)$ that is given by

$$f(\theta) \equiv \mathbb{E}[z|\theta] = \int zp(z|\theta)\,\mathrm{d}z \tag{2.127}$$

and is illustrated schematically in Figure 2.10. Functions defined in this way are called *regression functions*.

Our goal is to find the root $\theta^\star$ at which $f(\theta^\star) = 0$. If we had a large data set of observations of z and θ, then we could model the regression function directly and then obtain an estimate of its root. Suppose, however, that we observe values of z one at a time and we wish to find a corresponding sequential estimation scheme for $\theta^\star$. The following general procedure for solving such problems was given by

Robbins and Monro (1951). We shall assume that the conditional variance of z is finite so that

$$\mathbb{E}\left[(z-f)^2 \mid \theta\right] < \infty \tag{2.128}$$

and we shall also, without loss of generality, consider the case where $f(\theta) > 0$ for $\theta > \theta^\star$ and $f(\theta) < 0$ for $\theta < \theta^\star$, as is the case in Figure 2.10. The Robbins-Monro procedure then defines a sequence of successive estimates of the root $\theta^\star$ given by

$$\theta^{(N)} = \theta^{(N-1)} + a_{N-1} z(\theta^{(N-1)}) \tag{2.129}$$

where $z(\theta^{(N)})$ is an observed value of z when θ takes the value $\theta^{(N)}$. The coefficients $\{a_N\}$ represent a sequence of positive numbers that satisfy the conditions

$$\lim_{N\to\infty} a_N = 0 \tag{2.130}$$

$$\sum_{N=1}^{\infty} a_N = \infty \tag{2.131}$$

$$\sum_{N=1}^{\infty} a_N^2 < \infty. \tag{2.132}$$

It can then be shown (Robbins and Monro, 1951; Fukunaga, 1990) that the sequence of estimates given by (2.129) does indeed converge to the root with probability one. Note that the first condition (2.130) ensures that the successive corrections decrease in magnitude so that the process can converge to a limiting value. The second condition (2.131) is required to ensure that the algorithm does not converge short of the root, and the third condition (2.132) is needed to ensure that the accumulated noise has finite variance and hence does not spoil convergence.

Now let us consider how a general maximum likelihood problem can be solved sequentially using the Robbins-Monro algorithm. By definition, the maximum likelihood solution θ_{ML} is a stationary point of the log likelihood function and hence satisfies

$$\frac{\partial}{\partial\theta}\left\{\frac{1}{N}\sum_{n=1}^{N}\ln p(\mathbf{x}_n|\theta)\right\}\bigg|_{\theta_{\mathrm{ML}}} = 0. \tag{2.133}$$

Exchanging the derivative and the summation, and taking the limit $N \to \infty$ we have

$$\lim_{N\to\infty}\frac{1}{N}\sum_{n=1}^{N}\frac{\partial}{\partial\theta}\ln p(x_n|\theta) = \mathbb{E}_x\left[\frac{\partial}{\partial\theta}\ln p(x|\theta)\right] \tag{2.134}$$

and so we see that finding the maximum likelihood solution corresponds to finding the root of a regression function. We can therefore apply the Robbins-Monro procedure, which now takes the form

$$\theta^{(N)} = \theta^{(N-1)} + a_{N-1}\frac{\partial}{\partial\theta^{(N-1)}}\ln p(x_N|\theta^{(N-1)}). \tag{2.135}$$

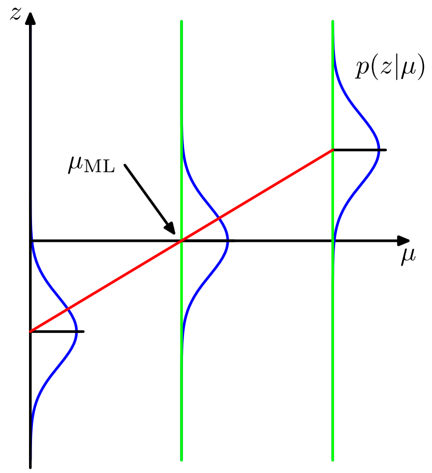

Figure 2.11 In the case of a Gaussian distribution, with θ corresponding to the mean μ, the regression function illustrated in Figure 2.10 takes the form of a straight line, as shown in red. In this case, the random variable z corresponds to the derivative of the log likelihood function and is given by $(x - \mu_{\mathrm{ML}})/\sigma^2$, and its expectation that defines the regression function is a straight line given by $(\mu - \mu_{\mathrm{ML}})/\sigma^2$. The root of the regression function corresponds to the maximum likelihood estimator μ_{ML}.

As a specific example, we consider once again the sequential estimation of the mean of a Gaussian distribution, in which case the parameter $\theta^{(N)}$ is the estimate $\mu_{\mathrm{ML}}^{(N)}$ of the mean of the Gaussian, and the random variable z is given by

$$z = \frac{\partial}{\partial \mu_{\mathrm{ML}}} \ln p(x|\mu_{\mathrm{ML}}, \sigma^2) = \frac{1}{\sigma^2}(x - \mu_{\mathrm{ML}}). \tag{2.136}$$

Thus the distribution of z is Gaussian with mean $\mu - \mu_{\mathrm{ML}}$, as illustrated in Figure 2.11. Substituting (2.136) into (2.135), we obtain the univariate form of (2.126), provided we choose the coefficients a_N to have the form $a_N = \sigma^2/N$. Note that although we have focussed on the case of a single variable, the same technique, together with the same restrictions (2.130)–(2.132) on the coefficients a_N, apply equally to the multivariate case (Blum, 1965).

2.3.6 Bayesian inference for the Gaussian

The maximum likelihood framework gave point estimates for the parameters $\boldsymbol{\mu}$ and $\boldsymbol{\Sigma}$. Now we develop a Bayesian treatment by introducing prior distributions over these parameters. Let us begin with a simple example in which we consider a single Gaussian random variable x. We shall suppose that the variance σ^2 is known, and we consider the task of inferring the mean μ given a set of N observations $\mathbf{X} = \{x_1, \ldots, x_N\}$. The likelihood function, that is the probability of the observed data given μ, viewed as a function of μ, is given by

$$p(\mathbf{X}|\mu) = \prod_{n=1}^{N} p(x_n|\mu) = \frac{1}{(2\pi\sigma^2)^{N/2}} \exp\left\{-\frac{1}{2\sigma^2}\sum_{n=1}^{N}(x_n - \mu)^2\right\}. \tag{2.137}$$

Again we emphasize that the likelihood function $p(\mathbf{X}|\mu)$ is not a probability distribution over μ and is not normalized.

We see that the likelihood function takes the form of the exponential of a quadratic form in μ. Thus if we choose a prior $p(\mu)$ given by a Gaussian, it will be a conjugate distribution for this likelihood function because the corresponding posterior will be a product of two exponentials of quadratic functions of μ and hence will also be Gaussian. We therefore take our prior distribution to be

$$p(\mu) = \mathcal{N}\left(\mu|\mu_0, \sigma_0^2\right) \tag{2.138}$$

and the posterior distribution is given by

$$p(\mu|\mathbf{X}) \propto p(\mathbf{X}|\mu)p(\mu). \tag{2.139}$$

Exercise 2.38

Simple manipulation involving completing the square in the exponent shows that the posterior distribution is given by

$$p(\mu|\mathbf{X}) = \mathcal{N}\left(\mu|\mu_N, \sigma_N^2\right) \tag{2.140}$$

where

$$\mu_N = \frac{\sigma^2}{N\sigma_0^2 + \sigma^2}\mu_0 + \frac{N\sigma_0^2}{N\sigma_0^2 + \sigma^2}\mu_{\mathrm{ML}} \tag{2.141}$$

$$\frac{1}{\sigma_N^2} = \frac{1}{\sigma_0^2} + \frac{N}{\sigma^2} \tag{2.142}$$

in which μ_{ML} is the maximum likelihood solution for μ given by the sample mean

$$\mu_{\mathrm{ML}} = \frac{1}{N}\sum_{n=1}^{N} x_n. \tag{2.143}$$

It is worth spending a moment studying the form of the posterior mean and variance. First of all, we note that the mean of the posterior distribution given by (2.141) is a compromise between the prior mean μ_0 and the maximum likelihood solution μ_{ML}. If the number of observed data points $N = 0$, then (2.141) reduces to the prior mean as expected. For $N \to \infty$, the posterior mean is given by the maximum likelihood solution. Similarly, consider the result (2.142) for the variance of the posterior distribution. We see that this is most naturally expressed in terms of the inverse variance, which is called the precision. Furthermore, the precisions are additive, so that the precision of the posterior is given by the precision of the prior plus one contribution of the data precision from each of the observed data points. As we increase the number of observed data points, the precision steadily increases, corresponding to a posterior distribution with steadily decreasing variance. With no observed data points, we have the prior variance, whereas if the number of data points $N \to \infty$, the variance σ_N^2 goes to zero and the posterior distribution becomes infinitely peaked around the maximum likelihood solution. We therefore see that the maximum likelihood result of a point estimate for μ given by (2.143) is recovered precisely from the Bayesian formalism in the limit of an infinite number of observations. Note also that for finite N, if we take the limit $\sigma_0^2 \to \infty$ in which the prior has infinite variance then the posterior mean (2.141) reduces to the maximum likelihood result, while from (2.142) the posterior variance is given by $\sigma_N^2 = \sigma^2/N$.

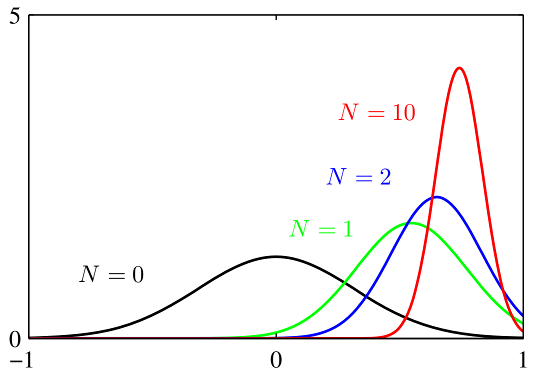

Figure 2.12 Illustration of Bayesian inference for the mean μ of a Gaussian distribution, in which the variance is assumed to be known. The curves show the prior distribution over μ (the curve labelled $N = 0$), which in this case is itself Gaussian, along with the posterior distribution given by (2.140) for increasing numbers N of data points. The data points are generated from a Gaussian of mean 0.8 and variance 0.1, and the prior is chosen to have mean 0. In both the prior and the likelihood function, the variance is set to the true value.

We illustrate our analysis of Bayesian inference for the mean of a Gaussian distribution in Figure 2.12. The generalization of this result to the case of a D-dimensional Gaussian random variable $\mathbf{x}$ with known covariance and unknown mean is straightforward. *Exercise 2.40*

Section 2.3.5 We have already seen how the maximum likelihood expression for the mean of a Gaussian can be re-cast as a sequential update formula in which the mean after observing N data points was expressed in terms of the mean after observing $N-1$ data points together with the contribution from data point $\mathbf{x}_N$. In fact, the Bayesian paradigm leads very naturally to a sequential view of the inference problem. To see this in the context of the inference of the mean of a Gaussian, we write the posterior distribution with the contribution from the final data point $\mathbf{x}_N$ separated out so that

$$p(\boldsymbol{\mu}|D) \propto \left[p(\boldsymbol{\mu}) \prod_{n=1}^{N-1} p(\mathbf{x}_n|\boldsymbol{\mu}) \right] p(\mathbf{x}_N|\boldsymbol{\mu}). \tag{2.144}$$

The term in square brackets is (up to a normalization coefficient) just the posterior distribution after observing $N-1$ data points. We see that this can be viewed as a prior distribution, which is combined using Bayes' theorem with the likelihood function associated with data point $\mathbf{x}_N$ to arrive at the posterior distribution after observing N data points. This sequential view of Bayesian inference is very general and applies to any problem in which the observed data are assumed to be independent and identically distributed.

So far, we have assumed that the variance of the Gaussian distribution over the data is known and our goal is to infer the mean. Now let us suppose that the mean is known and we wish to infer the variance. Again, our calculations will be greatly simplified if we choose a conjugate form for the prior distribution. It turns out to be most convenient to work with the precision $\lambda \equiv 1/\sigma^2$. The likelihood function for λ takes the form

$$p(\mathbf{X}|\lambda) = \prod_{n=1}^{N} \mathcal{N}(x_n|\mu, \lambda^{-1}) \propto \lambda^{N/2} \exp\left\{ -\frac{\lambda}{2} \sum_{n=1}^{N} (x_n - \mu)^2 \right\}. \tag{2.145}$$

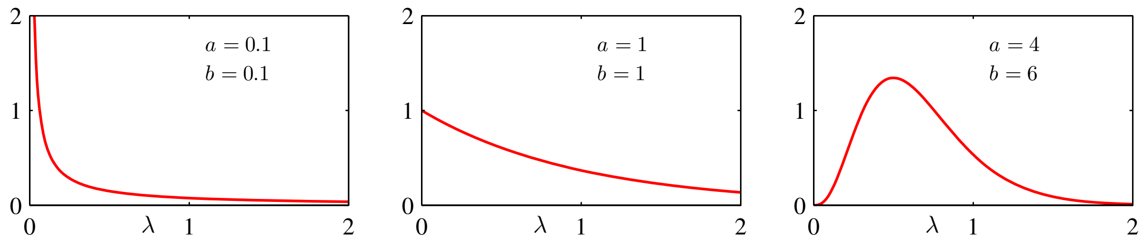

Figure 2.13 Plot of the gamma distribution $\mathrm{Gam}(\lambda|a, b)$ defined by (2.146) for various values of the parameters a and b.

The corresponding conjugate prior should therefore be proportional to the product of a power of λ and the exponential of a linear function of λ. This corresponds to the *gamma* distribution which is defined by

$$\mathrm{Gam}(\lambda|a, b) = \frac{1}{\Gamma(a)} b^a \lambda^{a-1} \exp(-b\lambda). \tag{2.146}$$

Here $\Gamma(a)$ is the gamma function that is defined by (1.141) and that ensures that (2.146) is correctly normalized. The gamma distribution has a finite integral if $a > 0$, and the distribution itself is finite if $a \geqslant 1$. It is plotted, for various values of a and b, in Figure 2.13. The mean and variance of the gamma distribution are given by

Exercise 2.41

Exercise 2.42

$$\mathbb{E}[\lambda] = \frac{a}{b} \tag{2.147}$$

$$\mathrm{var}[\lambda] = \frac{a}{b^2}. \tag{2.148}$$

Consider a prior distribution $\mathrm{Gam}(\lambda|a_0, b_0)$. If we multiply by the likelihood function (2.145), then we obtain a posterior distribution

$$p(\lambda|\mathbf{X}) \propto \lambda^{a_0-1}\lambda^{N/2} \exp\left\{-b_0\lambda - \frac{\lambda}{2}\sum_{n=1}^{N}(x_n - \mu)^2\right\} \tag{2.149}$$

which we recognize as a gamma distribution of the form $\mathrm{Gam}(\lambda|a_N, b_N)$ where

$$a_N = a_0 + \frac{N}{2} \tag{2.150}$$

$$b_N = b_0 + \frac{1}{2}\sum_{n=1}^{N}(x_n - \mu)^2 = b_0 + \frac{N}{2}\sigma^2_{\mathrm{ML}} \tag{2.151}$$

where σ^2_{ML} is the maximum likelihood estimator of the variance. Note that in (2.149) there is no need to keep track of the normalization constants in the prior and the likelihood function because, if required, the correct coefficient can be found at the end using the normalized form (2.146) for the gamma distribution.

From (2.150), we see that the effect of observing N data points is to increase the value of the coefficient a by $N/2$. Thus we can interpret the parameter a_0 in the prior in terms of $2a_0$ 'effective' prior observations. Similarly, from (2.151) we see that the N data points contribute $N\sigma^2_{\mathrm{ML}}/2$ to the parameter b, where σ^2_{ML} is the variance, and so we can interpret the parameter b_0 in the prior as arising from the $2a_0$ 'effective' prior observations having variance $2b_0/(2a_0) = b_0/a_0$. Recall that we made an analogous interpretation for the Dirichlet prior. These distributions are examples of the exponential family, and we shall see that the interpretation of a conjugate prior in terms of effective fictitious data points is a general one for the exponential family of distributions.

Section 2.2

Instead of working with the precision, we can consider the variance itself. The conjugate prior in this case is called the *inverse gamma* distribution, although we shall not discuss this further because we will find it more convenient to work with the precision.

Now suppose that both the mean and the precision are unknown. To find a conjugate prior, we consider the dependence of the likelihood function on μ and λ

$$\begin{aligned} p(\mathbf{X}|\mu,\lambda) &= \prod_{n=1}^{N}\left(\frac{\lambda}{2\pi}\right)^{1/2}\exp\left\{-\frac{\lambda}{2}(x_n-\mu)^2\right\} \\ &\propto \left[\lambda^{1/2}\exp\left(-\frac{\lambda\mu^2}{2}\right)\right]^N \exp\left\{\lambda\mu\sum_{n=1}^{N}x_n - \frac{\lambda}{2}\sum_{n=1}^{N}x_n^2\right\}. \end{aligned} \tag{2.152}$$

We now wish to identify a prior distribution $p(\mu,\lambda)$ that has the same functional dependence on μ and λ as the likelihood function and that should therefore take the form

$$\begin{aligned} p(\mu,\lambda) &\propto \left[\lambda^{1/2}\exp\left(-\frac{\lambda\mu^2}{2}\right)\right]^\beta \exp\left\{c\lambda\mu - d\lambda\right\} \\ &= \exp\left\{-\frac{\beta\lambda}{2}(\mu-c/\beta)^2\right\}\lambda^{\beta/2}\exp\left\{-\left(d-\frac{c^2}{2\beta}\right)\lambda\right\} \end{aligned} \tag{2.153}$$

where c, d, and β are constants. Since we can always write $p(\mu,\lambda) = p(\mu|\lambda)p(\lambda)$, we can find $p(\mu|\lambda)$ and $p(\lambda)$ by inspection. In particular, we see that $p(\mu|\lambda)$ is a Gaussian whose precision is a linear function of λ and that $p(\lambda)$ is a gamma distribution, so that the normalized prior takes the form

$$p(\mu,\lambda) = \mathcal{N}(\mu|\mu_0,(\beta\lambda)^{-1})\mathrm{Gam}(\lambda|a,b) \tag{2.154}$$

where we have defined new constants given by $\mu_0 = c/\beta$, $a = 1+\beta/2$, $b = d-c^2/2\beta$. The distribution (2.154) is called the *normal-gamma* or *Gaussian-gamma* distribution and is plotted in Figure 2.14. Note that this is not simply the product of an independent Gaussian prior over μ and a gamma prior over λ, because the precision of μ is a linear function of λ. Even if we chose a prior in which μ and λ were independent, the posterior distribution would exhibit a coupling between the precision of μ and the value of λ.

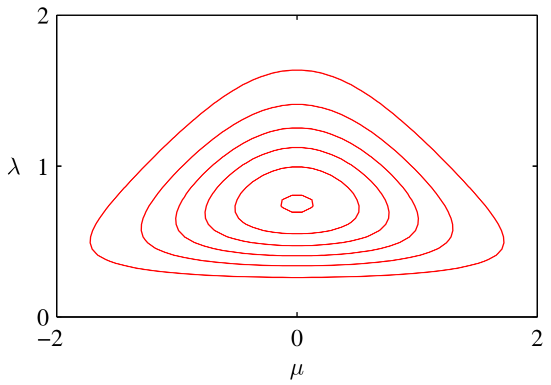

Figure 2.14 Contour plot of the normal-gamma distribution (2.154) for parameter values $\mu_0 = 0$, $\beta = 2$, $a = 5$ and $b = 6$.

In the case of the multivariate Gaussian distribution $\mathcal{N}\left(\mathbf{x}|\boldsymbol{\mu}, \boldsymbol{\Lambda}^{-1}\right)$ for a D-dimensional variable $\mathbf{x}$, the conjugate prior distribution for the mean $\boldsymbol{\mu}$, assuming the precision is known, is again a Gaussian. For known mean and unknown precision matrix $\boldsymbol{\Lambda}$, the conjugate prior is the *Wishart* distribution given by

Exercise 2.45

$$\mathcal{W}(\boldsymbol{\Lambda}|\mathbf{W}, \nu) = B|\boldsymbol{\Lambda}|^{(\nu-D-1)/2} \exp\left(-\frac{1}{2}\mathrm{Tr}(\mathbf{W}^{-1}\boldsymbol{\Lambda})\right) \tag{2.155}$$

where ν is called the number of *degrees of freedom* of the distribution, $\mathbf{W}$ is a $D \times D$ scale matrix, and $\mathrm{Tr}(\cdot)$ denotes the trace. The normalization constant B is given by

$$B(\mathbf{W}, \nu) = |\mathbf{W}|^{-\nu/2} \left(2^{\nu D/2}\, \pi^{D(D-1)/4} \prod_{i=1}^{D} \Gamma\left(\frac{\nu+1-i}{2}\right)\right)^{-1}. \tag{2.156}$$

Again, it is also possible to define a conjugate prior over the covariance matrix itself, rather than over the precision matrix, which leads to the *inverse Wishart* distribution, although we shall not discuss this further. If both the mean and the precision are unknown, then, following a similar line of reasoning to the univariate case, the conjugate prior is given by

$$p(\boldsymbol{\mu}, \boldsymbol{\Lambda}|\boldsymbol{\mu}_0, \beta, \mathbf{W}, \nu) = \mathcal{N}(\boldsymbol{\mu}|\boldsymbol{\mu}_0, (\beta\boldsymbol{\Lambda})^{-1})\, \mathcal{W}(\boldsymbol{\Lambda}|\mathbf{W}, \nu) \tag{2.157}$$

which is known as the *normal-Wishart* or *Gaussian-Wishart* distribution.

2.3.7 Student's t-distribution

We have seen that the conjugate prior for the precision of a Gaussian is given by a gamma distribution. If we have a univariate Gaussian $\mathcal{N}(x|\mu, \tau^{-1})$ together with a Gamma prior $\mathrm{Gam}(\tau|a, b)$ and we integrate out the precision, we obtain the marginal distribution of x in the form

Section 2.3.6

Exercise 2.46

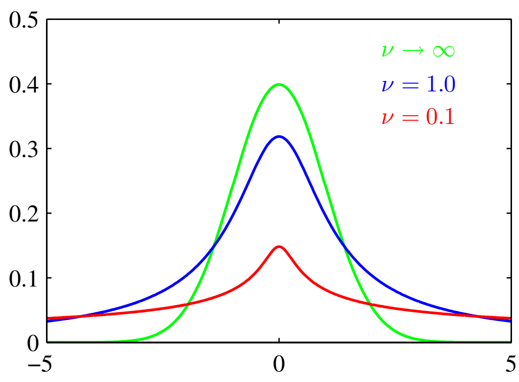

Figure 2.15 Plot of Student's t-distribution (2.159) for $\mu = 0$ and $\lambda = 1$ for various values of ν. The limit $\nu \to \infty$ corresponds to a Gaussian distribution with mean μ and precision λ.

$$\begin{aligned} p(x|\mu, a, b) &= \int_0^\infty \mathcal{N}(x|\mu, \tau^{-1})\mathrm{Gam}(\tau|a, b)\,\mathrm{d}\tau \qquad (2.158)\\ &= \int_0^\infty \frac{b^a e^{(-b\tau)}\tau^{a-1}}{\Gamma(a)} \left(\frac{\tau}{2\pi}\right)^{1/2} \exp\left\{-\frac{\tau}{2}(x-\mu)^2\right\} \mathrm{d}\tau \\ &= \frac{b^a}{\Gamma(a)} \left(\frac{1}{2\pi}\right)^{1/2} \left[b + \frac{(x-\mu)^2}{2}\right]^{-a-1/2} \Gamma(a + 1/2) \end{aligned}$$

where we have made the change of variable $z = \tau[b + (x-\mu)^2/2]$. By convention we define new parameters given by $\nu = 2a$ and $\lambda = a/b$, in terms of which the distribution $p(x|\mu, a, b)$ takes the form

$$\mathrm{St}(x|\mu, \lambda, \nu) = \frac{\Gamma(\nu/2 + 1/2)}{\Gamma(\nu/2)} \left(\frac{\lambda}{\pi\nu}\right)^{1/2} \left[1 + \frac{\lambda(x-\mu)^2}{\nu}\right]^{-\nu/2-1/2} \qquad (2.159)$$

which is known as *Student's t-distribution*. The parameter λ is sometimes called the *precision* of the t-distribution, even though it is not in general equal to the inverse of the variance. The parameter ν is called the *degrees of freedom*, and its effect is illustrated in Figure 2.15. For the particular case of $\nu = 1$, the t-distribution reduces to the *Cauchy* distribution, while in the limit $\nu \to \infty$ the t-distribution $\mathrm{St}(x|\mu, \lambda, \nu)$ becomes a Gaussian $\mathcal{N}(x|\mu, \lambda^{-1})$ with mean μ and precision λ.

Exercise 2.47

From (2.158), we see that Student's t-distribution is obtained by adding up an infinite number of Gaussian distributions having the same mean but different precisions. This can be interpreted as an infinite mixture of Gaussians (Gaussian mixtures will be discussed in detail in Section 2.3.9. The result is a distribution that in general has longer 'tails' than a Gaussian, as was seen in Figure 2.15. This gives the t-distribution an important property called *robustness*, which means that it is much less sensitive than the Gaussian to the presence of a few data points which are *outliers*. The robustness of the t-distribution is illustrated in Figure 2.16, which compares the maximum likelihood solutions for a Gaussian and a t-distribution. Note that the maximum likelihood solution for the t-distribution can be found using the expectation-maximization (EM) algorithm. Here we see that the effect of a small number of

Exercise 12.24

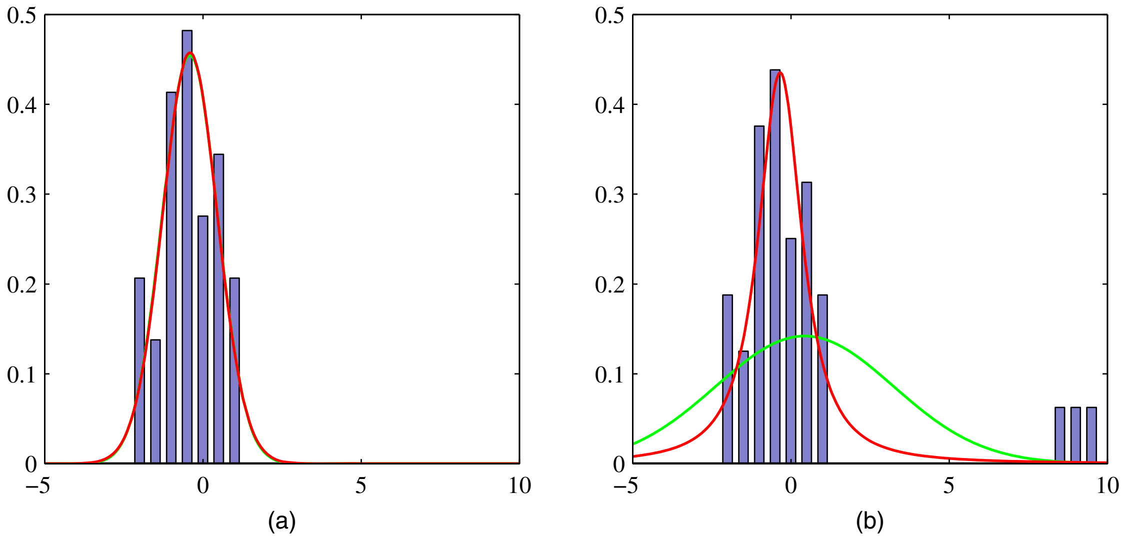

Figure 2.16 Illustration of the robustness of Student's t-distribution compared to a Gaussian. (a) Histogram distribution of 30 data points drawn from a Gaussian distribution, together with the maximum likelihood fit obtained from a t-distribution (red curve) and a Gaussian (green curve, largely hidden by the red curve). Because the t-distribution contains the Gaussian as a special case it gives almost the same solution as the Gaussian. (b) The same data set but with three additional outlying data points showing how the Gaussian (green curve) is strongly distorted by the outliers, whereas the t-distribution (red curve) is relatively unaffected.

outliers is much less significant for the t-distribution than for the Gaussian. Outliers can arise in practical applications either because the process that generates the data corresponds to a distribution having a heavy tail or simply through mislabelled data. Robustness is also an important property for regression problems. Unsurprisingly, the least squares approach to regression does not exhibit robustness, because it corresponds to maximum likelihood under a (conditional) Gaussian distribution. By basing a regression model on a heavy-tailed distribution such as a t-distribution, we obtain a more robust model.

If we go back to (2.158) and substitute the alternative parameters $\nu = 2a$, $\lambda = a/b$, and $\eta = \tau b/a$, we see that the t-distribution can be written in the form

$$\mathrm{St}(x|\mu, \lambda, \nu) = \int_0^{\infty} \mathcal{N}\left(x|\mu, (\eta\lambda)^{-1}\right) \mathrm{Gam}(\eta|\nu/2, \nu/2)\,\mathrm{d}\eta. \tag{2.160}$$

We can then generalize this to a multivariate Gaussian $\mathcal{N}(\mathbf{x}|\boldsymbol{\mu}, \boldsymbol{\Lambda})$ to obtain the corresponding multivariate Student's t-distribution in the form

$$\mathrm{St}(\mathbf{x}|\boldsymbol{\mu}, \boldsymbol{\Lambda}, \nu) = \int_0^{\infty} \mathcal{N}(\mathbf{x}|\boldsymbol{\mu}, (\eta\boldsymbol{\Lambda})^{-1})\mathrm{Gam}(\eta|\nu/2, \nu/2)\,\mathrm{d}\eta. \tag{2.161}$$

Exercise 2.48

Using the same technique as for the univariate case, we can evaluate this integral to give

$$\mathrm{St}(\mathbf{x}|\boldsymbol{\mu},\boldsymbol{\Lambda},\nu) = \frac{\Gamma(D/2+\nu/2)}{\Gamma(\nu/2)}\frac{|\boldsymbol{\Lambda}|^{1/2}}{(\pi\nu)^{D/2}}\left[1+\frac{\Delta^2}{\nu}\right]^{-D/2-\nu/2} \tag{2.162}$$

where D is the dimensionality of $\mathbf{x}$, and Δ^2 is the squared Mahalanobis distance defined by

$$\Delta^2 = (\mathbf{x}-\boldsymbol{\mu})^{\mathrm{T}}\boldsymbol{\Lambda}(\mathbf{x}-\boldsymbol{\mu}). \tag{2.163}$$

Exercise 2.49

This is the multivariate form of Student's t-distribution and satisfies the following properties

$$\begin{aligned}
\mathbb{E}[\mathbf{x}] &= \boldsymbol{\mu}, && \text{if} \quad \nu > 1 && (2.164)\\
\mathrm{cov}[\mathbf{x}] &= \frac{\nu}{(\nu-2)}\boldsymbol{\Lambda}^{-1}, && \text{if} \quad \nu > 2 && (2.165)\\
\mathrm{mode}[\mathbf{x}] &= \boldsymbol{\mu} && && (2.166)
\end{aligned}$$

with corresponding results for the univariate case.

2.3.8 Periodic variables

Although Gaussian distributions are of great practical significance, both in their own right and as building blocks for more complex probabilistic models, there are situations in which they are inappropriate as density models for continuous variables. One important case, which arises in practical applications, is that of periodic variables.

An example of a periodic variable would be the wind direction at a particular geographical location. We might, for instance, measure values of wind direction on a number of days and wish to summarize this using a parametric distribution. Another example is calendar time, where we may be interested in modelling quantities that are believed to be periodic over 24 hours or over an annual cycle. Such quantities can conveniently be represented using an angular (polar) coordinate $0 \leqslant \theta < 2\pi$.

We might be tempted to treat periodic variables by choosing some direction as the origin and then applying a conventional distribution such as the Gaussian. Such an approach, however, would give results that were strongly dependent on the arbitrary choice of origin. Suppose, for instance, that we have two observations at $\theta_1 = 1^\circ$ and $\theta_2 = 359^\circ$, and we model them using a standard univariate Gaussian distribution. If we choose the origin at 0°, then the sample mean of this data set will be 180° with standard deviation 179°, whereas if we choose the origin at 180°, then the mean will be 0° and the standard deviation will be 1°. We clearly need to develop a special approach for the treatment of periodic variables.

Let us consider the problem of evaluating the mean of a set of observations $\mathcal{D} = \{\theta_1,\ldots,\theta_N\}$ of a periodic variable. From now on, we shall assume that θ is measured in radians. We have already seen that the simple average $(\theta_1+\cdots+\theta_N)/N$ will be strongly coordinate dependent. To find an invariant measure of the mean, we note that the observations can be viewed as points on the unit circle and can therefore be described instead by two-dimensional unit vectors $\mathbf{x}_1,\ldots,\mathbf{x}_N$ where $\|\mathbf{x}_n\| = 1$ for $n = 1,\ldots,N$, as illustrated in Figure 2.17. We can average the vectors $\{\mathbf{x}_n\}$

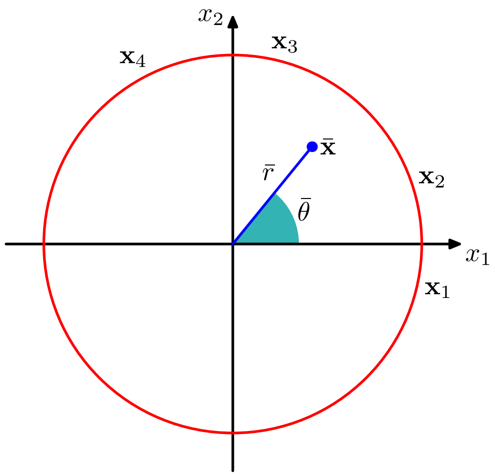

Figure 2.17 Illustration of the representation of values θ_n of a periodic variable as two-dimensional vectors $\mathbf{x}_n$ living on the unit circle. Also shown is the average $\overline{\mathbf{x}}$ of those vectors.

instead to give

$$\overline{\mathbf{x}} = \frac{1}{N}\sum_{n=1}^{N}\mathbf{x}_n \tag{2.167}$$

and then find the corresponding angle $\overline{\theta}$ of this average. Clearly, this definition will ensure that the location of the mean is independent of the origin of the angular coordinate. Note that $\overline{\mathbf{x}}$ will typically lie inside the unit circle. The Cartesian coordinates of the observations are given by $\mathbf{x}_n = (\cos\theta_n, \sin\theta_n)$, and we can write the Cartesian coordinates of the sample mean in the form $\overline{\mathbf{x}} = (\overline{r}\cos\overline{\theta}, \overline{r}\sin\overline{\theta})$. Substituting into (2.167) and equating the x_1 and x_2 components then gives

$$\overline{r}\cos\overline{\theta} = \frac{1}{N}\sum_{n=1}^{N}\cos\theta_n, \qquad \overline{r}\sin\overline{\theta} = \frac{1}{N}\sum_{n=1}^{N}\sin\theta_n. \tag{2.168}$$

Taking the ratio, and using the identity $\tan\theta = \sin\theta/\cos\theta$, we can solve for $\overline{\theta}$ to give

$$\overline{\theta} = \tan^{-1}\left\{\frac{\sum_n \sin\theta_n}{\sum_n \cos\theta_n}\right\}. \tag{2.169}$$

Shortly, we shall see how this result arises naturally as the maximum likelihood estimator for an appropriately defined distribution over a periodic variable.

We now consider a periodic generalization of the Gaussian called the *von Mises* distribution. Here we shall limit our attention to univariate distributions, although periodic distributions can also be found over hyperspheres of arbitrary dimension. For an extensive discussion of periodic distributions, see Mardia and Jupp (2000).

By convention, we will consider distributions $p(\theta)$ that have period 2π. Any probability density $p(\theta)$ defined over θ must not only be nonnegative and integrate

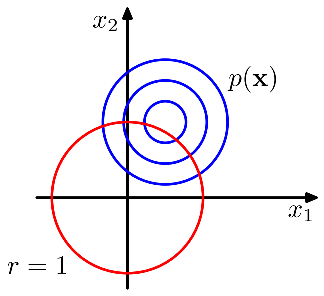

Figure 2.18 The von Mises distribution can be derived by considering a two-dimensional Gaussian of the form (2.173), whose density contours are shown in blue and conditioning on the unit circle shown in red.

to one, but it must also be periodic. Thus $p(\theta)$ must satisfy the three conditions

$$\begin{aligned} p(\theta) &\geqslant 0 && (2.170)\\ \int_0^{2\pi} p(\theta)\,\mathrm{d}\theta &= 1 && (2.171)\\ p(\theta + 2\pi) &= p(\theta). && (2.172) \end{aligned}$$

From (2.172), it follows that $p(\theta + M2\pi) = p(\theta)$ for any integer M.

We can easily obtain a Gaussian-like distribution that satisfies these three properties as follows. Consider a Gaussian distribution over two variables $\mathbf{x} = (x_1, x_2)$ having mean $\boldsymbol{\mu} = (\mu_1, \mu_2)$ and a covariance matrix $\boldsymbol{\Sigma} = \sigma^2\mathbf{I}$ where $\mathbf{I}$ is the 2×2 identity matrix, so that

$$p(x_1, x_2) = \frac{1}{2\pi\sigma^2} \exp\left\{-\frac{(x_1 - \mu_1)^2 + (x_2 - \mu_2)^2}{2\sigma^2}\right\}. \tag{2.173}$$

The contours of constant $p(\mathbf{x})$ are circles, as illustrated in Figure 2.18. Now suppose we consider the value of this distribution along a circle of fixed radius. Then by construction this distribution will be periodic, although it will not be normalized. We can determine the form of this distribution by transforming from Cartesian coordinates (x_1, x_2) to polar coordinates (r, θ) so that

$$x_1 = r\cos\theta, \qquad x_2 = r\sin\theta. \tag{2.174}$$

We also map the mean $\boldsymbol{\mu}$ into polar coordinates by writing

$$\mu_1 = r_0\cos\theta_0, \qquad \mu_2 = r_0\sin\theta_0. \tag{2.175}$$

Next we substitute these transformations into the two-dimensional Gaussian distribution (2.173), and then condition on the unit circle $r = 1$, noting that we are interested only in the dependence on θ. Focussing on the exponent in the Gaussian distribution we have

$$\begin{aligned} &-\frac{1}{2\sigma^2}\left\{(r\cos\theta - r_0\cos\theta_0)^2 + (r\sin\theta - r_0\sin\theta_0)^2\right\}\\ &\quad= -\frac{1}{2\sigma^2}\left\{1 + r_0^2 - 2r_0\cos\theta\cos\theta_0 - 2r_0\sin\theta\sin\theta_0\right\}\\ &\quad= \frac{r_0}{\sigma^2}\cos(\theta - \theta_0) + \text{const} && (2.176) \end{aligned}$$

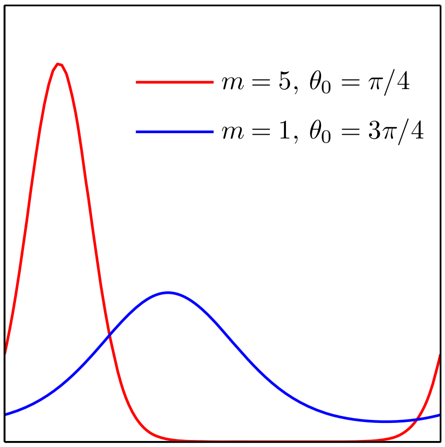

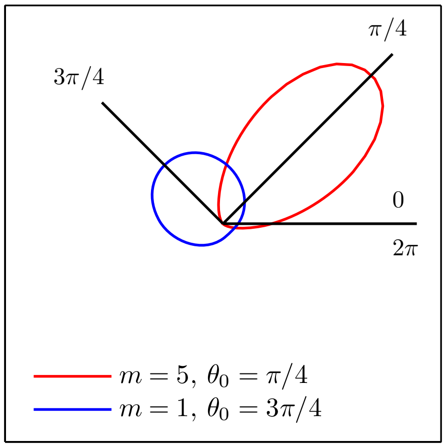

Figure 2.19 The von Mises distribution plotted for two different parameter values, shown as a Cartesian plot on the left and as the corresponding polar plot on the right.

where 'const' denotes terms independent of θ, and we have made use of the following trigonometrical identities

Exercise 2.51

$$\cos^2 A + \sin^2 A = 1 \qquad (2.177)$$
$$\cos A \cos B + \sin A \sin B = \cos(A - B). \qquad (2.178)$$

If we now define $m = r_0/\sigma^2$, we obtain our final expression for the distribution of $p(\theta)$ along the unit circle $r = 1$ in the form

$$p(\theta|\theta_0, m) = \frac{1}{2\pi I_0(m)} \exp\{m \cos(\theta - \theta_0)\} \qquad (2.179)$$

which is called the *von Mises* distribution, or the *circular normal*. Here the parameter θ_0 corresponds to the mean of the distribution, while m, which is known as the *concentration* parameter, is analogous to the inverse variance (precision) for the Gaussian. The normalization coefficient in (2.179) is expressed in terms of $I_0(m)$, which is the zeroth-order Bessel function of the first kind (Abramowitz and Stegun, 1965) and is defined by

$$I_0(m) = \frac{1}{2\pi} \int_0^{2\pi} \exp\{m \cos\theta\}\, \mathrm{d}\theta. \qquad (2.180)$$

Exercise 2.52

For large m, the distribution becomes approximately Gaussian. The von Mises distribution is plotted in Figure 2.19, and the function $I_0(m)$ is plotted in Figure 2.20.

Now consider the maximum likelihood estimators for the parameters θ_0 and m for the von Mises distribution. The log likelihood function is given by

$$\ln p(\mathcal{D}|\theta_0, m) = -N \ln(2\pi) - N \ln I_0(m) + m \sum_{n=1}^{N} \cos(\theta_n - \theta_0). \qquad (2.181)$$

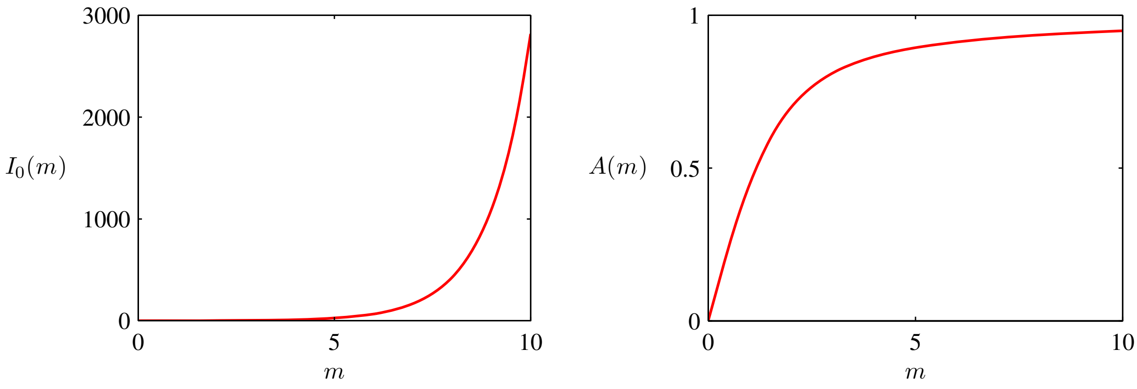

Figure 2.20 Plot of the Bessel function $I_0(m)$ defined by (2.180), together with the function $A(m)$ defined by (2.186).

Setting the derivative with respect to θ_0 equal to zero gives

$$\sum_{n=1}^{N} \sin(\theta_n - \theta_0) = 0. \tag{2.182}$$

To solve for θ_0, we make use of the trigonometric identity

$$\sin(A - B) = \cos B \sin A - \cos A \sin B \tag{2.183}$$

Exercise 2.53 from which we obtain

$$\theta_0^{\mathrm{ML}} = \tan^{-1}\left\{\frac{\sum_n \sin\theta_n}{\sum_n \cos\theta_n}\right\} \tag{2.184}$$

which we recognize as the result (2.169) obtained earlier for the mean of the observations viewed in a two-dimensional Cartesian space.

Similarly, maximizing (2.181) with respect to m, and making use of $I_0'(m) = I_1(m)$ (Abramowitz and Stegun, 1965), we have

$$A(m) = \frac{1}{N}\sum_{n=1}^{N} \cos(\theta_n - \theta_0^{\mathrm{ML}}) \tag{2.185}$$

where we have substituted for the maximum likelihood solution for θ_0^{ML} (recalling that we are performing a joint optimization over θ and m), and we have defined

$$A(m) = \frac{I_1(m)}{I_0(m)}. \tag{2.186}$$

The function $A(m)$ is plotted in Figure 2.20. Making use of the trigonometric identity (2.178), we can write (2.185) in the form

$$A(m_{\mathrm{ML}}) = \left(\frac{1}{N}\sum_{n=1}^{N}\cos\theta_n\right)\cos\theta_0^{\mathrm{ML}} - \left(\frac{1}{N}\sum_{n=1}^{N}\sin\theta_n\right)\sin\theta_0^{\mathrm{ML}}. \tag{2.187}$$

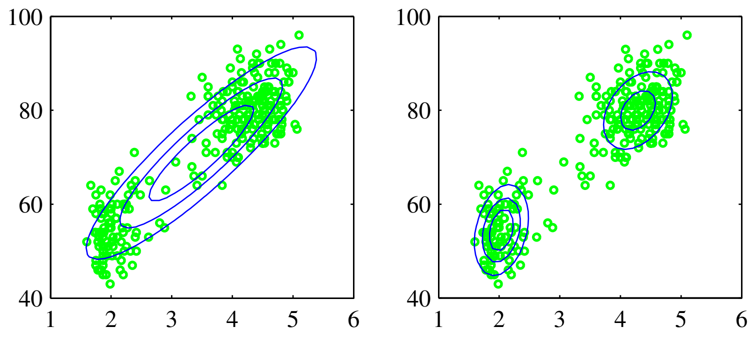

Figure 2.21 Plots of the 'old faithful' data in which the blue curves show contours of constant probability density. On the left is a single Gaussian distribution which has been fitted to the data using maximum likelihood. Note that this distribution fails to capture the two clumps in the data and indeed places much of its probability mass in the central region between the clumps where the data are relatively sparse. On the right the distribution is given by a linear combination of two Gaussians which has been fitted to the data by maximum likelihood using techniques discussed Chapter 9, and which gives a better representation of the data.

The right-hand side of (2.187) is easily evaluated, and the function $A(m)$ can be inverted numerically.

For completeness, we mention briefly some alternative techniques for the construction of periodic distributions. The simplest approach is to use a histogram of observations in which the angular coordinate is divided into fixed bins. This has the virtue of simplicity and flexibility but also suffers from significant limitations, as we shall see when we discuss histogram methods in more detail in Section 2.5. Another approach starts, like the von Mises distribution, from a Gaussian distribution over a Euclidean space but now marginalizes onto the unit circle rather than conditioning (Mardia and Jupp, 2000). However, this leads to more complex forms of distribution and will not be discussed further. Finally, any valid distribution over the real axis (such as a Gaussian) can be turned into a periodic distribution by mapping successive intervals of width 2π onto the periodic variable $(0, 2\pi)$, which corresponds to 'wrapping' the real axis around unit circle. Again, the resulting distribution is more complex to handle than the von Mises distribution.

One limitation of the von Mises distribution is that it is unimodal. By forming *mixtures* of von Mises distributions, we obtain a flexible framework for modelling periodic variables that can handle multimodality. For an example of a machine learning application that makes use of von Mises distributions, see Lawrence *et al.* (2002), and for extensions to modelling conditional densities for regression problems, see Bishop and Nabney (1996).

2.3.9 Mixtures of Gaussians

While the Gaussian distribution has some important analytical properties, it suffers from significant limitations when it comes to modelling real data sets. Consider the example shown in Figure 2.21. This is known as the 'Old Faithful' data set, and comprises 272 measurements of the eruption of the Old Faithful geyser at Yellowstone National Park in the USA. Each measurement comprises the duration of

Appendix A

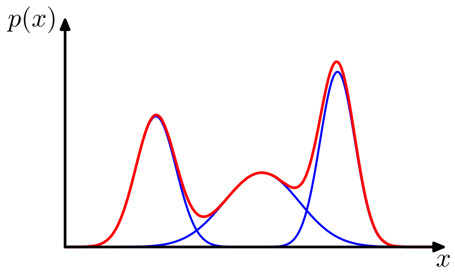

Figure 2.22 Example of a Gaussian mixture distribution in one dimension showing three Gaussians (each scaled by a coefficient) in blue and their sum in red.

the eruption in minutes (horizontal axis) and the time in minutes to the next eruption (vertical axis). We see that the data set forms two dominant clumps, and that a simple Gaussian distribution is unable to capture this structure, whereas a linear superposition of two Gaussians gives a better characterization of the data set.

Such superpositions, formed by taking linear combinations of more basic distributions such as Gaussians, can be formulated as probabilistic models known as *mixture distributions* (McLachlan and Basford, 1988; McLachlan and Peel, 2000). In Figure 2.22 we see that a linear combination of Gaussians can give rise to very complex densities. By using a sufficient number of Gaussians, and by adjusting their means and covariances as well as the coefficients in the linear combination, almost any continuous density can be approximated to arbitrary accuracy.

We therefore consider a superposition of K Gaussian densities of the form

$$p(\mathbf{x}) = \sum_{k=1}^{K} \pi_k \mathcal{N}(\mathbf{x}|\boldsymbol{\mu}_k, \boldsymbol{\Sigma}_k) \tag{2.188}$$

which is called a *mixture of Gaussians*. Each Gaussian density $\mathcal{N}(\mathbf{x}|\boldsymbol{\mu}_k, \boldsymbol{\Sigma}_k)$ is called a *component* of the mixture and has its own mean $\boldsymbol{\mu}_k$ and covariance $\boldsymbol{\Sigma}_k$. Contour and surface plots for a Gaussian mixture having 3 components are shown in Figure 2.23.

In this section we shall consider Gaussian components to illustrate the framework of mixture models. More generally, mixture models can comprise linear combinations of other distributions. For instance, in Section 9.3.3 we shall consider mixtures of Bernoulli distributions as an example of a mixture model for discrete variables. *Section 9.3.3*

The parameters π_k in (2.188) are called *mixing coefficients*. If we integrate both sides of (2.188) with respect to $\mathbf{x}$, and note that both $p(\mathbf{x})$ and the individual Gaussian components are normalized, we obtain

$$\sum_{k=1}^{K} \pi_k = 1. \tag{2.189}$$

Also, the requirement that $p(\mathbf{x}) \geqslant 0$, together with $\mathcal{N}(\mathbf{x}|\boldsymbol{\mu}_k, \boldsymbol{\Sigma}_k) \geqslant 0$, implies $\pi_k \geqslant 0$ for all k. Combining this with the condition (2.189) we obtain

$$0 \leqslant \pi_k \leqslant 1. \tag{2.190}$$

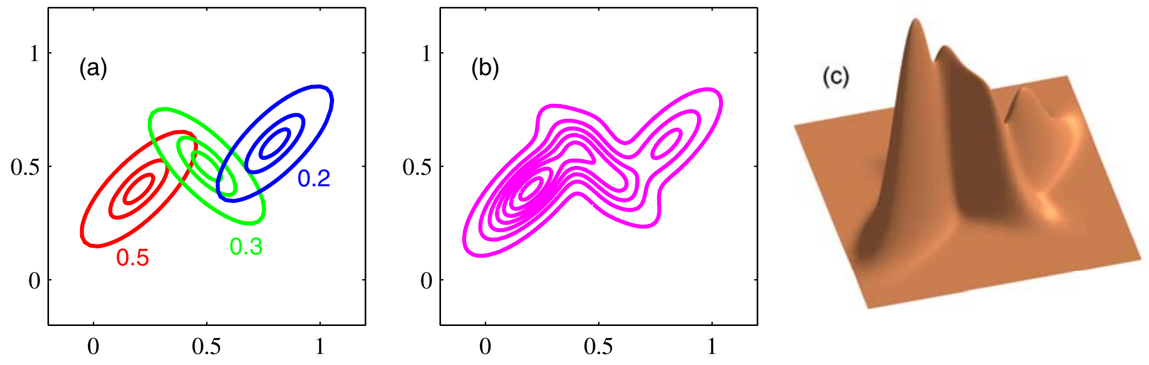

Figure 2.23 Illustration of a mixture of 3 Gaussians in a two-dimensional space. (a) Contours of constant density for each of the mixture components, in which the 3 components are denoted red, blue and green, and the values of the mixing coefficients are shown below each component. (b) Contours of the marginal probability density $p(\mathbf{x})$ of the mixture distribution. (c) A surface plot of the distribution $p(\mathbf{x})$.

We therefore see that the mixing coefficients satisfy the requirements to be probabilities.

From the sum and product rules, the marginal density is given by

$$p(\mathbf{x}) = \sum_{k=1}^{K} p(k)p(\mathbf{x}|k) \tag{2.191}$$

which is equivalent to (2.188) in which we can view $\pi_k = p(k)$ as the prior probability of picking the k^{th} component, and the density $\mathcal{N}(\mathbf{x}|\boldsymbol{\mu}_k, \boldsymbol{\Sigma}_k) = p(\mathbf{x}|k)$ as the probability of $\mathbf{x}$ conditioned on k. As we shall see in later chapters, an important role is played by the posterior probabilities $p(k|\mathbf{x})$, which are also known as *responsibilities*. From Bayes' theorem these are given by

$$\begin{aligned}\gamma_k(\mathbf{x}) &\equiv p(k|\mathbf{x}) \\ &= \frac{p(k)p(\mathbf{x}|k)}{\sum_l p(l)p(\mathbf{x}|l)} \\ &= \frac{\pi_k \mathcal{N}(\mathbf{x}|\boldsymbol{\mu}_k, \boldsymbol{\Sigma}_k)}{\sum_l \pi_l \mathcal{N}(\mathbf{x}|\boldsymbol{\mu}_l, \boldsymbol{\Sigma}_l)}.\end{aligned} \tag{2.192}$$

We shall discuss the probabilistic interpretation of the mixture distribution in greater detail in Chapter 9.

The form of the Gaussian mixture distribution is governed by the parameters $\boldsymbol{\pi}$, $\boldsymbol{\mu}$ and $\boldsymbol{\Sigma}$, where we have used the notation $\boldsymbol{\pi} \equiv \{\pi_1, \ldots, \pi_K\}$, $\boldsymbol{\mu} \equiv \{\boldsymbol{\mu}_1, \ldots, \boldsymbol{\mu}_K\}$ and $\boldsymbol{\Sigma} \equiv \{\boldsymbol{\Sigma}_1, \ldots \boldsymbol{\Sigma}_K\}$. One way to set the values of these parameters is to use maximum likelihood. From (2.188) the log of the likelihood function is given by

$$\ln p(\mathbf{X}|\boldsymbol{\pi}, \boldsymbol{\mu}, \boldsymbol{\Sigma}) = \sum_{n=1}^{N} \ln \left\{ \sum_{k=1}^{K} \pi_k \mathcal{N}(\mathbf{x}_n|\boldsymbol{\mu}_k, \boldsymbol{\Sigma}_k) \right\} \tag{2.193}$$

where $\mathbf{X} = \{\mathbf{x}_1, \ldots, \mathbf{x}_N\}$. We immediately see that the situation is now much more complex than with a single Gaussian, due to the presence of the summation over k inside the logarithm. As a result, the maximum likelihood solution for the parameters no longer has a closed-form analytical solution. One approach to maximizing the likelihood function is to use iterative numerical optimization techniques (Fletcher, 1987; Nocedal and Wright, 1999; Bishop and Nabney, 2008). Alternatively we can employ a powerful framework called *expectation maximization*, which will be discussed at length in Chapter 9.

2.4. The Exponential Family

The probability distributions that we have studied so far in this chapter (with the exception of the Gaussian mixture) are specific examples of a broad class of distributions called the *exponential family* (Duda and Hart, 1973; Bernardo and Smith, 1994). Members of the exponential family have many important properties in common, and it is illuminating to discuss these properties in some generality.

The exponential family of distributions over $\mathbf{x}$, given parameters $\boldsymbol{\eta}$, is defined to be the set of distributions of the form

$$p(\mathbf{x}|\boldsymbol{\eta}) = h(\mathbf{x})g(\boldsymbol{\eta}) \exp\left\{\boldsymbol{\eta}^{\mathrm{T}}\mathbf{u}(\mathbf{x})\right\} \tag{2.194}$$

where $\mathbf{x}$ may be scalar or vector, and may be discrete or continuous. Here $\boldsymbol{\eta}$ are called the *natural parameters* of the distribution, and $\mathbf{u}(\mathbf{x})$ is some function of $\mathbf{x}$. The function $g(\boldsymbol{\eta})$ can be interpreted as the coefficient that ensures that the distribution is normalized and therefore satisfies

$$g(\boldsymbol{\eta}) \int h(\mathbf{x}) \exp\left\{\boldsymbol{\eta}^{\mathrm{T}}\mathbf{u}(\mathbf{x})\right\} \,\mathrm{d}\mathbf{x} = 1 \tag{2.195}$$

where the integration is replaced by summation if $\mathbf{x}$ is a discrete variable.

We begin by taking some examples of the distributions introduced earlier in the chapter and showing that they are indeed members of the exponential family. Consider first the Bernoulli distribution

$$p(x|\mu) = \mathrm{Bern}(x|\mu) = \mu^x(1-\mu)^{1-x}. \tag{2.196}$$

Expressing the right-hand side as the exponential of the logarithm, we have

$$\begin{aligned} p(x|\mu) &= \exp\left\{x \ln \mu + (1-x)\ln(1-\mu)\right\} \\ &= (1-\mu)\exp\left\{\ln\left(\frac{\mu}{1-\mu}\right)x\right\}. \end{aligned} \tag{2.197}$$

Comparison with (2.194) allows us to identify

$$\eta = \ln\left(\frac{\mu}{1-\mu}\right) \tag{2.198}$$

which we can solve for μ to give $\mu = \sigma(\eta)$, where

$$\sigma(\eta) = \frac{1}{1 + \exp(-\eta)} \tag{2.199}$$

is called the *logistic sigmoid* function. Thus we can write the Bernoulli distribution using the standard representation (2.194) in the form

$$p(x|\eta) = \sigma(-\eta) \exp(\eta x) \tag{2.200}$$

where we have used $1 - \sigma(\eta) = \sigma(-\eta)$, which is easily proved from (2.199). Comparison with (2.194) shows that

$$\begin{aligned} u(x) &= x && (2.201)\\ h(x) &= 1 && (2.202)\\ g(\eta) &= \sigma(-\eta). && (2.203) \end{aligned}$$

Next consider the multinomial distribution that, for a single observation $\mathbf{x}$, takes the form

$$p(\mathbf{x}|\boldsymbol{\mu}) = \prod_{k=1}^{M} \mu_k^{x_k} = \exp\left\{ \sum_{k=1}^{M} x_k \ln \mu_k \right\} \tag{2.204}$$

where $\mathbf{x} = (x_1, \ldots, x_N)^{\mathrm{T}}$. Again, we can write this in the standard representation (2.194) so that

$$p(\mathbf{x}|\boldsymbol{\eta}) = \exp(\boldsymbol{\eta}^{\mathrm{T}}\mathbf{x}) \tag{2.205}$$

where $\eta_k = \ln \mu_k$, and we have defined $\boldsymbol{\eta} = (\eta_1, \ldots, \eta_M)^{\mathrm{T}}$. Again, comparing with (2.194) we have

$$\begin{aligned} \mathbf{u}(\mathbf{x}) &= \mathbf{x} && (2.206)\\ h(\mathbf{x}) &= 1 && (2.207)\\ g(\boldsymbol{\eta}) &= 1. && (2.208) \end{aligned}$$

Note that the parameters η_k are not independent because the parameters μ_k are subject to the constraint

$$\sum_{k=1}^{M} \mu_k = 1 \tag{2.209}$$

so that, given any $M-1$ of the parameters μ_k, the value of the remaining parameter is fixed. In some circumstances, it will be convenient to remove this constraint by expressing the distribution in terms of only $M-1$ parameters. This can be achieved by using the relationship (2.209) to eliminate μ_M by expressing it in terms of the remaining $\{\mu_k\}$ where $k = 1, \ldots, M-1$, thereby leaving $M-1$ parameters. Note that these remaining parameters are still subject to the constraints

$$0 \leqslant \mu_k \leqslant 1, \qquad \sum_{k=1}^{M-1} \mu_k \leqslant 1. \tag{2.210}$$

Making use of the constraint (2.209), the multinomial distribution in this representation then becomes

$$\begin{aligned}
&\exp\left\{\sum_{k=1}^{M} x_k \ln \mu_k\right\} \\
&\quad= \exp\left\{\sum_{k=1}^{M-1} x_k \ln \mu_k + \left(1-\sum_{k=1}^{M-1} x_k\right) \ln\left(1-\sum_{k=1}^{M-1}\mu_k\right)\right\} \\
&\quad= \exp\left\{\sum_{k=1}^{M-1} x_k \ln\left(\frac{\mu_k}{1-\sum_{j=1}^{M-1}\mu_j}\right) + \ln\left(1-\sum_{k=1}^{M-1}\mu_k\right)\right\}. \qquad (2.211)
\end{aligned}$$

We now identify

$$\ln\left(\frac{\mu_k}{1-\sum_j \mu_j}\right) = \eta_k \qquad (2.212)$$

which we can solve for μ_k by first summing both sides over k and then rearranging and back-substituting to give

$$\mu_k = \frac{\exp(\eta_k)}{1+\sum_j \exp(\eta_j)}. \qquad (2.213)$$

This is called the *softmax* function, or the *normalized exponential*. In this representation, the multinomial distribution therefore takes the form

$$p(\mathbf{x}|\boldsymbol{\eta}) = \left(1+\sum_{k=1}^{M-1}\exp(\eta_k)\right)^{-1} \exp(\boldsymbol{\eta}^{\mathrm{T}}\mathbf{x}). \qquad (2.214)$$

This is the standard form of the exponential family, with parameter vector $\boldsymbol{\eta} = (\eta_1, \ldots, \eta_{M-1})^{\mathrm{T}}$ in which

$$\begin{aligned}
\mathbf{u}(\mathbf{x}) &= \mathbf{x} && (2.215)\\
h(\mathbf{x}) &= 1 && (2.216)\\
g(\boldsymbol{\eta}) &= \left(1+\sum_{k=1}^{M-1}\exp(\eta_k)\right)^{-1}. && (2.217)
\end{aligned}$$

Finally, let us consider the Gaussian distribution. For the univariate Gaussian, we have

$$\begin{aligned}
p(x|\mu,\sigma^2) &= \frac{1}{(2\pi\sigma^2)^{1/2}} \exp\left\{-\frac{1}{2\sigma^2}(x-\mu)^2\right\} && (2.218)\\
&= \frac{1}{(2\pi\sigma^2)^{1/2}} \exp\left\{-\frac{1}{2\sigma^2}x^2 + \frac{\mu}{\sigma^2}x - \frac{1}{2\sigma^2}\mu^2\right\} && (2.219)
\end{aligned}$$

Exercise 2.57 which, after some simple rearrangement, can be cast in the standard exponential family form (2.194) with

$$\boldsymbol{\eta} = \begin{pmatrix} \mu/\sigma^2 \\ -1/2\sigma^2 \end{pmatrix} \tag{2.220}$$

$$\mathbf{u}(x) = \begin{pmatrix} x \\ x^2 \end{pmatrix} \tag{2.221}$$

$$h(\mathbf{x}) = (2\pi)^{-1/2} \tag{2.222}$$

$$g(\boldsymbol{\eta}) = (-2\eta_2)^{1/2} \exp\left(\frac{\eta_1^2}{4\eta_2}\right). \tag{2.223}$$

2.4.1 Maximum likelihood and sufficient statistics

Let us now consider the problem of estimating the parameter vector $\boldsymbol{\eta}$ in the general exponential family distribution (2.194) using the technique of maximum likelihood. Taking the gradient of both sides of (2.195) with respect to $\boldsymbol{\eta}$, we have

$$\nabla g(\boldsymbol{\eta}) \int h(\mathbf{x}) \exp\left\{\boldsymbol{\eta}^{\mathrm{T}}\mathbf{u}(\mathbf{x})\right\} \mathrm{d}\mathbf{x} + g(\boldsymbol{\eta}) \int h(\mathbf{x}) \exp\left\{\boldsymbol{\eta}^{\mathrm{T}}\mathbf{u}(\mathbf{x})\right\} \mathbf{u}(\mathbf{x})\,\mathrm{d}\mathbf{x} = 0. \tag{2.224}$$

Rearranging, and making use again of (2.195) then gives

$$-\frac{1}{g(\boldsymbol{\eta})}\nabla g(\boldsymbol{\eta}) = g(\boldsymbol{\eta}) \int h(\mathbf{x}) \exp\left\{\boldsymbol{\eta}^{\mathrm{T}}\mathbf{u}(\mathbf{x})\right\} \mathbf{u}(\mathbf{x})\,\mathrm{d}\mathbf{x} = \mathbb{E}[\mathbf{u}(\mathbf{x})] \tag{2.225}$$

where we have used (2.194). We therefore obtain the result

$$-\nabla \ln g(\boldsymbol{\eta}) = \mathbb{E}[\mathbf{u}(\mathbf{x})]. \tag{2.226}$$

Exercise 2.58 Note that the covariance of $\mathbf{u}(\mathbf{x})$ can be expressed in terms of the second derivatives of $g(\boldsymbol{\eta})$, and similarly for higher order moments. Thus, provided we can normalize a distribution from the exponential family, we can always find its moments by simple differentiation.

Now consider a set of independent identically distributed data denoted by $\mathbf{X} = \{\mathbf{x}_1, \ldots, \mathbf{x}_n\}$, for which the likelihood function is given by

$$p(\mathbf{X}|\boldsymbol{\eta}) = \left(\prod_{n=1}^{N} h(\mathbf{x}_n)\right) g(\boldsymbol{\eta})^N \exp\left\{\boldsymbol{\eta}^{\mathrm{T}} \sum_{n=1}^{N} \mathbf{u}(\mathbf{x}_n)\right\}. \tag{2.227}$$

Setting the gradient of $\ln p(\mathbf{X}|\boldsymbol{\eta})$ with respect to $\boldsymbol{\eta}$ to zero, we get the following condition to be satisfied by the maximum likelihood estimator $\boldsymbol{\eta}_{\mathrm{ML}}$

$$-\nabla \ln g(\boldsymbol{\eta}_{\mathrm{ML}}) = \frac{1}{N}\sum_{n=1}^{N} \mathbf{u}(\mathbf{x}_n) \tag{2.228}$$

which can in principle be solved to obtain $\boldsymbol{\eta}_{\mathrm{ML}}$. We see that the solution for the maximum likelihood estimator depends on the data only through $\sum_n \mathbf{u}(\mathbf{x}_n)$, which is therefore called the *sufficient statistic* of the distribution (2.194). We do not need to store the entire data set itself but only the value of the sufficient statistic. For the Bernoulli distribution, for example, the function $\mathbf{u}(x)$ is given just by x and so we need only keep the sum of the data points $\{x_n\}$, whereas for the Gaussian $\mathbf{u}(x) = (x, x^2)^{\mathrm{T}}$, and so we should keep both the sum of $\{x_n\}$ and the sum of $\{x_n^2\}$.

If we consider the limit $N \to \infty$, then the right-hand side of (2.228) becomes $\mathbb{E}[\mathbf{u}(\mathbf{x})]$, and so by comparing with (2.226) we see that in this limit $\boldsymbol{\eta}_{\mathrm{ML}}$ will equal the true value $\boldsymbol{\eta}$.

In fact, this sufficiency property holds also for Bayesian inference, although we shall defer discussion of this until Chapter 8 when we have equipped ourselves with the tools of graphical models and can thereby gain a deeper insight into these important concepts.

2.4.2 Conjugate priors

We have already encountered the concept of a conjugate prior several times, for example in the context of the Bernoulli distribution (for which the conjugate prior is the beta distribution) or the Gaussian (where the conjugate prior for the mean is a Gaussian, and the conjugate prior for the precision is the Wishart distribution). In general, for a given probability distribution $p(\mathbf{x}|\boldsymbol{\eta})$, we can seek a prior $p(\boldsymbol{\eta})$ that is conjugate to the likelihood function, so that the posterior distribution has the same functional form as the prior. For any member of the exponential family (2.194), there exists a conjugate prior that can be written in the form

$$p(\boldsymbol{\eta}|\boldsymbol{\chi}, \nu) = f(\boldsymbol{\chi}, \nu) g(\boldsymbol{\eta})^{\nu} \exp\left\{\nu \boldsymbol{\eta}^{\mathrm{T}} \boldsymbol{\chi}\right\} \tag{2.229}$$

where $f(\boldsymbol{\chi}, \nu)$ is a normalization coefficient, and $g(\boldsymbol{\eta})$ is the same function as appears in (2.194). To see that this is indeed conjugate, let us multiply the prior (2.229) by the likelihood function (2.227) to obtain the posterior distribution, up to a normalization coefficient, in the form

$$p(\boldsymbol{\eta}|\mathbf{X}, \boldsymbol{\chi}, \nu) \propto g(\boldsymbol{\eta})^{\nu+N} \exp\left\{\boldsymbol{\eta}^{\mathrm{T}} \left(\sum_{n=1}^{N} \mathbf{u}(\mathbf{x}_n) + \nu \boldsymbol{\chi}\right)\right\}. \tag{2.230}$$

This again takes the same functional form as the prior (2.229), confirming conjugacy. Furthermore, we see that the parameter ν can be interpreted as a effective number of pseudo-observations in the prior, each of which has a value for the sufficient statistic $\mathbf{u}(\mathbf{x})$ given by $\boldsymbol{\chi}$.

2.4.3 Noninformative priors

In some applications of probabilistic inference, we may have prior knowledge that can be conveniently expressed through the prior distribution. For example, if the prior assigns zero probability to some value of variable, then the posterior distribution will necessarily also assign zero probability to that value, irrespective of any subsequent observations of data. In many cases, however, we may have little idea of what form the distribution should take. We may then seek a form of prior distribution, called a *noninformative prior*, which is intended to have as little influence on the posterior distribution as possible (Jeffries, 1946; Box and Tao, 1973; Bernardo and Smith, 1994). This is sometimes referred to as 'letting the data speak for themselves'.

If we have a distribution $p(x|\lambda)$ governed by a parameter λ, we might be tempted to propose a prior distribution $p(\lambda) = \text{const}$ as a suitable prior. If λ is a discrete variable with K states, this simply amounts to setting the prior probability of each state to $1/K$. In the case of continuous parameters, however, there are two potential difficulties with this approach. The first is that, if the domain of λ is unbounded, this prior distribution cannot be correctly normalized because the integral over λ diverges. Such priors are called *improper*. In practice, improper priors can often be used provided the corresponding posterior distribution is *proper*, i.e., that it can be correctly normalized. For instance, if we put a uniform prior distribution over the mean of a Gaussian, then the posterior distribution for the mean, once we have observed at least one data point, will be proper.

A second difficulty arises from the transformation behaviour of a probability density under a nonlinear change of variables, given by (1.27). If a function $h(\lambda)$ is constant, and we change variables to $\lambda = \eta^2$, then $\widehat{h}(\eta) = h(\eta^2)$ will also be constant. However, if we choose the density $p_\lambda(\lambda)$ to be constant, then the density of η will be given, from (1.27), by

$$p_\eta(\eta) = p_\lambda(\lambda)\left|\frac{\mathrm{d}\lambda}{\mathrm{d}\eta}\right| = p_\lambda(\eta^2)2\eta \propto \eta \tag{2.231}$$

and so the density over η will not be constant. This issue does not arise when we use maximum likelihood, because the likelihood function $p(x|\lambda)$ is a simple function of λ and so we are free to use any convenient parameterization. If, however, we are to choose a prior distribution that is constant, we must take care to use an appropriate representation for the parameters.

Here we consider two simple examples of noninformative priors (Berger, 1985). First of all, if a density takes the form

$$p(x|\mu) = f(x - \mu) \tag{2.232}$$

then the parameter μ is known as a *location parameter*. This family of densities exhibits *translation invariance* because if we shift x by a constant to give $\widehat{x} = x + c$, then

$$p(\widehat{x}|\widehat{\mu}) = f(\widehat{x} - \widehat{\mu}) \tag{2.233}$$

where we have defined $\widehat{\mu} = \mu + c$. Thus the density takes the same form in the new variable as in the original one, and so the density is independent of the choice of origin. We would like to choose a prior distribution that reflects this translation invariance property, and so we choose a prior that assigns equal probability mass to an interval $A \leqslant \mu \leqslant B$ as to the shifted interval $A - c \leqslant \mu \leqslant B - c$. This implies

$$\int_A^B p(\mu)\,\mathrm{d}\mu = \int_{A-c}^{B-c} p(\mu)\,\mathrm{d}\mu = \int_A^B p(\mu - c)\,\mathrm{d}\mu \tag{2.234}$$

and because this must hold for all choices of A and B, we have

$$p(\mu - c) = p(\mu) \tag{2.235}$$

which implies that $p(\mu)$ is constant. An example of a location parameter would be the mean μ of a Gaussian distribution. As we have seen, the conjugate prior distribution for μ in this case is a Gaussian $p(\mu|\mu_0, \sigma_0^2) = \mathcal{N}(\mu|\mu_0, \sigma_0^2)$, and we obtain a noninformative prior by taking the limit $\sigma_0^2 \to \infty$. Indeed, from (2.141) and (2.142) we see that this gives a posterior distribution over μ in which the contributions from the prior vanish.

As a second example, consider a density of the form

$$p(x|\sigma) = \frac{1}{\sigma} f\left(\frac{x}{\sigma}\right) \tag{2.236}$$

Exercise 2.59

where $\sigma > 0$. Note that this will be a normalized density provided $f(x)$ is correctly normalized. The parameter σ is known as a *scale parameter*, and the density exhibits *scale invariance* because if we scale x by a constant to give $\widehat{x} = cx$, then

$$p(\widehat{x}|\widehat{\sigma}) = \frac{1}{\widehat{\sigma}} f\left(\frac{\widehat{x}}{\widehat{\sigma}}\right) \tag{2.237}$$

where we have defined $\widehat{\sigma} = c\sigma$. This transformation corresponds to a change of scale, for example from meters to kilometers if x is a length, and we would like to choose a prior distribution that reflects this scale invariance. If we consider an interval $A \leqslant \sigma \leqslant B$, and a scaled interval $A/c \leqslant \sigma \leqslant B/c$, then the prior should assign equal probability mass to these two intervals. Thus we have

$$\int_A^B p(\sigma)\,\mathrm{d}\sigma = \int_{A/c}^{B/c} p(\sigma)\,\mathrm{d}\sigma = \int_A^B p\left(\frac{1}{c}\sigma\right)\frac{1}{c}\,\mathrm{d}\sigma \tag{2.238}$$

and because this must hold for choices of A and B, we have

$$p(\sigma) = p\left(\frac{1}{c}\sigma\right)\frac{1}{c} \tag{2.239}$$

and hence $p(\sigma) \propto 1/\sigma$. Note that again this is an improper prior because the integral of the distribution over $0 \leqslant \sigma \leqslant \infty$ is divergent. It is sometimes also convenient to think of the prior distribution for a scale parameter in terms of the density of the log of the parameter. Using the transformation rule (1.27) for densities we see that $p(\ln\sigma) = \text{const}$. Thus, for this prior there is the same probability mass in the range $1 \leqslant \sigma \leqslant 10$ as in the range $10 \leqslant \sigma \leqslant 100$ and in $100 \leqslant \sigma \leqslant 1000$.

An example of a scale parameter would be the standard deviation σ of a Gaussian distribution, after we have taken account of the location parameter μ, because

$$\mathcal{N}(x|\mu,\sigma^2) \propto \sigma^{-1}\exp\left\{-(\widetilde{x}/\sigma)^2\right\} \tag{2.240}$$

where $\widetilde{x} = x - \mu$. As discussed earlier, it is often more convenient to work in terms of the precision $\lambda = 1/\sigma^2$ rather than σ itself. Using the transformation rule for densities, we see that a distribution $p(\sigma) \propto 1/\sigma$ corresponds to a distribution over λ of the form $p(\lambda) \propto 1/\lambda$. We have seen that the conjugate prior for λ was the gamma distribution $\mathrm{Gam}(\lambda|a_0, b_0)$ given by (2.146). The noninformative prior is obtained as the special case $a_0 = b_0 = 0$. Again, if we examine the results (2.150) and (2.151) for the posterior distribution of λ, we see that for $a_0 = b_0 = 0$, the posterior depends only on terms arising from the data and not from the prior.

Section 2.3

2.5. Nonparametric Methods

Throughout this chapter, we have focussed on the use of probability distributions having specific functional forms governed by a small number of parameters whose values are to be determined from a data set. This is called the *parametric* approach to density modelling. An important limitation of this approach is that the chosen density might be a poor model of the distribution that generates the data, which can result in poor predictive performance. For instance, if the process that generates the data is multimodal, then this aspect of the distribution can never be captured by a Gaussian, which is necessarily unimodal.

In this final section, we consider some *nonparametric* approaches to density estimation that make few assumptions about the form of the distribution. Here we shall focus mainly on simple frequentist methods. The reader should be aware, however, that nonparametric Bayesian methods are attracting increasing interest (Walker *et al.*, 1999; Neal, 2000; Müller and Quintana, 2004; Teh *et al.*, 2006).

Let us start with a discussion of histogram methods for density estimation, which we have already encountered in the context of marginal and conditional distributions in Figure 1.11 and in the context of the central limit theorem in Figure 2.6. Here we explore the properties of histogram density models in more detail, focussing on the case of a single continuous variable x. Standard histograms simply partition x into distinct bins of width Δ_i and then count the number n_i of observations of x falling in bin i. In order to turn this count into a normalized probability density, we simply divide by the total number N of observations and by the width Δ_i of the bins to obtain probability values for each bin given by

$$p_i = \frac{n_i}{N\Delta_i} \tag{2.241}$$

for which it is easily seen that $\int p(x)\,\mathrm{d}x = 1$. This gives a model for the density $p(x)$ that is constant over the width of each bin, and often the bins are chosen to have the same width $\Delta_i = \Delta$.

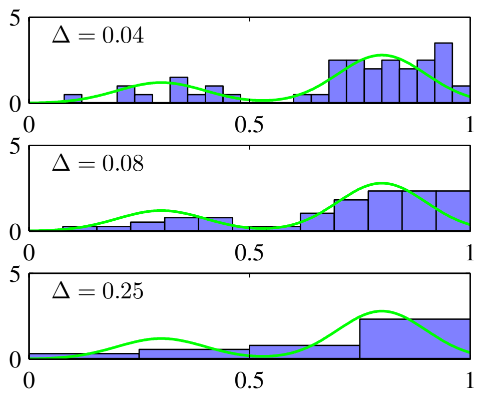

Figure 2.24 An illustration of the histogram approach to density estimation, in which a data set of 50 data points is generated from the distribution shown by the green curve. Histogram density estimates, based on (2.241), with a common bin width Δ are shown for various values of Δ.

In Figure 2.24, we show an example of histogram density estimation. Here the data is drawn from the distribution, corresponding to the green curve, which is formed from a mixture of two Gaussians. Also shown are three examples of histogram density estimates corresponding to three different choices for the bin width Δ. We see that when Δ is very small (top figure), the resulting density model is very spiky, with a lot of structure that is not present in the underlying distribution that generated the data set. Conversely, if Δ is too large (bottom figure) then the result is a model that is too smooth and that consequently fails to capture the bimodal property of the green curve. The best results are obtained for some intermediate value of Δ (middle figure). In principle, a histogram density model is also dependent on the choice of edge location for the bins, though this is typically much less significant than the value of Δ.

Note that the histogram method has the property (unlike the methods to be discussed shortly) that, once the histogram has been computed, the data set itself can be discarded, which can be advantageous if the data set is large. Also, the histogram approach is easily applied if the data points are arriving sequentially.

In practice, the histogram technique can be useful for obtaining a quick visualization of data in one or two dimensions but is unsuited to most density estimation applications. One obvious problem is that the estimated density has discontinuities that are due to the bin edges rather than any property of the underlying distribution that generated the data. Another major limitation of the histogram approach is its scaling with dimensionality. If we divide each variable in a D-dimensional space into M bins, then the total number of bins will be M^D. This exponential scaling with D is an example of the curse of dimensionality. In a space of high dimensionality, the quantity of data needed to provide meaningful estimates of local probability density would be prohibitive.

Section 1.4

The histogram approach to density estimation does, however, teach us two important lessons. First, to estimate the probability density at a particular location, we should consider the data points that lie within some local neighbourhood of that point. Note that the concept of locality requires that we assume some form of distance measure, and here we have been assuming Euclidean distance. For histograms, this neighbourhood property was defined by the bins, and there is a natural 'smoothing' parameter describing the spatial extent of the local region, in this case the bin width. Second, the value of the smoothing parameter should be neither too large nor too small in order to obtain good results. This is reminiscent of the choice of model complexity in polynomial curve fitting discussed in Chapter 1 where the degree M of the polynomial, or alternatively the value α of the regularization parameter, was optimal for some intermediate value, neither too large nor too small. Armed with these insights, we turn now to a discussion of two widely used nonparametric techniques for density estimation, kernel estimators and nearest neighbours, which have better scaling with dimensionality than the simple histogram model.

2.5.1 Kernel density estimators

Let us suppose that observations are being drawn from some unknown probability density $p(\mathbf{x})$ in some D-dimensional space, which we shall take to be Euclidean, and we wish to estimate the value of $p(\mathbf{x})$. From our earlier discussion of locality, let us consider some small region $\mathcal{R}$ containing $\mathbf{x}$. The probability mass associated with this region is given by

$$P = \int_{\mathcal{R}} p(\mathbf{x})\,\mathrm{d}\mathbf{x}. \tag{2.242}$$

Now suppose that we have collected a data set comprising N observations drawn from $p(\mathbf{x})$. Because each data point has a probability P of falling within $\mathcal{R}$, the total number K of points that lie inside $\mathcal{R}$ will be distributed according to the binomial distribution

Section 2.1

$$\mathrm{Bin}(K|N,P) = \frac{N!}{K!(N-K)!}P^K(1-P)^{1-K}. \tag{2.243}$$

Using (2.11), we see that the mean fraction of points falling inside the region is $\mathbb{E}[K/N] = P$, and similarly using (2.12) we see that the variance around this mean is $\mathrm{var}[K/N] = P(1-P)/N$. For large N, this distribution will be sharply peaked around the mean and so

$$K \simeq NP. \tag{2.244}$$

If, however, we also assume that the region $\mathcal{R}$ is sufficiently small that the probability density $p(\mathbf{x})$ is roughly constant over the region, then we have

$$P \simeq p(\mathbf{x})V \tag{2.245}$$

where V is the volume of $\mathcal{R}$. Combining (2.244) and (2.245), we obtain our density estimate in the form

$$p(\mathbf{x}) = \frac{K}{NV}. \tag{2.246}$$

Note that the validity of (2.246) depends on two contradictory assumptions, namely that the region $\mathcal{R}$ be sufficiently small that the density is approximately constant over the region and yet sufficiently large (in relation to the value of that density) that the number K of points falling inside the region is sufficient for the binomial distribution to be sharply peaked.

We can exploit the result (2.246) in two different ways. Either we can fix K and determine the value of V from the data, which gives rise to the K-nearest-neighbour technique discussed shortly, or we can fix V and determine K from the data, giving rise to the kernel approach. It can be shown that both the K-nearest-neighbour density estimator and the kernel density estimator converge to the true probability density in the limit $N \to \infty$ provided V shrinks suitably with N, and K grows with N (Duda and Hart, 1973).

We begin by discussing the kernel method in detail, and to start with we take the region $\mathcal{R}$ to be a small hypercube centred on the point $\mathbf{x}$ at which we wish to determine the probability density. In order to count the number K of points falling within this region, it is convenient to define the following function

$$k(\mathbf{u}) = \begin{cases} 1, & |u_i| \leqslant 1/2, \qquad i = 1, \ldots, D, \\ 0, & \text{otherwise} \end{cases} \tag{2.247}$$

which represents a unit cube centred on the origin. The function $k(\mathbf{u})$ is an example of a *kernel function*, and in this context is also called a *Parzen window*. From (2.247), the quantity $k((\mathbf{x} - \mathbf{x}_n)/h)$ will be one if the data point $\mathbf{x}_n$ lies inside a cube of side h centred on $\mathbf{x}$, and zero otherwise. The total number of data points lying inside this cube will therefore be

$$K = \sum_{n=1}^{N} k\left(\frac{\mathbf{x} - \mathbf{x}_n}{h}\right). \tag{2.248}$$

Substituting this expression into (2.246) then gives the following result for the estimated density at $\mathbf{x}$

$$p(\mathbf{x}) = \frac{1}{N} \sum_{n=1}^{N} \frac{1}{h^D} k\left(\frac{\mathbf{x} - \mathbf{x}_n}{h}\right) \tag{2.249}$$

where we have used $V = h^D$ for the volume of a hypercube of side h in D dimensions. Using the symmetry of the function $k(\mathbf{u})$, we can now re-interpret this equation, not as a single cube centred on $\mathbf{x}$ but as the sum over N cubes centred on the N data points $\mathbf{x}_n$.

As it stands, the kernel density estimator (2.249) will suffer from one of the same problems that the histogram method suffered from, namely the presence of artificial discontinuities, in this case at the boundaries of the cubes. We can obtain a smoother density model if we choose a smoother kernel function, and a common choice is the Gaussian, which gives rise to the following kernel density model

$$p(\mathbf{x}) = \frac{1}{N} \sum_{n=1}^{N} \frac{1}{(2\pi h^2)^{1/2}} \exp\left\{ -\frac{\|\mathbf{x} - \mathbf{x}_n\|^2}{2h^2} \right\} \tag{2.250}$$

where h represents the standard deviation of the Gaussian components. Thus our density model is obtained by placing a Gaussian over each data point and then adding up the contributions over the whole data set, and then dividing by N so that the density is correctly normalized. In Figure 2.25, we apply the model (2.250) to the data

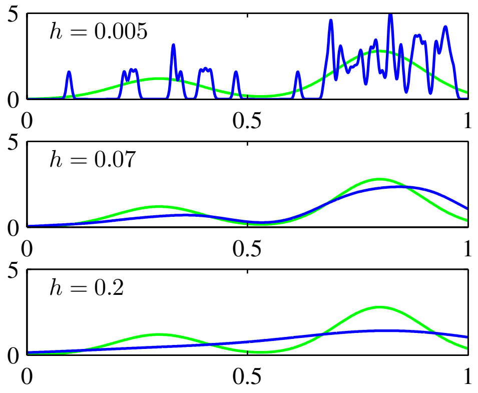

Figure 2.25 Illustration of the kernel density model (2.250) applied to the same data set used to demonstrate the histogram approach in Figure 2.24. We see that h acts as a smoothing parameter and that if it is set too small (top panel), the result is a very noisy density model, whereas if it is set too large (bottom panel), then the bimodal nature of the underlying distribution from which the data is generated (shown by the green curve) is washed out. The best density model is obtained for some intermediate value of h (middle panel).

set used earlier to demonstrate the histogram technique. We see that, as expected, the parameter h plays the role of a smoothing parameter, and there is a trade-off between sensitivity to noise at small h and over-smoothing at large h. Again, the optimization of h is a problem in model complexity, analogous to the choice of bin width in histogram density estimation, or the degree of the polynomial used in curve fitting.

We can choose any other kernel function $k(\mathbf{u})$ in (2.249) subject to the conditions

$$k(\mathbf{u}) \geqslant 0, \tag{2.251}$$

$$\int k(\mathbf{u})\,\mathrm{d}\mathbf{u} = 1 \tag{2.252}$$

which ensure that the resulting probability distribution is nonnegative everywhere and integrates to one. The class of density model given by (2.249) is called a kernel density estimator, or *Parzen* estimator. It has a great merit that there is no computation involved in the 'training' phase because this simply requires storage of the training set. However, this is also one of its great weaknesses because the computational cost of evaluating the density grows linearly with the size of the data set.

2.5.2 Nearest-neighbour methods

One of the difficulties with the kernel approach to density estimation is that the parameter h governing the kernel width is fixed for all kernels. In regions of high data density, a large value of h may lead to over-smoothing and a washing out of structure that might otherwise be extracted from the data. However, reducing h may lead to noisy estimates elsewhere in data space where the density is smaller. Thus the optimal choice for h may be dependent on location within the data space. This issue is addressed by nearest-neighbour methods for density estimation.

We therefore return to our general result (2.246) for local density estimation, and instead of fixing V and determining the value of K from the data, we consider a fixed value of K and use the data to find an appropriate value for V. To do this, we consider a small sphere centred on the point $\mathbf{x}$ at which we wish to estimate the

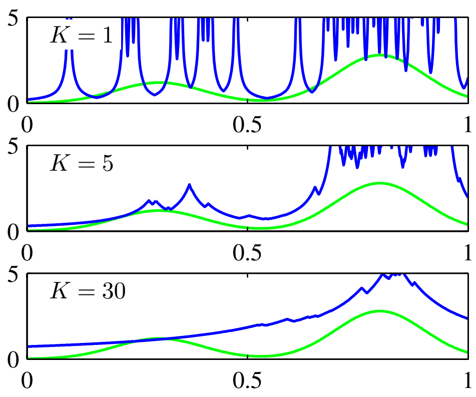

Figure 2.26 Illustration of K-nearest-neighbour density estimation using the same data set as in Figures 2.25 and 2.24. We see that the parameter K governs the degree of smoothing, so that a small value of K leads to a very noisy density model (top panel), whereas a large value (bottom panel) smoothes out the bimodal nature of the true distribution (shown by the green curve) from which the data set was generated.

density $p(\mathbf{x})$, and we allow the radius of the sphere to grow until it contains precisely K data points. The estimate of the density $p(\mathbf{x})$ is then given by (2.246) with V set to the volume of the resulting sphere. This technique is known as K *nearest neighbours* and is illustrated in Figure 2.26, for various choices of the parameter K, using the same data set as used in Figure 2.24 and Figure 2.25. We see that the value of K now governs the degree of smoothing and that again there is an optimum choice for K that is neither too large nor too small. Note that the model produced by K nearest neighbours is not a true density model because the integral over all space diverges. *Exercise 2.61*

We close this chapter by showing how the K-nearest-neighbour technique for density estimation can be extended to the problem of classification. To do this, we apply the K-nearest-neighbour density estimation technique to each class separately and then make use of Bayes' theorem. Let us suppose that we have a data set comprising N_k points in class $\mathcal{C}_k$ with N points in total, so that $\sum_k N_k = N$. If we wish to classify a new point $\mathbf{x}$, we draw a sphere centred on $\mathbf{x}$ containing precisely K points irrespective of their class. Suppose this sphere has volume V and contains K_k points from class $\mathcal{C}_k$. Then (2.246) provides an estimate of the density associated with each class

$$p(\mathbf{x}|\mathcal{C}_k) = \frac{K_k}{N_k V}. \tag{2.253}$$

Similarly, the unconditional density is given by

$$p(\mathbf{x}) = \frac{K}{NV} \tag{2.254}$$

while the class priors are given by

$$p(\mathcal{C}_k) = \frac{N_k}{N}. \tag{2.255}$$

We can now combine (2.253), (2.254), and (2.255) using Bayes' theorem to obtain the posterior probability of class membership

$$p(\mathcal{C}_k|\mathbf{x}) = \frac{p(\mathbf{x}|\mathcal{C}_k)p(\mathcal{C}_k)}{p(\mathbf{x})} = \frac{K_k}{K}. \tag{2.256}$$

Figure 2.27 (a) In the K-nearest-neighbour classifier, a new point, shown by the black diamond, is classified according to the majority class membership of the K closest training data points, in this case $K = 3$. (b) In the nearest-neighbour ($K = 1$) approach to classification, the resulting decision boundary is composed of hyperplanes that form perpendicular bisectors of pairs of points from different classes.

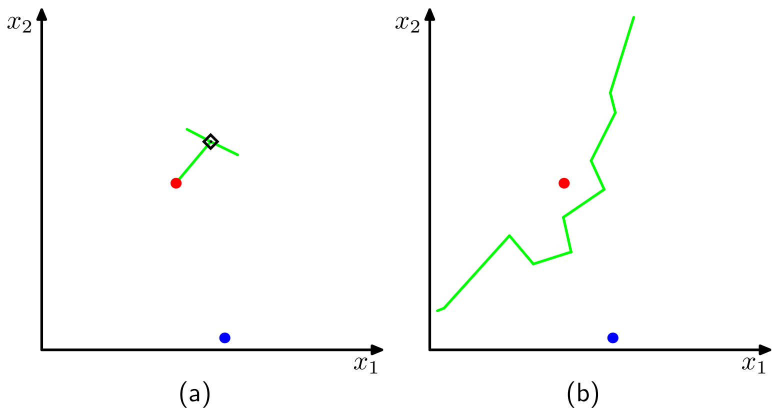

If we wish to minimize the probability of misclassification, this is done by assigning the test point $\mathbf{x}$ to the class having the largest posterior probability, corresponding to the largest value of K_k/K. Thus to classify a new point, we identify the K nearest points from the training data set and then assign the new point to the class having the largest number of representatives amongst this set. Ties can be broken at random. The particular case of $K = 1$ is called the *nearest-neighbour* rule, because a test point is simply assigned to the same class as the nearest point from the training set. These concepts are illustrated in Figure 2.27.

In Figure 2.28, we show the results of applying the K-nearest-neighbour algorithm to the oil flow data, introduced in Chapter 1, for various values of K. As expected, we see that K controls the degree of smoothing, so that small K produces many small regions of each class, whereas large K leads to fewer larger regions.

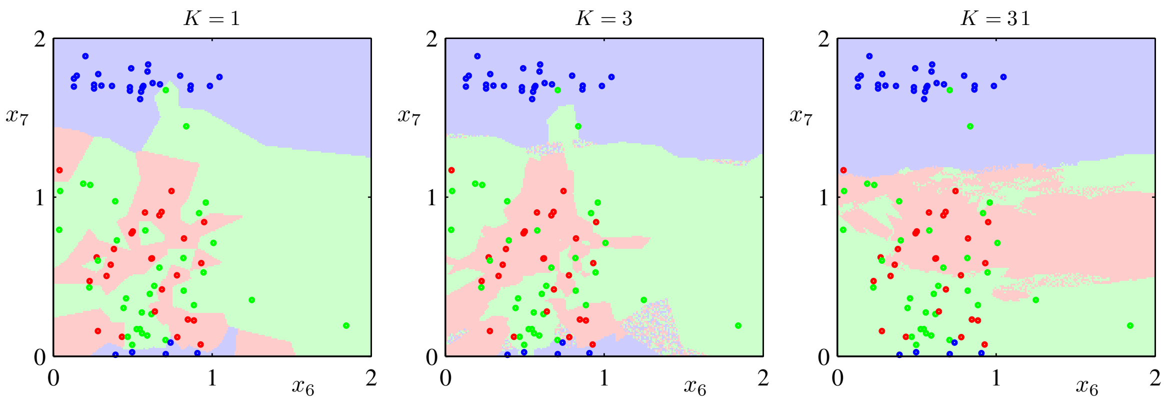

Figure 2.28 Plot of 200 data points from the oil data set showing values of x_6 plotted against x_7, where the red, green, and blue points correspond to the 'laminar', 'annular', and 'homogeneous' classes, respectively. Also shown are the classifications of the input space given by the K-nearest-neighbour algorithm for various values of K.

An interesting property of the nearest-neighbour ($K = 1$) classifier is that, in the limit $N \to \infty$, the error rate is never more than twice the minimum achievable error rate of an optimal classifier, i.e., one that uses the true class distributions (Cover and Hart, 1967) .

As discussed so far, both the K-nearest-neighbour method, and the kernel density estimator, require the entire training data set to be stored, leading to expensive computation if the data set is large. This effect can be offset, at the expense of some additional one-off computation, by constructing tree-based search structures to allow (approximate) near neighbours to be found efficiently without doing an exhaustive search of the data set. Nevertheless, these nonparametric methods are still severely limited. On the other hand, we have seen that simple parametric models are very restricted in terms of the forms of distribution that they can represent. We therefore need to find density models that are very flexible and yet for which the complexity of the models can be controlled independently of the size of the training set, and we shall see in subsequent chapters how to achieve this.

Exercises

2.1 ($\star$) **www** Verify that the Bernoulli distribution (2.2) satisfies the following properties

$$\sum_{x=0}^{1} p(x|\mu) = 1 \tag{2.257}$$

$$\mathbb{E}[x] = \mu \tag{2.258}$$

$$\mathrm{var}[x] = \mu(1-\mu). \tag{2.259}$$

Show that the entropy $\mathrm{H}[x]$ of a Bernoulli distributed random binary variable x is given by

$$\mathrm{H}[x] = -\mu \ln \mu - (1-\mu)\ln(1-\mu). \tag{2.260}$$

2.2 ($\star\star$) The form of the Bernoulli distribution given by (2.2) is not symmetric between the two values of x. In some situations, it will be more convenient to use an equivalent formulation for which $x \in \{-1, 1\}$, in which case the distribution can be written

$$p(x|\mu) = \left(\frac{1-\mu}{2}\right)^{(1-x)/2}\left(\frac{1+\mu}{2}\right)^{(1+x)/2} \tag{2.261}$$

where $\mu \in [-1, 1]$. Show that the distribution (2.261) is normalized, and evaluate its mean, variance, and entropy.

2.3 ($\star\star$) **www** In this exercise, we prove that the binomial distribution (2.9) is normalized. First use the definition (2.10) of the number of combinations of m identical objects chosen from a total of N to show that

$$\binom{N}{m} + \binom{N}{m-1} = \binom{N+1}{m}. \tag{2.262}$$

6 Kernel Methods

In Chapters 3 and 4, we considered linear parametric models for regression and classification in which the form of the mapping $y(\mathbf{x}, \mathbf{w})$ from input $\mathbf{x}$ to output y is governed by a vector $\mathbf{w}$ of adaptive parameters. During the learning phase, a set of training data is used either to obtain a point estimate of the parameter vector or to determine a posterior distribution over this vector. The training data is then discarded, and predictions for new inputs are based purely on the learned parameter vector $\mathbf{w}$. This approach is also used in nonlinear parametric models such as neural networks. *Chapter 5*

However, there is a class of pattern recognition techniques, in which the training data points, or a subset of them, are kept and used also during the prediction phase. For instance, the Parzen probability density model comprised a linear combination of 'kernel' functions each one centred on one of the training data points. Similarly, in Section 2.5.2 we introduced a simple technique for classification called nearest neighbours, which involved assigning to each new test vector the same label as the *Section 2.5.1* closest example from the training set. These are examples of *memory-based* methods that involve storing the entire training set in order to make predictions for future data points. They typically require a metric to be defined that measures the similarity of any two vectors in input space, and are generally fast to 'train' but slow at making predictions for test data points.

Many linear parametric models can be re-cast into an equivalent 'dual representation' in which the predictions are also based on linear combinations of a *kernel function* evaluated at the training data points. As we shall see, for models which are based on a fixed nonlinear *feature space* mapping $\boldsymbol{\phi}(\mathbf{x})$, the kernel function is given by the relation

$$k(\mathbf{x}, \mathbf{x}') = \boldsymbol{\phi}(\mathbf{x})^{\mathrm{T}}\boldsymbol{\phi}(\mathbf{x}'). \tag{6.1}$$

From this definition, we see that the kernel is a symmetric function of its arguments so that $k(\mathbf{x}, \mathbf{x}') = k(\mathbf{x}', \mathbf{x})$. The kernel concept was introduced into the field of pattern recognition by Aizerman *et al.* (1964) in the context of the method of potential functions, so-called because of an analogy with electrostatics. Although neglected for many years, it was re-introduced into machine learning in the context of large-margin classifiers by Boser *et al.* (1992) giving rise to the technique of *support vector machines*. Since then, there has been considerable interest in this topic, both in terms of theory and applications. One of the most significant developments has been the extension of kernels to handle symbolic objects, thereby greatly expanding the range of problems that can be addressed.

Chapter 7

The simplest example of a kernel function is obtained by considering the identity mapping for the feature space in (6.1) so that $\boldsymbol{\phi}(\mathbf{x}) = \mathbf{x}$, in which case $k(\mathbf{x}, \mathbf{x}') = \mathbf{x}^{\mathrm{T}}\mathbf{x}'$. We shall refer to this as the linear kernel.

The concept of a kernel formulated as an inner product in a feature space allows us to build interesting extensions of many well-known algorithms by making use of the *kernel trick*, also known as *kernel substitution*. The general idea is that, if we have an algorithm formulated in such a way that the input vector $\mathbf{x}$ enters only in the form of scalar products, then we can replace that scalar product with some other choice of kernel. For instance, the technique of kernel substitution can be applied to principal component analysis in order to develop a nonlinear variant of PCA (Schölkopf *et al.*, 1998). Other examples of kernel substitution include nearest-neighbour classifiers and the kernel Fisher discriminant (Mika *et al.*, 1999; Roth and Steinhage, 2000; Baudat and Anouar, 2000).

Section 12.3

There are numerous forms of kernel functions in common use, and we shall encounter several examples in this chapter. Many have the property of being a function only of the difference between the arguments, so that $k(\mathbf{x}, \mathbf{x}') = k(\mathbf{x} - \mathbf{x}')$, which are known as *stationary* kernels because they are invariant to translations in input space. A further specialization involves *homogeneous* kernels, also known as *radial basis functions*, which depend only on the magnitude of the distance (typically Euclidean) between the arguments so that $k(\mathbf{x}, \mathbf{x}') = k(\|\mathbf{x} - \mathbf{x}'\|)$.

Section 6.3

For recent textbooks on kernel methods, see Schölkopf and Smola (2002), Herbrich (2002), and Shawe-Taylor and Cristianini (2004).

6.1. Dual Representations

Many linear models for regression and classification can be reformulated in terms of a dual representation in which the kernel function arises naturally. This concept will play an important role when we consider support vector machines in the next chapter. Here we consider a linear regression model whose parameters are determined by minimizing a regularized sum-of-squares error function given by

$$J(\mathbf{w}) = \frac{1}{2}\sum_{n=1}^{N}\left\{\mathbf{w}^{\mathrm{T}}\boldsymbol{\phi}(\mathbf{x}_n) - t_n\right\}^2 + \frac{\lambda}{2}\mathbf{w}^{\mathrm{T}}\mathbf{w} \tag{6.2}$$

where $\lambda \geqslant 0$. If we set the gradient of $J(\mathbf{w})$ with respect to $\mathbf{w}$ equal to zero, we see that the solution for $\mathbf{w}$ takes the form of a linear combination of the vectors $\boldsymbol{\phi}(\mathbf{x}_n)$, with coefficients that are functions of $\mathbf{w}$, of the form

$$\mathbf{w} = -\frac{1}{\lambda}\sum_{n=1}^{N}\left\{\mathbf{w}^{\mathrm{T}}\boldsymbol{\phi}(\mathbf{x}_n) - t_n\right\}\boldsymbol{\phi}(\mathbf{x}_n) = \sum_{n=1}^{N} a_n\boldsymbol{\phi}(\mathbf{x}_n) = \boldsymbol{\Phi}^{\mathrm{T}}\mathbf{a} \tag{6.3}$$

where $\boldsymbol{\Phi}$ is the design matrix, whose n^{th} row is given by $\boldsymbol{\phi}(\mathbf{x}_n)^{\mathrm{T}}$. Here the vector $\mathbf{a} = (a_1, \ldots, a_N)^{\mathrm{T}}$, and we have defined

$$a_n = -\frac{1}{\lambda}\left\{\mathbf{w}^{\mathrm{T}}\boldsymbol{\phi}(\mathbf{x}_n) - t_n\right\}. \tag{6.4}$$

Instead of working with the parameter vector $\mathbf{w}$, we can now reformulate the least-squares algorithm in terms of the parameter vector $\mathbf{a}$, giving rise to a *dual representation*. If we substitute $\mathbf{w} = \boldsymbol{\Phi}^{\mathrm{T}}\mathbf{a}$ into $J(\mathbf{w})$, we obtain

$$J(\mathbf{a}) = \frac{1}{2}\mathbf{a}^{\mathrm{T}}\boldsymbol{\Phi}\boldsymbol{\Phi}^{\mathrm{T}}\boldsymbol{\Phi}\boldsymbol{\Phi}^{\mathrm{T}}\mathbf{a} - \mathbf{a}^{\mathrm{T}}\boldsymbol{\Phi}\boldsymbol{\Phi}^{\mathrm{T}}\mathbf{t} + \frac{1}{2}\mathbf{t}^{\mathrm{T}}\mathbf{t} + \frac{\lambda}{2}\mathbf{a}^{\mathrm{T}}\boldsymbol{\Phi}\boldsymbol{\Phi}^{\mathrm{T}}\mathbf{a} \tag{6.5}$$

where $\mathbf{t} = (t_1, \ldots, t_N)^{\mathrm{T}}$. We now define the *Gram* matrix $\mathbf{K} = \boldsymbol{\Phi}\boldsymbol{\Phi}^{\mathrm{T}}$, which is an $N \times N$ symmetric matrix with elements

$$K_{nm} = \boldsymbol{\phi}(\mathbf{x}_n)^{\mathrm{T}}\boldsymbol{\phi}(\mathbf{x}_m) = k(\mathbf{x}_n, \mathbf{x}_m) \tag{6.6}$$

where we have introduced the *kernel function* $k(\mathbf{x}, \mathbf{x}')$ defined by (6.1). In terms of the Gram matrix, the sum-of-squares error function can be written as

$$J(\mathbf{a}) = \frac{1}{2}\mathbf{a}^{\mathrm{T}}\mathbf{K}\mathbf{K}\mathbf{a} - \mathbf{a}^{\mathrm{T}}\mathbf{K}\mathbf{t} + \frac{1}{2}\mathbf{t}^{\mathrm{T}}\mathbf{t} + \frac{\lambda}{2}\mathbf{a}^{\mathrm{T}}\mathbf{K}\mathbf{a}. \tag{6.7}$$

Setting the gradient of $J(\mathbf{a})$ with respect to $\mathbf{a}$ to zero, we obtain the following solution

$$\mathbf{a} = (\mathbf{K} + \lambda\mathbf{I}_N)^{-1}\mathbf{t}. \tag{6.8}$$

If we substitute this back into the linear regression model, we obtain the following prediction for a new input $\mathbf{x}$

$$y(\mathbf{x}) = \mathbf{w}^{\mathrm{T}}\boldsymbol{\phi}(\mathbf{x}) = \mathbf{a}^{\mathrm{T}}\boldsymbol{\Phi}\boldsymbol{\phi}(\mathbf{x}) = \mathbf{k}(\mathbf{x})^{\mathrm{T}}\left(\mathbf{K} + \lambda\mathbf{I}_N\right)^{-1}\mathbf{t} \tag{6.9}$$

where we have defined the vector $\mathbf{k}(\mathbf{x})$ with elements $k_n(\mathbf{x}) = k(\mathbf{x}_n, \mathbf{x})$. Thus we see that the dual formulation allows the solution to the least-squares problem to be expressed entirely in terms of the kernel function $k(\mathbf{x}, \mathbf{x}')$. This is known as a dual formulation because, by noting that the solution for $\mathbf{a}$ can be expressed as a linear combination of the elements of $\boldsymbol{\phi}(\mathbf{x})$, we recover the original formulation in terms of the parameter vector $\mathbf{w}$. Note that the prediction at $\mathbf{x}$ is given by a linear combination of the target values from the training set. In fact, we have already obtained this result, using a slightly different notation, in Section 3.3.3.

Exercise 6.1

In the dual formulation, we determine the parameter vector $\mathbf{a}$ by inverting an $N \times N$ matrix, whereas in the original parameter space formulation we had to invert an $M \times M$ matrix in order to determine $\mathbf{w}$. Because N is typically much larger than M, the dual formulation does not seem to be particularly useful. However, the advantage of the dual formulation, as we shall see, is that it is expressed entirely in terms of the kernel function $k(\mathbf{x}, \mathbf{x}')$. We can therefore work directly in terms of kernels and avoid the explicit introduction of the feature vector $\boldsymbol{\phi}(\mathbf{x})$, which allows us implicitly to use feature spaces of high, even infinite, dimensionality.

The existence of a dual representation based on the Gram matrix is a property of many linear models, including the perceptron. In Section 6.4, we will develop a duality between probabilistic linear models for regression and the technique of Gaussian processes. Duality will also play an important role when we discuss support vector machines in Chapter 7.

Exercise 6.2

6.2. Constructing Kernels

In order to exploit kernel substitution, we need to be able to construct valid kernel functions. One approach is to choose a feature space mapping $\boldsymbol{\phi}(\mathbf{x})$ and then use this to find the corresponding kernel, as is illustrated in Figure 6.1. Here the kernel function is defined for a one-dimensional input space by

$$k(x, x') = \boldsymbol{\phi}(x)^{\mathrm{T}}\boldsymbol{\phi}(x') = \sum_{i=1}^{M} \phi_i(x)\phi_i(x') \tag{6.10}$$

where $\phi_i(x)$ are the basis functions.

An alternative approach is to construct kernel functions directly. In this case, we must ensure that the function we choose is a valid kernel, in other words that it corresponds to a scalar product in some (perhaps infinite dimensional) feature space. As a simple example, consider a kernel function given by

$$k(\mathbf{x}, \mathbf{z}) = \left(\mathbf{x}^{\mathrm{T}}\mathbf{z}\right)^2. \tag{6.11}$$

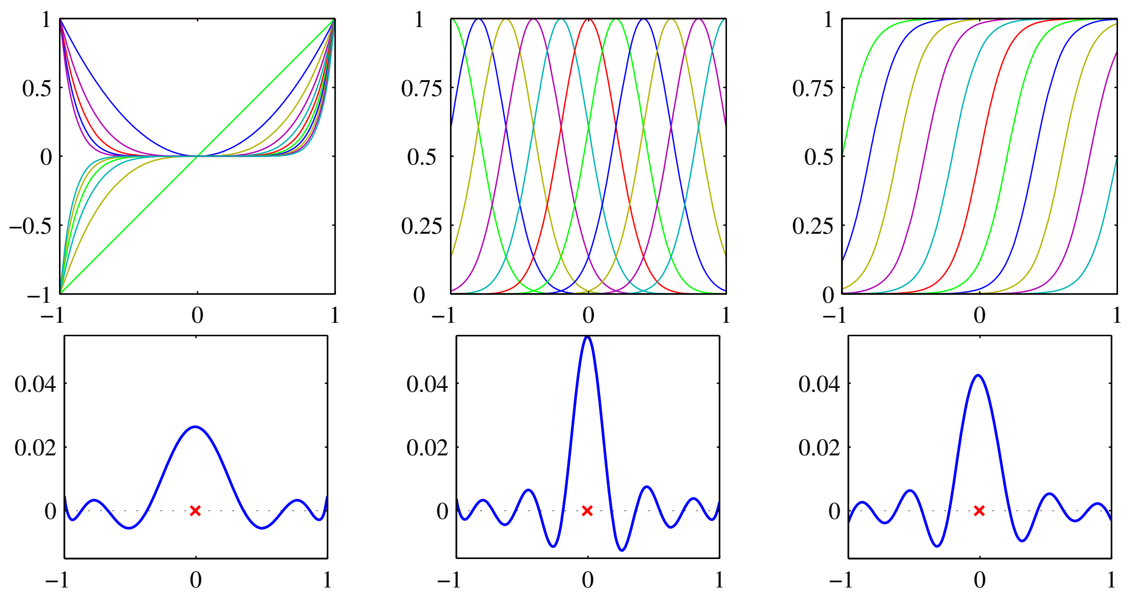

Figure 6.1 Illustration of the construction of kernel functions starting from a corresponding set of basis functions. In each column the lower plot shows the kernel function $k(x, x')$ defined by (6.10) plotted as a function of x for $x' = 0$, while the upper plot shows the corresponding basis functions given by polynomials (left column), 'Gaussians' (centre column), and logistic sigmoids (right column).

If we take the particular case of a two-dimensional input space $\mathbf{x} = (x_1, x_2)$ we can expand out the terms and thereby identify the corresponding nonlinear feature mapping

$$\begin{aligned} k(\mathbf{x}, \mathbf{z}) &= \left(\mathbf{x}^{\mathrm{T}}\mathbf{z}\right)^2 = (x_1 z_1 + x_2 z_2)^2 \\ &= x_1^2 z_1^2 + 2x_1 z_1 x_2 z_2 + x_2^2 z_2^2 \\ &= (x_1^2, \sqrt{2}x_1 x_2, x_2^2)(z_1^2, \sqrt{2}z_1 z_2, z_2^2)^{\mathrm{T}} \\ &= \boldsymbol{\phi}(\mathbf{x})^{\mathrm{T}}\boldsymbol{\phi}(\mathbf{z}). \end{aligned} \tag{6.12}$$

We see that the feature mapping takes the form $\boldsymbol{\phi}(\mathbf{x}) = (x_1^2, \sqrt{2}x_1 x_2, x_2^2)^{\mathrm{T}}$ and therefore comprises all possible second order terms, with a specific weighting between them.

More generally, however, we need a simple way to test whether a function constitutes a valid kernel without having to construct the function $\boldsymbol{\phi}(\mathbf{x})$ explicitly. A necessary and sufficient condition for a function $k(\mathbf{x}, \mathbf{x}')$ to be a valid kernel (Shawe-Taylor and Cristianini, 2004) is that the Gram matrix $\mathbf{K}$, whose elements are given by $k(\mathbf{x}_n, \mathbf{x}_m)$, should be positive semidefinite for all possible choices of the set $\{\mathbf{x}_n\}$. Note that a positive semidefinite matrix is not the same thing as a matrix whose elements are nonnegative.

Appendix C

One powerful technique for constructing new kernels is to build them out of simpler kernels as building blocks. This can be done using the following properties:

Techniques for Constructing New Kernels.

Given valid kernels $k_1(\mathbf{x}, \mathbf{x}')$ and $k_2(\mathbf{x}, \mathbf{x}')$, the following new kernels will also be valid:

$$\begin{aligned}
k(\mathbf{x}, \mathbf{x}') &= ck_1(\mathbf{x}, \mathbf{x}') && (6.13)\\
k(\mathbf{x}, \mathbf{x}') &= f(\mathbf{x})k_1(\mathbf{x}, \mathbf{x}')f(\mathbf{x}') && (6.14)\\
k(\mathbf{x}, \mathbf{x}') &= q\left(k_1(\mathbf{x}, \mathbf{x}')\right) && (6.15)\\
k(\mathbf{x}, \mathbf{x}') &= \exp\left(k_1(\mathbf{x}, \mathbf{x}')\right) && (6.16)\\
k(\mathbf{x}, \mathbf{x}') &= k_1(\mathbf{x}, \mathbf{x}') + k_2(\mathbf{x}, \mathbf{x}') && (6.17)\\
k(\mathbf{x}, \mathbf{x}') &= k_1(\mathbf{x}, \mathbf{x}')k_2(\mathbf{x}, \mathbf{x}') && (6.18)\\
k(\mathbf{x}, \mathbf{x}') &= k_3\left(\boldsymbol{\phi}(\mathbf{x}), \boldsymbol{\phi}(\mathbf{x}')\right) && (6.19)\\
k(\mathbf{x}, \mathbf{x}') &= \mathbf{x}^{\mathrm{T}}\mathbf{A}\mathbf{x}' && (6.20)\\
k(\mathbf{x}, \mathbf{x}') &= k_a(\mathbf{x}_a, \mathbf{x}'_a) + k_b(\mathbf{x}_b, \mathbf{x}'_b) && (6.21)\\
k(\mathbf{x}, \mathbf{x}') &= k_a(\mathbf{x}_a, \mathbf{x}'_a)k_b(\mathbf{x}_b, \mathbf{x}'_b) && (6.22)
\end{aligned}$$

where $c > 0$ is a constant, $f(\cdot)$ is any function, $q(\cdot)$ is a polynomial with nonnegative coefficients, $\boldsymbol{\phi}(\mathbf{x})$ is a function from $\mathbf{x}$ to $\mathbb{R}^M$, $k_3(\cdot, \cdot)$ is a valid kernel in $\mathbb{R}^M$, $\mathbf{A}$ is a symmetric positive semidefinite matrix, $\mathbf{x}_a$ and $\mathbf{x}_b$ are variables (not necessarily disjoint) with $\mathbf{x} = (\mathbf{x}_a, \mathbf{x}_b)$, and k_a and k_b are valid kernel functions over their respective spaces.

Equipped with these properties, we can now embark on the construction of more complex kernels appropriate to specific applications. We require that the kernel $k(\mathbf{x}, \mathbf{x}')$ be symmetric and positive semidefinite and that it expresses the appropriate form of similarity between $\mathbf{x}$ and $\mathbf{x}'$ according to the intended application. Here we consider a few common examples of kernel functions. For a more extensive discussion of 'kernel engineering', see Shawe-Taylor and Cristianini (2004).

We saw that the simple polynomial kernel $k(\mathbf{x}, \mathbf{x}') = \left(\mathbf{x}^{\mathrm{T}}\mathbf{x}'\right)^2$ contains only terms of degree two. If we consider the slightly generalized kernel $k(\mathbf{x}, \mathbf{x}') = \left(\mathbf{x}^{\mathrm{T}}\mathbf{x}' + c\right)^2$ with $c > 0$, then the corresponding feature mapping $\boldsymbol{\phi}(\mathbf{x})$ contains constant and linear terms as well as terms of order two. Similarly, $k(\mathbf{x}, \mathbf{x}') = \left(\mathbf{x}^{\mathrm{T}}\mathbf{x}'\right)^M$ contains all monomials of order M. For instance, if $\mathbf{x}$ and $\mathbf{x}'$ are two images, then the kernel represents a particular weighted sum of all possible products of M pixels in the first image with M pixels in the second image. This can similarly be generalized to include all terms up to degree M by considering $k(\mathbf{x}, \mathbf{x}') = \left(\mathbf{x}^{\mathrm{T}}\mathbf{x}' + c\right)^M$ with $c > 0$. Using the results (6.17) and (6.18) for combining kernels we see that these will all be valid kernel functions.

Another commonly used kernel takes the form

$$k(\mathbf{x}, \mathbf{x}') = \exp\left(-\|\mathbf{x} - \mathbf{x}'\|^2/2\sigma^2\right) \tag{6.23}$$

and is often called a 'Gaussian' kernel. Note, however, that in this context it is not interpreted as a probability density, and hence the normalization coefficient is omitted. We can see that this is a valid kernel by expanding the square

$$\|\mathbf{x} - \mathbf{x}'\|^2 = \mathbf{x}^{\mathrm{T}}\mathbf{x} + (\mathbf{x}')^{\mathrm{T}}\mathbf{x}' - 2\mathbf{x}^{\mathrm{T}}\mathbf{x}' \tag{6.24}$$

to give

$$k(\mathbf{x}, \mathbf{x}') = \exp\left(-\mathbf{x}^{\mathrm{T}}\mathbf{x}/2\sigma^2\right) \exp\left(\mathbf{x}^{\mathrm{T}}\mathbf{x}'/\sigma^2\right) \exp\left(-(\mathbf{x}')^{\mathrm{T}}\mathbf{x}'/2\sigma^2\right) \tag{6.25}$$

and then making use of (6.14) and (6.16), together with the validity of the linear kernel $k(\mathbf{x}, \mathbf{x}') = \mathbf{x}^{\mathrm{T}}\mathbf{x}'$. Note that the feature vector that corresponds to the Gaussian kernel has infinite dimensionality. *Exercise 6.11*

The Gaussian kernel is not restricted to the use of Euclidean distance. If we use kernel substitution in (6.24) to replace $\mathbf{x}^{\mathrm{T}}\mathbf{x}'$ with a nonlinear kernel $\kappa(\mathbf{x}, \mathbf{x}')$, we obtain

$$k(\mathbf{x}, \mathbf{x}') = \exp\left\{-\frac{1}{2\sigma^2}\left(\kappa(\mathbf{x}, \mathbf{x}) + \kappa(\mathbf{x}', \mathbf{x}') - 2\kappa(\mathbf{x}, \mathbf{x}')\right)\right\}. \tag{6.26}$$

An important contribution to arise from the kernel viewpoint has been the extension to inputs that are symbolic, rather than simply vectors of real numbers. Kernel functions can be defined over objects as diverse as graphs, sets, strings, and text documents. Consider, for instance, a fixed set and define a nonvectorial space consisting of all possible subsets of this set. If A_1 and A_2 are two such subsets then one simple choice of kernel would be

$$k(A_1, A_2) = 2^{|A_1 \cap A_2|} \tag{6.27}$$

where $A_1 \cap A_2$ denotes the intersection of sets A_1 and A_2, and $|A|$ denotes the number of subsets in A. This is a valid kernel function because it can be shown to correspond to an inner product in a feature space. *Exercise 6.12*

One powerful approach to the construction of kernels starts from a probabilistic generative model (Haussler, 1999), which allows us to apply generative models in a discriminative setting. Generative models can deal naturally with missing data and in the case of hidden Markov models can handle sequences of varying length. By contrast, discriminative models generally give better performance on discriminative tasks than generative models. It is therefore of some interest to combine these two approaches (Lasserre *et al.*, 2006). One way to combine them is to use a generative model to define a kernel, and then use this kernel in a discriminative approach.

Given a generative model $p(\mathbf{x})$ we can define a kernel by

$$k(\mathbf{x}, \mathbf{x}') = p(\mathbf{x})p(\mathbf{x}'). \tag{6.28}$$

This is clearly a valid kernel function because we can interpret it as an inner product in the one-dimensional feature space defined by the mapping $p(\mathbf{x})$. It says that two inputs $\mathbf{x}$ and $\mathbf{x}'$ are similar if they both have high probabilities. We can use (6.13) and (6.17) to extend this class of kernels by considering sums over products of different probability distributions, with positive weighting coefficients $p(i)$, of the form

$$k(\mathbf{x}, \mathbf{x}') = \sum_i p(\mathbf{x}|i)p(\mathbf{x}'|i)p(i). \tag{6.29}$$

This is equivalent, up to an overall multiplicative constant, to a mixture distribution in which the components factorize, with the index i playing the role of a 'latent' variable. Two inputs $\mathbf{x}$ and $\mathbf{x}'$ will give a large value for the kernel function, and hence appear similar, if they have significant probability under a range of different components. Taking the limit of an infinite sum, we can also consider kernels of the form

Section 9.2

$$k(\mathbf{x}, \mathbf{x}') = \int p(\mathbf{x}|\mathbf{z})p(\mathbf{x}'|\mathbf{z})p(\mathbf{z})\,\mathrm{d}\mathbf{z} \tag{6.30}$$

where $\mathbf{z}$ is a continuous latent variable.

Now suppose that our data consists of ordered sequences of length L so that an observation is given by $\mathbf{X} = \{\mathbf{x}_1, \ldots, \mathbf{x}_L\}$. A popular generative model for sequences is the hidden Markov model, which expresses the distribution $p(\mathbf{X})$ as a marginalization over a corresponding sequence of hidden states $\mathbf{Z} = \{\mathbf{z}_1, \ldots, \mathbf{z}_L\}$. We can use this approach to define a kernel function measuring the similarity of two sequences $\mathbf{X}$ and $\mathbf{X}'$ by extending the mixture representation (6.29) to give

Section 13.2

$$k(\mathbf{X}, \mathbf{X}') = \sum_{\mathbf{Z}} p(\mathbf{X}|\mathbf{Z})p(\mathbf{X}'|\mathbf{Z})p(\mathbf{Z}) \tag{6.31}$$

so that both observed sequences are generated by the same hidden sequence $\mathbf{Z}$. This model can easily be extended to allow sequences of differing length to be compared.

An alternative technique for using generative models to define kernel functions is known as the *Fisher kernel* (Jaakkola and Haussler, 1999). Consider a parametric generative model $p(\mathbf{x}|\boldsymbol{\theta})$ where $\boldsymbol{\theta}$ denotes the vector of parameters. The goal is to find a kernel that measures the similarity of two input vectors $\mathbf{x}$ and $\mathbf{x}'$ induced by the generative model. Jaakkola and Haussler (1999) consider the gradient with respect to $\boldsymbol{\theta}$, which defines a vector in a 'feature' space having the same dimensionality as $\boldsymbol{\theta}$. In particular, they consider the *Fisher score*

$$\mathbf{g}(\boldsymbol{\theta}, \mathbf{x}) = \nabla_{\boldsymbol{\theta}} \ln p(\mathbf{x}|\boldsymbol{\theta}) \tag{6.32}$$

from which the Fisher kernel is defined by

$$k(\mathbf{x}, \mathbf{x}') = \mathbf{g}(\boldsymbol{\theta}, \mathbf{x})^{\mathrm{T}}\mathbf{F}^{-1}\mathbf{g}(\boldsymbol{\theta}, \mathbf{x}'). \tag{6.33}$$

Here $\mathbf{F}$ is the *Fisher information matrix*, given by

$$\mathbf{F} = \mathbb{E}_{\mathbf{x}}\left[\mathbf{g}(\boldsymbol{\theta}, \mathbf{x})\mathbf{g}(\boldsymbol{\theta}, \mathbf{x})^{\mathrm{T}}\right] \tag{6.34}$$

where the expectation is with respect to $\mathbf{x}$ under the distribution $p(\mathbf{x}|\boldsymbol{\theta})$. This can be motivated from the perspective of *information geometry* (Amari, 1998), which considers the differential geometry of the space of model parameters. Here we simply note that the presence of the Fisher information matrix causes this kernel to be invariant under a nonlinear re-parameterization of the density model $\boldsymbol{\theta} \rightarrow \boldsymbol{\psi}(\boldsymbol{\theta})$.

Exercise 6.13

In practice, it is often infeasible to evaluate the Fisher information matrix. One approach is simply to replace the expectation in the definition of the Fisher information with the sample average, giving

$$\mathbf{F} \simeq \frac{1}{N}\sum_{n=1}^{N} \mathbf{g}(\boldsymbol{\theta}, \mathbf{x}_n)\mathbf{g}(\boldsymbol{\theta}, \mathbf{x}_n)^{\mathrm{T}}. \tag{6.35}$$

Section 12.1.3

This is the covariance matrix of the Fisher scores, and so the Fisher kernel corresponds to a whitening of these scores. More simply, we can just omit the Fisher information matrix altogether and use the noninvariant kernel

$$k(\mathbf{x}, \mathbf{x}') = \mathbf{g}(\boldsymbol{\theta}, \mathbf{x})^{\mathrm{T}} \mathbf{g}(\boldsymbol{\theta}, \mathbf{x}'). \tag{6.36}$$

An application of Fisher kernels to document retrieval is given by Hofmann (2000).

A final example of a kernel function is the sigmoidal kernel given by

$$k(\mathbf{x}, \mathbf{x}') = \tanh\left(a\mathbf{x}^{\mathrm{T}}\mathbf{x}' + b\right) \tag{6.37}$$

whose Gram matrix in general is not positive semidefinite. This form of kernel has, however, been used in practice (Vapnik, 1995), possibly because it gives kernel expansions such as the support vector machine a superficial resemblance to neural network models. As we shall see, in the limit of an infinite number of basis functions, a Bayesian neural network with an appropriate prior reduces to a Gaussian process, thereby providing a deeper link between neural networks and kernel methods.

Section 6.4.7

6.3. Radial Basis Function Networks

In Chapter 3, we discussed regression models based on linear combinations of fixed basis functions, although we did not discuss in detail what form those basis functions might take. One choice that has been widely used is that of *radial basis functions*, which have the property that each basis function depends only on the radial distance (typically Euclidean) from a centre $\boldsymbol{\mu}_j$, so that $\phi_j(\mathbf{x}) = h(\|\mathbf{x} - \boldsymbol{\mu}_j\|)$.

Historically, radial basis functions were introduced for the purpose of exact function interpolation (Powell, 1987). Given a set of input vectors $\{\mathbf{x}_1, \ldots, \mathbf{x}_N\}$ along with corresponding target values $\{t_1, \ldots, t_N\}$, the goal is to find a smooth function $f(\mathbf{x})$ that fits every target value exactly, so that $f(\mathbf{x}_n) = t_n$ for $n = 1, \ldots, N$. This is achieved by expressing $f(\mathbf{x})$ as a linear combination of radial basis functions, one centred on every data point

$$f(\mathbf{x}) = \sum_{n=1}^{N} w_n h(\|\mathbf{x} - \mathbf{x}_n\|). \tag{6.38}$$

The values of the coefficients $\{w_n\}$ are found by least squares, and because there are the same number of coefficients as there are constraints, the result is a function that fits every target value exactly. In pattern recognition applications, however, the target values are generally noisy, and exact interpolation is undesirable because this corresponds to an over-fitted solution.

Expansions in radial basis functions also arise from regularization theory (Poggio and Girosi, 1990; Bishop, 1995a). For a sum-of-squares error function with a regularizer defined in terms of a differential operator, the optimal solution is given by an expansion in the *Green's functions* of the operator (which are analogous to the eigenvectors of a discrete matrix), again with one basis function centred on each data point. If the differential operator is isotropic then the Green's functions depend only on the radial distance from the corresponding data point. Due to the presence of the regularizer, the solution no longer interpolates the training data exactly.

Another motivation for radial basis functions comes from a consideration of the interpolation problem when the input (rather than the target) variables are noisy (Webb, 1994; Bishop, 1995a). If the noise on the input variable $\mathbf{x}$ is described by a variable $\boldsymbol{\xi}$ having a distribution $\nu(\boldsymbol{\xi})$, then the sum-of-squares error function becomes

$$E = \frac{1}{2}\sum_{n=1}^{N}\int \{y(\mathbf{x}_n + \boldsymbol{\xi}) - t_n\}^2 \, \nu(\boldsymbol{\xi})\, \mathrm{d}\boldsymbol{\xi}. \tag{6.39}$$

Appendix D
Exercise 6.17

Using the calculus of variations, we can optimize with respect to the function $f(\mathbf{x})$ to give

$$y(\mathbf{x}_n) = \sum_{n=1}^{N} t_n h(\mathbf{x} - \mathbf{x}_n) \tag{6.40}$$

where the basis functions are given by

$$h(\mathbf{x} - \mathbf{x}_n) = \frac{\nu(\mathbf{x} - \mathbf{x}_n)}{\displaystyle\sum_{n=1}^{N} \nu(\mathbf{x} - \mathbf{x}_n)}. \tag{6.41}$$

We see that there is one basis function centred on every data point. This is known as the *Nadaraya-Watson* model and will be derived again from a different perspective in Section 6.3.1. If the noise distribution $\nu(\boldsymbol{\xi})$ is isotropic, so that it is a function only of $\|\boldsymbol{\xi}\|$, then the basis functions will be radial.

Note that the basis functions (6.41) are normalized, so that $\sum_n h(\mathbf{x} - \mathbf{x}_n) = 1$ for any value of $\mathbf{x}$. The effect of such normalization is shown in Figure 6.2. Normalization is sometimes used in practice as it avoids having regions of input space where all of the basis functions take small values, which would necessarily lead to predictions in such regions that are either small or controlled purely by the bias parameter.

Another situation in which expansions in normalized radial basis functions arise is in the application of kernel density estimation to the problem of regression, as we shall discuss in Section 6.3.1.

Because there is one basis function associated with every data point, the corresponding model can be computationally costly to evaluate when making predictions for new data points. Models have therefore been proposed (Broomhead and Lowe, 1988; Moody and Darken, 1989; Poggio and Girosi, 1990), which retain the expansion in radial basis functions but where the number M of basis functions is smaller than the number N of data points. Typically, the number of basis functions, and the locations $\boldsymbol{\mu}_i$ of their centres, are determined based on the input data $\{\mathbf{x}_n\}$ alone. The basis functions are then kept fixed and the coefficients $\{w_i\}$ are determined by least squares by solving the usual set of linear equations, as discussed in Section 3.1.1.

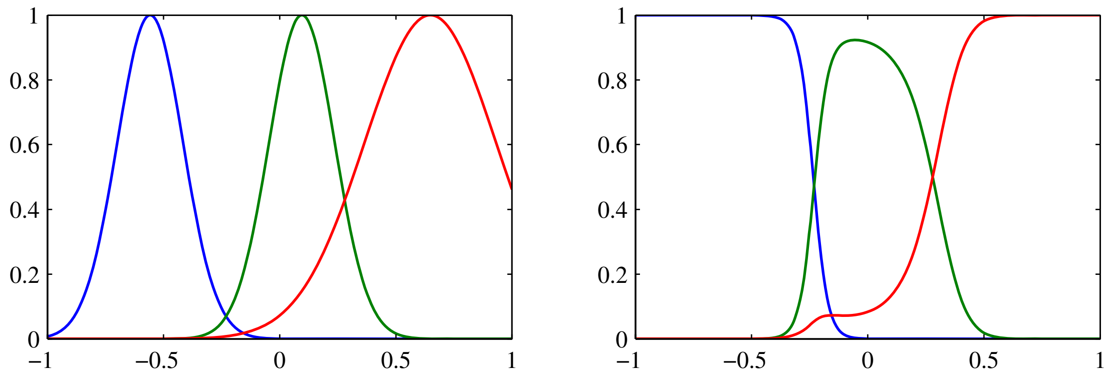

Figure 6.2 Plot of a set of Gaussian basis functions on the left, together with the corresponding normalized basis functions on the right.

One of the simplest ways of choosing basis function centres is to use a randomly chosen subset of the data points. A more systematic approach is called *orthogonal least squares* (Chen *et al.*, 1991). This is a sequential selection process in which at each step the next data point to be chosen as a basis function centre corresponds to the one that gives the greatest reduction in the sum-of-squares error. Values for the expansion coefficients are determined as part of the algorithm. Clustering algorithms such as K-means have also been used, which give a set of basis function centres that no longer coincide with training data points.

Section 9.1

6.3.1 Nadaraya-Watson model

In Section 3.3.3, we saw that the prediction of a linear regression model for a new input $\mathbf{x}$ takes the form of a linear combination of the training set target values with coefficients given by the 'equivalent kernel' (3.62) where the equivalent kernel satisfies the summation constraint (3.64).

We can motivate the kernel regression model (3.61) from a different perspective, starting with kernel density estimation. Suppose we have a training set $\{\mathbf{x}_n, t_n\}$ and we use a Parzen density estimator to model the joint distribution $p(\mathbf{x}, t)$, so that

Section 2.5.1

$$p(\mathbf{x}, t) = \frac{1}{N} \sum_{n=1}^{N} f(\mathbf{x} - \mathbf{x}_n, t - t_n) \tag{6.42}$$

where $f(\mathbf{x}, t)$ is the component density function, and there is one such component centred on each data point. We now find an expression for the regression function $y(\mathbf{x})$, corresponding to the conditional average of the target variable conditioned on the input variable, which is given by

$$\begin{aligned} y(\mathbf{x}) &= \mathbb{E}[t|\mathbf{x}] = \int_{-\infty}^{\infty} tp(t|\mathbf{x})\,\mathrm{d}t \\ &= \frac{\displaystyle\int tp(\mathbf{x},t)\,\mathrm{d}t}{\displaystyle\int p(\mathbf{x},t)\,\mathrm{d}t} \\ &= \frac{\displaystyle\sum_n \int tf(\mathbf{x}-\mathbf{x}_n, t-t_n)\,\mathrm{d}t}{\displaystyle\sum_m \int f(\mathbf{x}-\mathbf{x}_m, t-t_m)\,\mathrm{d}t}. \end{aligned} \tag{6.43}$$

We now assume for simplicity that the component density functions have zero mean so that

$$\int_{-\infty}^{\infty} f(\mathbf{x},t)t\,\mathrm{d}t = 0 \tag{6.44}$$

for all values of $\mathbf{x}$. Using a simple change of variable, we then obtain

$$\begin{aligned} y(\mathbf{x}) &= \frac{\displaystyle\sum_n g(\mathbf{x}-\mathbf{x}_n)t_n}{\displaystyle\sum_m g(\mathbf{x}-\mathbf{x}_m)} \\ &= \sum_n k(\mathbf{x},\mathbf{x}_n)t_n \end{aligned} \tag{6.45}$$

where $n, m = 1, \ldots, N$ and the kernel function $k(\mathbf{x},\mathbf{x}_n)$ is given by

$$k(\mathbf{x},\mathbf{x}_n) = \frac{g(\mathbf{x}-\mathbf{x}_n)}{\displaystyle\sum_m g(\mathbf{x}-\mathbf{x}_m)} \tag{6.46}$$

and we have defined

$$g(\mathbf{x}) = \int_{-\infty}^{\infty} f(\mathbf{x},t)\,\mathrm{d}t. \tag{6.47}$$

The result (6.45) is known as the *Nadaraya-Watson* model, or *kernel regression* (Nadaraya, 1964; Watson, 1964). For a localized kernel function, it has the property of giving more weight to the data points $\mathbf{x}_n$ that are close to $\mathbf{x}$. Note that the kernel (6.46) satisfies the summation constraint

$$\sum_{n=1}^{N} k(\mathbf{x},\mathbf{x}_n) = 1.$$

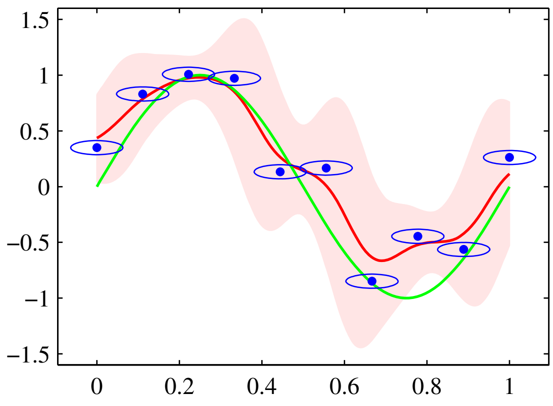

Figure 6.3 Illustration of the Nadaraya-Watson kernel regression model using isotropic Gaussian kernels, for the sinusoidal data set. The original sine function is shown by the green curve, the data points are shown in blue, and each is the centre of an isotropic Gaussian kernel. The resulting regression function, given by the conditional mean, is shown by the red line, along with the two-standard-deviation region for the conditional distribution $p(t|x)$ shown by the red shading. The blue ellipse around each data point shows one standard deviation contour for the corresponding kernel. These appear noncircular due to the different scales on the horizontal and vertical axes.

In fact, this model defines not only a conditional expectation but also a full conditional distribution given by

$$p(t|\mathbf{x}) = \frac{p(t,\mathbf{x})}{\displaystyle\int p(t,\mathbf{x})\,\mathrm{d}t} = \frac{\displaystyle\sum_n f(\mathbf{x}-\mathbf{x}_n, t-t_n)}{\displaystyle\sum_m \int f(\mathbf{x}-\mathbf{x}_m, t-t_m)\,\mathrm{d}t} \tag{6.48}$$

from which other expectations can be evaluated.

As an illustration we consider the case of a single input variable x in which $f(x,t)$ is given by a zero-mean isotropic Gaussian over the variable $\mathbf{z} = (x,t)$ with variance σ^2. The corresponding conditional distribution (6.48) is given by a Gaussian mixture, and is shown, together with the conditional mean, for the sinusoidal synthetic data set in Figure 6.3.

Exercise 6.18

An obvious extension of this model is to allow for more flexible forms of Gaussian components, for instance having different variance parameters for the input and target variables. More generally, we could model the joint distribution $p(t,\mathbf{x})$ using a Gaussian mixture model, trained using techniques discussed in Chapter 9 (Ghahramani and Jordan, 1994), and then find the corresponding conditional distribution $p(t|\mathbf{x})$. In this latter case we no longer have a representation in terms of kernel functions evaluated at the training set data points. However, the number of components in the mixture model can be smaller than the number of training set points, resulting in a model that is faster to evaluate for test data points. We have thereby accepted an increased computational cost during the training phase in order to have a model that is faster at making predictions.

6.4. Gaussian Processes

In Section 6.1, we introduced kernels by applying the concept of duality to a non-probabilistic model for regression. Here we extend the role of kernels to probabilistic discriminative models, leading to the framework of Gaussian processes. We shall thereby see how kernels arise naturally in a Bayesian setting.

In Chapter 3, we considered linear regression models of the form $y(\mathbf{x}, \mathbf{w}) = \mathbf{w}^{\mathrm{T}}\boldsymbol{\phi}(\mathbf{x})$ in which $\mathbf{w}$ is a vector of parameters and $\boldsymbol{\phi}(\mathbf{x})$ is a vector of fixed nonlinear basis functions that depend on the input vector $\mathbf{x}$. We showed that a prior distribution over $\mathbf{w}$ induced a corresponding prior distribution over functions $y(\mathbf{x}, \mathbf{w})$. Given a training data set, we then evaluated the posterior distribution over $\mathbf{w}$ and thereby obtained the corresponding posterior distribution over regression functions, which in turn (with the addition of noise) implies a predictive distribution $p(t|\mathbf{x})$ for new input vectors $\mathbf{x}$.

In the Gaussian process viewpoint, we dispense with the parametric model and instead define a prior probability distribution over functions directly. At first sight, it might seem difficult to work with a distribution over the uncountably infinite space of functions. However, as we shall see, for a finite training set we only need to consider the values of the function at the discrete set of input values $\mathbf{x}_n$ corresponding to the training set and test set data points, and so in practice we can work in a finite space.

Models equivalent to Gaussian processes have been widely studied in many different fields. For instance, in the geostatistics literature Gaussian process regression is known as *kriging* (Cressie, 1993). Similarly, ARMA (autoregressive moving average) models, Kalman filters, and radial basis function networks can all be viewed as forms of Gaussian process models. Reviews of Gaussian processes from a machine learning perspective can be found in MacKay (1998), Williams (1999), and MacKay (2003), and a comparison of Gaussian process models with alternative approaches is given in Rasmussen (1996). See also Rasmussen and Williams (2006) for a recent textbook on Gaussian processes.

6.4.1 Linear regression revisited

In order to motivate the Gaussian process viewpoint, let us return to the linear regression example and re-derive the predictive distribution by working in terms of distributions over functions $y(\mathbf{x}, \mathbf{w})$. This will provide a specific example of a Gaussian process.

Consider a model defined in terms of a linear combination of M fixed basis functions given by the elements of the vector $\boldsymbol{\phi}(\mathbf{x})$ so that

$$y(\mathbf{x}) = \mathbf{w}^{\mathrm{T}}\boldsymbol{\phi}(\mathbf{x}) \tag{6.49}$$

where $\mathbf{x}$ is the input vector and $\mathbf{w}$ is the M-dimensional weight vector. Now consider a prior distribution over $\mathbf{w}$ given by an isotropic Gaussian of the form

$$p(\mathbf{w}) = \mathcal{N}(\mathbf{w}|\mathbf{0}, \alpha^{-1}\mathbf{I}) \tag{6.50}$$

governed by the hyperparameter α, which represents the precision (inverse variance) of the distribution. For any given value of $\mathbf{w}$, the definition (6.49) defines a particular function of $\mathbf{x}$. The probability distribution over $\mathbf{w}$ defined by (6.50) therefore induces a probability distribution over functions $y(\mathbf{x})$. In practice, we wish to evaluate this function at specific values of $\mathbf{x}$, for example at the training data points

$\mathbf{x}_1, \ldots, \mathbf{x}_N$. We are therefore interested in the joint distribution of the function values $y(\mathbf{x}_1), \ldots, y(\mathbf{x}_N)$, which we denote by the vector y with elements $y_n = y(\mathbf{x}_n)$ for $n = 1, \ldots, N$. From (6.49), this vector is given by

$$\mathsf{y} = \mathbf{\Phi}\mathbf{w} \tag{6.51}$$

where $\mathbf{\Phi}$ is the design matrix with elements $\Phi_{nk} = \phi_k(\mathbf{x}_n)$. We can find the probability distribution of y as follows. First of all we note that y is a linear combination of Gaussian distributed variables given by the elements of $\mathbf{w}$ and hence is itself Gaussian. We therefore need only to find its mean and covariance, which are given from (6.50) by

Exercise 2.31

$$\mathbb{E}[\mathsf{y}] = \mathbf{\Phi}\mathbb{E}[\mathbf{w}] = \mathbf{0} \tag{6.52}$$

$$\operatorname{cov}[\mathsf{y}] = \mathbb{E}\left[\mathsf{y}\mathsf{y}^{\mathrm{T}}\right] = \mathbf{\Phi}\mathbb{E}\left[\mathbf{w}\mathbf{w}^{\mathrm{T}}\right]\mathbf{\Phi}^{\mathrm{T}} = \frac{1}{\alpha}\mathbf{\Phi}\mathbf{\Phi}^{\mathrm{T}} = \mathbf{K} \tag{6.53}$$

where $\mathbf{K}$ is the Gram matrix with elements

$$K_{nm} = k(\mathbf{x}_n, \mathbf{x}_m) = \frac{1}{\alpha}\boldsymbol{\phi}(\mathbf{x}_n)^{\mathrm{T}}\boldsymbol{\phi}(\mathbf{x}_m) \tag{6.54}$$

and $k(\mathbf{x}, \mathbf{x}')$ is the kernel function.

This model provides us with a particular example of a Gaussian process. In general, a Gaussian process is defined as a probability distribution over functions $y(\mathbf{x})$ such that the set of values of $y(\mathbf{x})$ evaluated at an arbitrary set of points $\mathbf{x}_1, \ldots, \mathbf{x}_N$ jointly have a Gaussian distribution. In cases where the input vector $\mathbf{x}$ is two dimensional, this may also be known as a *Gaussian random field*. More generally, a *stochastic process* $y(\mathbf{x})$ is specified by giving the joint probability distribution for any finite set of values $y(\mathbf{x}_1), \ldots, y(\mathbf{x}_N)$ in a consistent manner.

A key point about Gaussian stochastic processes is that the joint distribution over N variables $y_1, \ldots, y_N$ is specified completely by the second-order statistics, namely the mean and the covariance. In most applications, we will not have any prior knowledge about the mean of $y(\mathbf{x})$ and so by symmetry we take it to be zero. This is equivalent to choosing the mean of the prior over weight values $p(\mathbf{w}|\alpha)$ to be zero in the basis function viewpoint. The specification of the Gaussian process is then completed by giving the covariance of $y(\mathbf{x})$ evaluated at any two values of $\mathbf{x}$, which is given by the kernel function

$$\mathbb{E}\left[y(\mathbf{x}_n)y(\mathbf{x}_m)\right] = k(\mathbf{x}_n, \mathbf{x}_m). \tag{6.55}$$

For the specific case of a Gaussian process defined by the linear regression model (6.49) with a weight prior (6.50), the kernel function is given by (6.54).

We can also define the kernel function directly, rather than indirectly through a choice of basis function. Figure 6.4 shows samples of functions drawn from Gaussian processes for two different choices of kernel function. The first of these is a 'Gaussian' kernel of the form (6.23), and the second is the exponential kernel given by

$$k(x, x') = \exp\left(-\theta\,|x - x'|\right) \tag{6.56}$$

which corresponds to the *Ornstein-Uhlenbeck process* originally introduced by Uhlenbeck and Ornstein (1930) to describe Brownian motion.

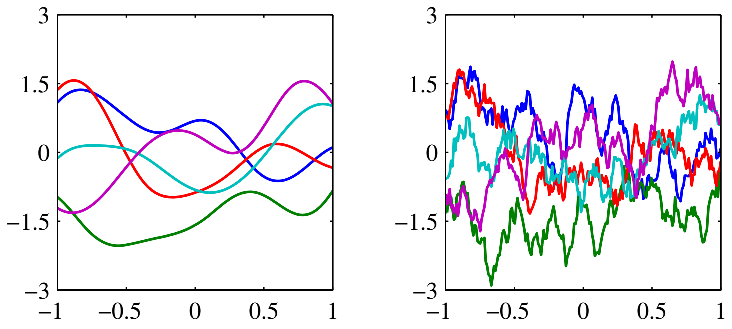

Figure 6.4 Samples from Gaussian processes for a 'Gaussian' kernel (left) and an exponential kernel (right).

6.4.2 Gaussian processes for regression

In order to apply Gaussian process models to the problem of regression, we need to take account of the noise on the observed target values, which are given by

$$t_n = y_n + \epsilon_n \tag{6.57}$$

where $y_n = y(\mathbf{x}_n)$, and ϵ_n is a random noise variable whose value is chosen independently for each observation n. Here we shall consider noise processes that have a Gaussian distribution, so that

$$p(t_n|y_n) = \mathcal{N}(t_n|y_n, \beta^{-1}) \tag{6.58}$$

where β is a hyperparameter representing the precision of the noise. Because the noise is independent for each data point, the joint distribution of the target values $\mathbf{t} = (t_1, \ldots, t_N)^{\mathrm{T}}$ conditioned on the values of $\mathbf{y} = (y_1, \ldots, y_N)^{\mathrm{T}}$ is given by an isotropic Gaussian of the form

$$p(\mathbf{t}|\mathbf{y}) = \mathcal{N}(\mathbf{t}|\mathbf{y}, \beta^{-1}\mathbf{I}_N) \tag{6.59}$$

where $\mathbf{I}_N$ denotes the $N \times N$ unit matrix. From the definition of a Gaussian process, the marginal distribution $p(\mathbf{y})$ is given by a Gaussian whose mean is zero and whose covariance is defined by a Gram matrix $\mathbf{K}$ so that

$$p(\mathbf{y}) = \mathcal{N}(\mathbf{y}|\mathbf{0}, \mathbf{K}). \tag{6.60}$$

The kernel function that determines $\mathbf{K}$ is typically chosen to express the property that, for points $\mathbf{x}_n$ and $\mathbf{x}_m$ that are similar, the corresponding values $y(\mathbf{x}_n)$ and $y(\mathbf{x}_m)$ will be more strongly correlated than for dissimilar points. Here the notion of similarity will depend on the application.

In order to find the marginal distribution $p(\mathbf{t})$, conditioned on the input values $\mathbf{x}_1, \ldots, \mathbf{x}_N$, we need to integrate over $\mathbf{y}$. This can be done by making use of the results from Section 2.3.3 for the linear-Gaussian model. Using (2.115), we see that the marginal distribution of $\mathbf{t}$ is given by

$$p(\mathbf{t}) = \int p(\mathbf{t}|\mathbf{y})p(\mathbf{y})\,\mathrm{d}\mathbf{y} = \mathcal{N}(\mathbf{t}|\mathbf{0}, \mathbf{C}) \tag{6.61}$$

where the covariance matrix $\mathbf{C}$ has elements

$$C(\mathbf{x}_n, \mathbf{x}_m) = k(\mathbf{x}_n, \mathbf{x}_m) + \beta^{-1}\delta_{nm}. \tag{6.62}$$

This result reflects the fact that the two Gaussian sources of randomness, namely that associated with $y(\mathbf{x})$ and that associated with ϵ, are independent and so their covariances simply add.

One widely used kernel function for Gaussian process regression is given by the exponential of a quadratic form, with the addition of constant and linear terms to give

$$k(\mathbf{x}_n, \mathbf{x}_m) = \theta_0 \exp\left\{-\frac{\theta_1}{2}\|\mathbf{x}_n - \mathbf{x}_m\|^2\right\} + \theta_2 + \theta_3\mathbf{x}_n^{\mathrm{T}}\mathbf{x}_m. \tag{6.63}$$

Note that the term involving θ_3 corresponds to a parametric model that is a linear function of the input variables. Samples from this prior are plotted for various values of the parameters $\theta_0, \ldots, \theta_3$ in Figure 6.5, and Figure 6.6 shows a set of points sampled from the joint distribution (6.60) along with the corresponding values defined by (6.61).

So far, we have used the Gaussian process viewpoint to build a model of the joint distribution over sets of data points. Our goal in regression, however, is to make predictions of the target variables for new inputs, given a set of training data. Let us suppose that $\mathbf{t}_N = (t_1, \ldots, t_N)^{\mathrm{T}}$, corresponding to input values $\mathbf{x}_1, \ldots, \mathbf{x}_N$, comprise the observed training set, and our goal is to predict the target variable t_{N+1} for a new input vector $\mathbf{x}_{N+1}$. This requires that we evaluate the predictive distribution $p(t_{N+1}|\mathbf{t}_N)$. Note that this distribution is conditioned also on the variables $\mathbf{x}_1, \ldots, \mathbf{x}_N$ and $\mathbf{x}_{N+1}$. However, to keep the notation simple we will not show these conditioning variables explicitly.

To find the conditional distribution $p(t_{N+1}|\mathbf{t})$, we begin by writing down the joint distribution $p(\mathbf{t}_{N+1})$, where $\mathbf{t}_{N+1}$ denotes the vector $(t_1, \ldots, t_N, t_{N+1})^{\mathrm{T}}$. We then apply the results from Section 2.3.1 to obtain the required conditional distribution, as illustrated in Figure 6.7.

From (6.61), the joint distribution over $t_1, \ldots, t_{N+1}$ will be given by

$$p(\mathbf{t}_{N+1}) = \mathcal{N}(\mathbf{t}_{N+1}|\mathbf{0}, \mathbf{C}_{N+1}) \tag{6.64}$$

where $\mathbf{C}_{N+1}$ is an $(N+1) \times (N+1)$ covariance matrix with elements given by (6.62). Because this joint distribution is Gaussian, we can apply the results from Section 2.3.1 to find the conditional Gaussian distribution. To do this, we partition the covariance matrix as follows

$$\mathbf{C}_{N+1} = \begin{pmatrix} \mathbf{C}_N & \mathbf{k} \\ \mathbf{k}^{\mathrm{T}} & c \end{pmatrix} \tag{6.65}$$

where $\mathbf{C}_N$ is the $N \times N$ covariance matrix with elements given by (6.62) for $n, m = 1, \ldots, N$, the vector $\mathbf{k}$ has elements $k(\mathbf{x}_n, \mathbf{x}_{N+1})$ for $n = 1, \ldots, N$, and the scalar

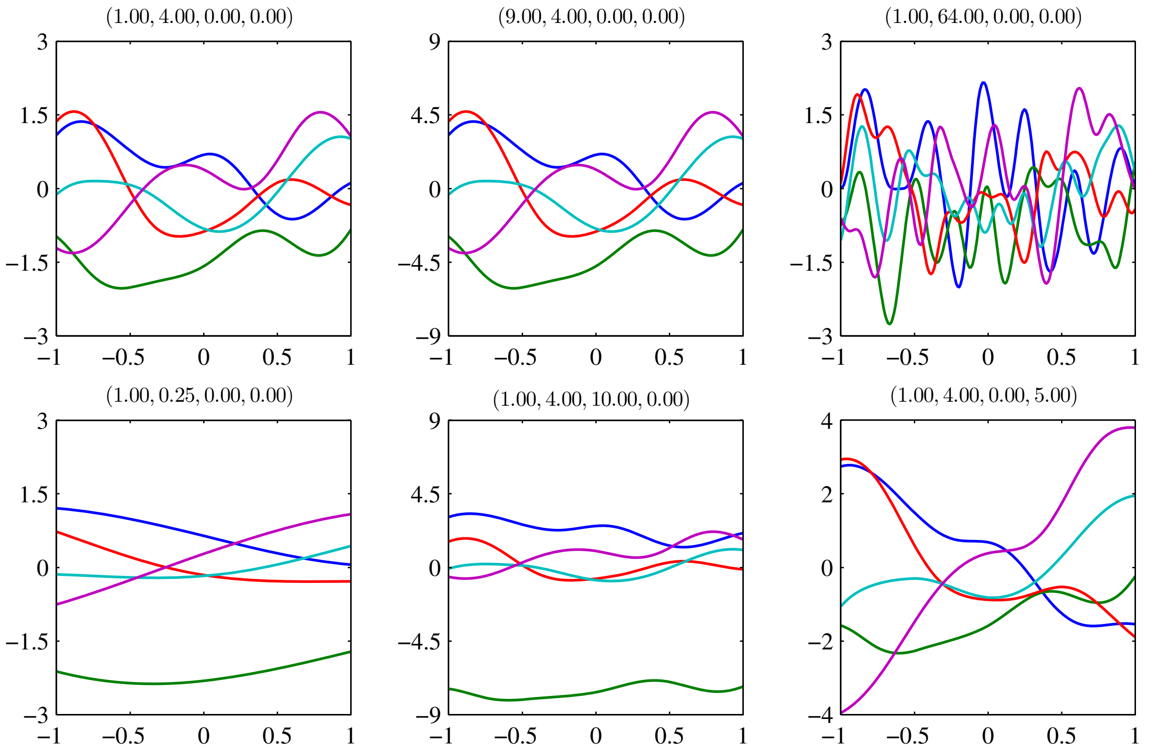

Figure 6.5 Samples from a Gaussian process prior defined by the covariance function (6.63). The title above each plot denotes $(\theta_0, \theta_1, \theta_2, \theta_3)$.

$c = k(\mathbf{x}_{N+1}, \mathbf{x}_{N+1}) + \beta^{-1}$. Using the results (2.81) and (2.82), we see that the conditional distribution $p(t_{N+1}|\mathbf{t})$ is a Gaussian distribution with mean and covariance given by

$$m(\mathbf{x}_{N+1}) = \mathbf{k}^{\mathrm{T}}\mathbf{C}_N^{-1}\mathbf{t} \tag{6.66}$$

$$\sigma^2(\mathbf{x}_{N+1}) = c - \mathbf{k}^{\mathrm{T}}\mathbf{C}_N^{-1}\mathbf{k}. \tag{6.67}$$

These are the key results that define Gaussian process regression. Because the vector $\mathbf{k}$ is a function of the test point input value $\mathbf{x}_{N+1}$, we see that the predictive distribution is a Gaussian whose mean and variance both depend on $\mathbf{x}_{N+1}$. An example of Gaussian process regression is shown in Figure 6.8.

The only restriction on the kernel function is that the covariance matrix given by (6.62) must be positive definite. If λ_i is an eigenvalue of $\mathbf{K}$, then the corresponding eigenvalue of $\mathbf{C}$ will be $\lambda_i + \beta^{-1}$. It is therefore sufficient that the kernel matrix $k(\mathbf{x}_n, \mathbf{x}_m)$ be positive semidefinite for any pair of points $\mathbf{x}_n$ and $\mathbf{x}_m$, so that $\lambda_i \geqslant 0$, because any eigenvalue λ_i that is zero will still give rise to a positive eigenvalue for $\mathbf{C}$ because $\beta > 0$. This is the same restriction on the kernel function discussed earlier, and so we can again exploit all of the techniques in Section 6.2 to construct

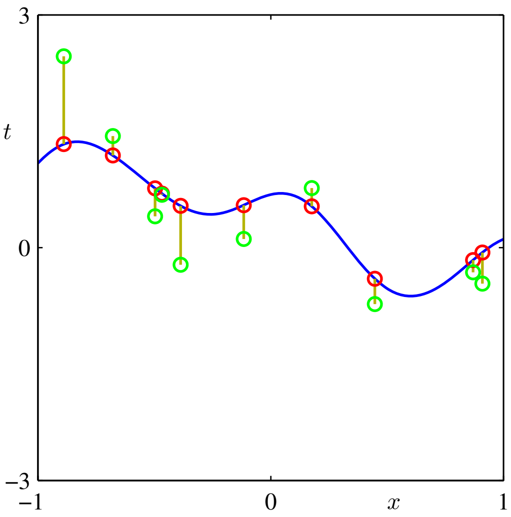

Figure 6.6 Illustration of the sampling of data points $\{t_n\}$ from a Gaussian process. The blue curve shows a sample function from the Gaussian process prior over functions, and the red points show the values of y_n obtained by evaluating the function at a set of input values $\{x_n\}$. The corresponding values of $\{t_n\}$, shown in green, are obtained by adding independent Gaussian noise to each of the $\{y_n\}$.

suitable kernels.

Note that the mean (6.66) of the predictive distribution can be written, as a function of $\mathbf{x}_{N+1}$, in the form

$$m(\mathbf{x}_{N+1}) = \sum_{n=1}^{N} a_n k(\mathbf{x}_n, \mathbf{x}_{N+1}) \tag{6.68}$$

where a_n is the n^{th} component of $\mathbf{C}_N^{-1}\mathbf{t}$. Thus, if the kernel function $k(\mathbf{x}_n, \mathbf{x}_m)$ depends only on the distance $\|\mathbf{x}_n - \mathbf{x}_m\|$, then we obtain an expansion in radial basis functions.

The results (6.66) and (6.67) define the predictive distribution for Gaussian process regression with an arbitrary kernel function $k(\mathbf{x}_n, \mathbf{x}_m)$. In the particular case in which the kernel function $k(\mathbf{x}, \mathbf{x}')$ is defined in terms of a finite set of basis functions, we can derive the results obtained previously in Section 3.3.2 for linear regression starting from the Gaussian process viewpoint.

Exercise 6.21

For such models, we can therefore obtain the predictive distribution either by taking a parameter space viewpoint and using the linear regression result or by taking a function space viewpoint and using the Gaussian process result.

The central computational operation in using Gaussian processes will involve the inversion of a matrix of size $N \times N$, for which standard methods require $O(N^3)$ computations. By contrast, in the basis function model we have to invert a matrix $\mathbf{S}_N$ of size $M \times M$, which has $O(M^3)$ computational complexity. Note that for both viewpoints, the matrix inversion must be performed once for the given training set. For each new test point, both methods require a vector-matrix multiply, which has cost $O(N^2)$ in the Gaussian process case and $O(M^2)$ for the linear basis function model. If the number M of basis functions is smaller than the number N of data points, it will be computationally more efficient to work in the basis function

Figure 6.7 Illustration of the mechanism of Gaussian process regression for the case of one training point and one test point, in which the red ellipses show contours of the joint distribution $p(t_1, t_2)$. Here t_1 is the training data point, and conditioning on the value of t_1, corresponding to the vertical blue line, we obtain $p(t_2|t_1)$ shown as a function of t_2 by the green curve.

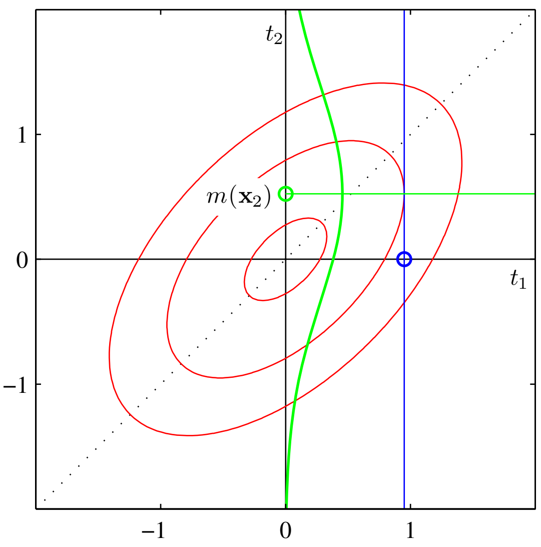

framework. However, an advantage of a Gaussian processes viewpoint is that we can consider covariance functions that can only be expressed in terms of an infinite number of basis functions.

For large training data sets, however, the direct application of Gaussian process methods can become infeasible, and so a range of approximation schemes have been developed that have better scaling with training set size than the exact approach (Gibbs, 1997; Tresp, 2001; Smola and Bartlett, 2001; Williams and Seeger, 2001; Csató and Opper, 2002; Seeger *et al.*, 2003). Practical issues in the application of Gaussian processes are discussed in Bishop and Nabney (2008).

We have introduced Gaussian process regression for the case of a single target variable. The extension of this formalism to multiple target variables, known as co-kriging (Cressie, 1993), is straightforward. Various other extensions of Gaus-

Exercise 6.23

Figure 6.8 Illustration of Gaussian process regression applied to the sinusoidal data set in Figure A.6 in which the three right-most data points have been omitted. The green curve shows the sinusoidal function from which the data points, shown in blue, are obtained by sampling and addition of Gaussian noise. The red line shows the mean of the Gaussian process predictive distribution, and the shaded region corresponds to plus and minus two standard deviations. Notice how the uncertainty increases in the region to the right of the data points.

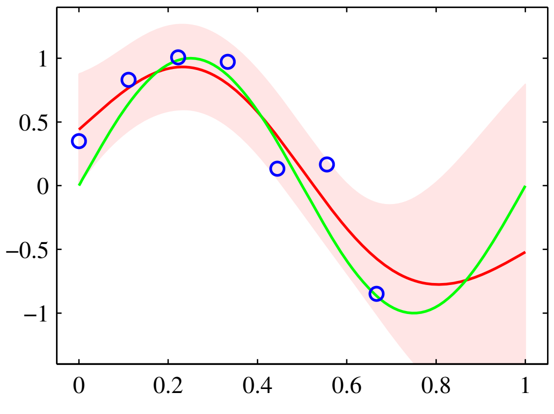

sian process regression have also been considered, for purposes such as modelling the distribution over low-dimensional manifolds for unsupervised learning (Bishop *et al.*, 1998a) and the solution of stochastic differential equations (Graepel, 2003).

6.4.3 Learning the hyperparameters

The predictions of a Gaussian process model will depend, in part, on the choice of covariance function. In practice, rather than fixing the covariance function, we may prefer to use a parametric family of functions and then infer the parameter values from the data. These parameters govern such things as the length scale of the correlations and the precision of the noise and correspond to the hyperparameters in a standard parametric model.

Techniques for learning the hyperparameters are based on the evaluation of the likelihood function $p(\mathbf{t}|\boldsymbol{\theta})$ where $\boldsymbol{\theta}$ denotes the hyperparameters of the Gaussian process model. The simplest approach is to make a point estimate of $\boldsymbol{\theta}$ by maximizing the log likelihood function. Because $\boldsymbol{\theta}$ represents a set of hyperparameters for the regression problem, this can be viewed as analogous to the type 2 maximum likelihood procedure for linear regression models. Maximization of the log likelihood can be done using efficient gradient-based optimization algorithms such as conjugate gradients (Fletcher, 1987; Nocedal and Wright, 1999; Bishop and Nabney, 2008).

Section 3.5

The log likelihood function for a Gaussian process regression model is easily evaluated using the standard form for a multivariate Gaussian distribution, giving

$$\ln p(\mathbf{t}|\boldsymbol{\theta}) = -\frac{1}{2}\ln|\mathbf{C}_N| - \frac{1}{2}\mathbf{t}^{\mathrm{T}}\mathbf{C}_N^{-1}\mathbf{t} - \frac{N}{2}\ln(2\pi). \tag{6.69}$$

For nonlinear optimization, we also need the gradient of the log likelihood function with respect to the parameter vector $\boldsymbol{\theta}$. We shall assume that evaluation of the derivatives of $\mathbf{C}_N$ is straightforward, as would be the case for the covariance functions considered in this chapter. Making use of the result (C.21) for the derivative of $\mathbf{C}_N^{-1}$, together with the result (C.22) for the derivative of $\ln|\mathbf{C}_N|$, we obtain

$$\frac{\partial}{\partial\theta_i}\ln p(\mathbf{t}|\boldsymbol{\theta}) = -\frac{1}{2}\mathrm{Tr}\left(\mathbf{C}_N^{-1}\frac{\partial\mathbf{C}_N}{\partial\theta_i}\right) + \frac{1}{2}\mathbf{t}^{\mathrm{T}}\mathbf{C}_N^{-1}\frac{\partial\mathbf{C}_N}{\partial\theta_i}\mathbf{C}_N^{-1}\mathbf{t}. \tag{6.70}$$

Because $\ln p(\mathbf{t}|\boldsymbol{\theta})$ will in general be a nonconvex function, it can have multiple maxima.

It is straightforward to introduce a prior over $\boldsymbol{\theta}$ and to maximize the log posterior using gradient-based methods. In a fully Bayesian treatment, we need to evaluate marginals over $\boldsymbol{\theta}$ weighted by the product of the prior $p(\boldsymbol{\theta})$ and the likelihood function $p(\mathbf{t}|\boldsymbol{\theta})$. In general, however, exact marginalization will be intractable, and we must resort to approximations.

The Gaussian process regression model gives a predictive distribution whose mean and variance are functions of the input vector $\mathbf{x}$. However, we have assumed that the contribution to the predictive variance arising from the additive noise, governed by the parameter β, is a constant. For some problems, known as *heteroscedastic*, the noise variance itself will also depend on $\mathbf{x}$. To model this, we can extend the

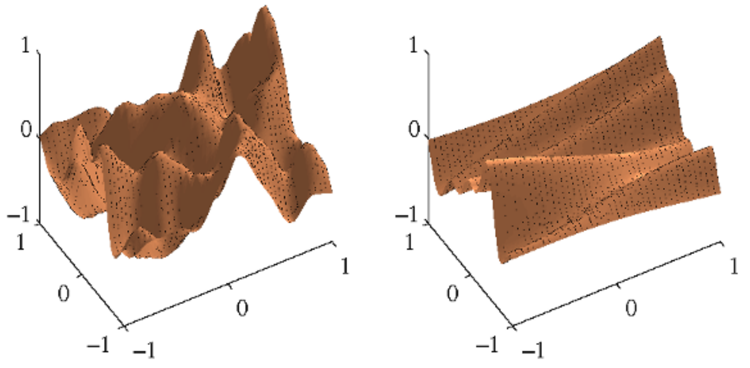

Figure 6.9 Samples from the ARD prior for Gaussian processes, in which the kernel function is given by (6.71). The left plot corresponds to $\eta_1 = \eta_2 = 1$, and the right plot corresponds to $\eta_1 = 1$, $\eta_2 = 0.01$.

Gaussian process framework by introducing a second Gaussian process to represent the dependence of β on the input $\mathbf{x}$ (Goldberg *et al.*, 1998). Because β is a variance, and hence nonnegative, we use the Gaussian process to model $\ln \beta(\mathbf{x})$.

6.4.4 Automatic relevance determination

In the previous section, we saw how maximum likelihood could be used to determine a value for the correlation length-scale parameter in a Gaussian process. This technique can usefully be extended by incorporating a separate parameter for each input variable (Rasmussen and Williams, 2006). The result, as we shall see, is that the optimization of these parameters by maximum likelihood allows the relative importance of different inputs to be inferred from the data. This represents an example in the Gaussian process context of *automatic relevance determination*, or *ARD*, which was originally formulated in the framework of neural networks (MacKay, 1994; Neal, 1996). The mechanism by which appropriate inputs are preferred is discussed in Section 7.2.2.

Consider a Gaussian process with a two-dimensional input space $\mathbf{x} = (x_1, x_2)$, having a kernel function of the form

$$k(\mathbf{x}, \mathbf{x}') = \theta_0 \exp\left\{ -\frac{1}{2} \sum_{i=1}^{2} \eta_i (x_i - x_i')^2 \right\}. \tag{6.71}$$

Samples from the resulting prior over functions $y(\mathbf{x})$ are shown for two different settings of the precision parameters η_i in Figure 6.9. We see that, as a particular parameter η_i becomes small, the function becomes relatively insensitive to the corresponding input variable x_i. By adapting these parameters to a data set using maximum likelihood, it becomes possible to detect input variables that have little effect on the predictive distribution, because the corresponding values of η_i will be small. This can be useful in practice because it allows such inputs to be discarded. ARD is illustrated using a simple synthetic data set having three inputs x_1, x_2 and x_3 (Nabney, 2002) in Figure 6.10. The target variable t, is generated by sampling 100 values of x_1 from a Gaussian, evaluating the function $\sin(2\pi x_1)$, and then adding

Figure 6.10 Illustration of automatic relevance determination in a Gaussian process for a synthetic problem having three inputs x_1, x_2, and x_3, for which the curves show the corresponding values of the hyperparameters η_1 (red), η_2 (green), and η_3 (blue) as a function of the number of iterations when optimizing the marginal likelihood. Details are given in the text. Note the logarithmic scale on the vertical axis.

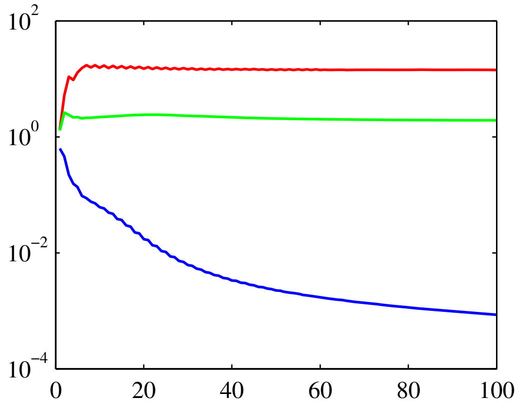

Gaussian noise. Values of x_2 are given by copying the corresponding values of x_1 and adding noise, and values of x_3 are sampled from an independent Gaussian distribution. Thus x_1 is a good predictor of t, x_2 is a more noisy predictor of t, and x_3 has only chance correlations with t. The marginal likelihood for a Gaussian process with ARD parameters η_1, η_2, η_3 is optimized using the scaled conjugate gradients algorithm. We see from Figure 6.10 that η_1 converges to a relatively large value, η_2 converges to a much smaller value, and η_3 becomes very small indicating that x_3 is irrelevant for predicting t.

The ARD framework is easily incorporated into the exponential-quadratic kernel (6.63) to give the following form of kernel function, which has been found useful for applications of Gaussian processes to a range of regression problems

$$k(\mathbf{x}_n, \mathbf{x}_m) = \theta_0 \exp\left\{-\frac{1}{2}\sum_{i=1}^{D} \eta_i (x_{ni} - x_{mi})^2\right\} + \theta_2 + \theta_3 \sum_{i=1}^{D} x_{ni} x_{mi} \qquad (6.72)$$

where D is the dimensionality of the input space.

6.4.5 Gaussian processes for classification

In a probabilistic approach to classification, our goal is to model the posterior probabilities of the target variable for a new input vector, given a set of training data. These probabilities must lie in the interval $(0, 1)$, whereas a Gaussian process model makes predictions that lie on the entire real axis. However, we can easily adapt Gaussian processes to classification problems by transforming the output of the Gaussian process using an appropriate nonlinear activation function.

Consider first the two-class problem with a target variable $t \in \{0, 1\}$. If we define a Gaussian process over a function $a(\mathbf{x})$ and then transform the function using a logistic sigmoid $y = \sigma(a)$, given by (4.59), then we will obtain a non-Gaussian stochastic process over functions $y(\mathbf{x})$ where $y \in (0, 1)$. This is illustrated for the case of a one-dimensional input space in Figure 6.11 in which the probability distri-

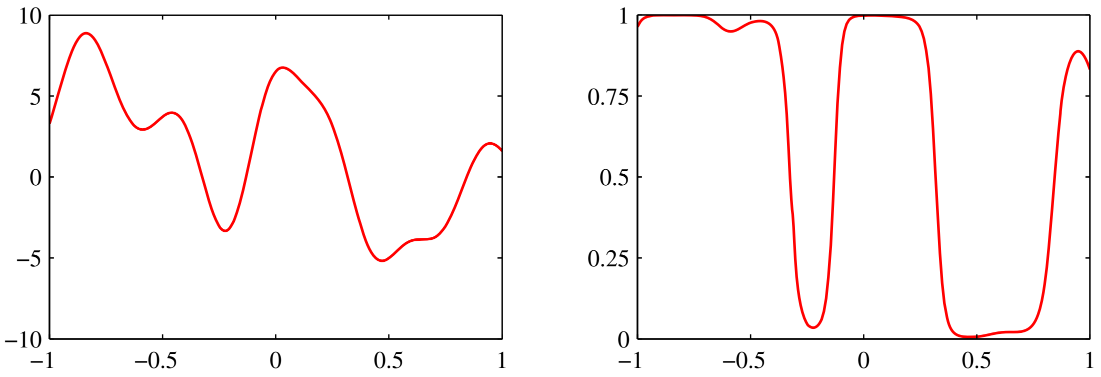

Figure 6.11 The left plot shows a sample from a Gaussian process prior over functions $a(\mathbf{x})$, and the right plot shows the result of transforming this sample using a logistic sigmoid function.

bution over the target variable t is then given by the Bernoulli distribution

$$p(t|a) = \sigma(a)^t (1 - \sigma(a))^{1-t}. \tag{6.73}$$

As usual, we denote the training set inputs by $\mathbf{x}_1, \ldots, \mathbf{x}_N$ with corresponding observed target variables $\mathbf{t} = (t_1, \ldots, t_N)^{\mathrm{T}}$. We also consider a single test point $\mathbf{x}_{N+1}$ with target value t_{N+1}. Our goal is to determine the predictive distribution $p(t_{N+1}|\mathbf{t})$, where we have left the conditioning on the input variables implicit. To do this we introduce a Gaussian process prior over the vector $\mathbf{a}_{N+1}$, which has components $a(\mathbf{x}_1), \ldots, a(\mathbf{x}_{N+1})$. This in turn defines a non-Gaussian process over $\mathbf{t}_{N+1}$, and by conditioning on the training data $\mathbf{t}_N$ we obtain the required predictive distribution. The Gaussian process prior for $\mathbf{a}_{N+1}$ takes the form

$$p(\mathbf{a}_{N+1}) = \mathcal{N}(\mathbf{a}_{N+1}|\mathbf{0}, \mathbf{C}_{N+1}). \tag{6.74}$$

Unlike the regression case, the covariance matrix no longer includes a noise term because we assume that all of the training data points are correctly labelled. However, for numerical reasons it is convenient to introduce a noise-like term governed by a parameter ν that ensures that the covariance matrix is positive definite. Thus the covariance matrix $\mathbf{C}_{N+1}$ has elements given by

$$C(\mathbf{x}_n, \mathbf{x}_m) = k(\mathbf{x}_n, \mathbf{x}_m) + \nu\delta_{nm} \tag{6.75}$$

where $k(\mathbf{x}_n, \mathbf{x}_m)$ is any positive semidefinite kernel function of the kind considered in Section 6.2, and the value of ν is typically fixed in advance. We shall assume that the kernel function $k(\mathbf{x}, \mathbf{x}')$ is governed by a vector $\boldsymbol{\theta}$ of parameters, and we shall later discuss how $\boldsymbol{\theta}$ may be learned from the training data.

For two-class problems, it is sufficient to predict $p(t_{N+1} = 1|\mathbf{t}_N)$ because the value of $p(t_{N+1} = 0|\mathbf{t}_N)$ is then given by $1 - p(t_{N+1} = 1|\mathbf{t}_N)$. The required predictive distribution is given by

$$p(t_{N+1} = 1|\mathbf{t}_N) = \int p(t_{N+1} = 1|a_{N+1})p(a_{N+1}|\mathbf{t}_N)\,\mathrm{d}a_{N+1} \tag{6.76}$$

where $p(t_{N+1} = 1|a_{N+1}) = \sigma(a_{N+1})$.

This integral is analytically intractable, and so may be approximated using sampling methods (Neal, 1997). Alternatively, we can consider techniques based on an analytical approximation. In Section 4.5.2, we derived the approximate formula (4.153) for the convolution of a logistic sigmoid with a Gaussian distribution. We can use this result to evaluate the integral in (6.76) provided we have a Gaussian approximation to the posterior distribution $p(a_{N+1}|\mathbf{t}_N)$. The usual justification for a Gaussian approximation to a posterior distribution is that the true posterior will tend to a Gaussian as the number of data points increases as a consequence of the central limit theorem. *Section 2.3* In the case of Gaussian processes, the number of variables grows with the number of data points, and so this argument does not apply directly. However, if we consider increasing the number of data points falling in a fixed region of $\mathbf{x}$ space, then the corresponding uncertainty in the function $a(\mathbf{x})$ will decrease, again leading asymptotically to a Gaussian (Williams and Barber, 1998).

Three different approaches to obtaining a Gaussian approximation have been considered. *Section 10.1* One technique is based on *variational inference* (Gibbs and MacKay, 2000) and makes use of the local variational bound (10.144) on the logistic sigmoid. This allows the product of sigmoid functions to be approximated by a product of Gaussians thereby allowing the marginalization over $\mathbf{a}_N$ to be performed analytically. The approach also yields a lower bound on the likelihood function $p(\mathbf{t}_N|\boldsymbol{\theta})$. The variational framework for Gaussian process classification can also be extended to multiclass ($K > 2$) problems by using a Gaussian approximation to the softmax function (Gibbs, 1997).

Section 10.7 A second approach uses *expectation propagation* (Opper and Winther, 2000b; Minka, 2001b; Seeger, 2003). Because the true posterior distribution is unimodal, as we shall see shortly, the expectation propagation approach can give good results.

6.4.6 Laplace approximation

The third approach to Gaussian process classification is based on the Laplace approximation, which we now consider in detail. *Section 4.4* In order to evaluate the predictive distribution (6.76), we seek a Gaussian approximation to the posterior distribution over a_{N+1}, which, using Bayes' theorem, is given by

$$\begin{aligned}
p(a_{N+1}|\mathbf{t}_N) &= \int p(a_{N+1}, \mathbf{a}_N|\mathbf{t}_N)\,\mathrm{d}\mathbf{a}_N \\
&= \frac{1}{p(\mathbf{t}_N)}\int p(a_{N+1}, \mathbf{a}_N)p(\mathbf{t}_N|a_{N+1}, \mathbf{a}_N)\,\mathrm{d}\mathbf{a}_N \\
&= \frac{1}{p(\mathbf{t}_N)}\int p(a_{N+1}|\mathbf{a}_N)p(\mathbf{a}_N)p(\mathbf{t}_N|\mathbf{a}_N)\,\mathrm{d}\mathbf{a}_N \\
&= \int p(a_{N+1}|\mathbf{a}_N)p(\mathbf{a}_N|\mathbf{t}_N)\,\mathrm{d}\mathbf{a}_N
\end{aligned} \tag{6.77}$$

where we have used $p(\mathbf{t}_N|a_{N+1}, \mathbf{a}_N) = p(\mathbf{t}_N|\mathbf{a}_N)$. The conditional distribution $p(a_{N+1}|\mathbf{a}_N)$ is obtained by invoking the results (6.66) and (6.67) for Gaussian process regression, to give

$$p(a_{N+1}|\mathbf{a}_N) = \mathcal{N}(a_{N+1}|\mathbf{k}^{\mathrm{T}}\mathbf{C}_N^{-1}\mathbf{a}_N, c - \mathbf{k}^{\mathrm{T}}\mathbf{C}_N^{-1}\mathbf{k}). \tag{6.78}$$

We can therefore evaluate the integral in (6.77) by finding a Laplace approximation for the posterior distribution $p(\mathbf{a}_N|\mathbf{t}_N)$, and then using the standard result for the convolution of two Gaussian distributions.

The prior $p(\mathbf{a}_N)$ is given by a zero-mean Gaussian process with covariance matrix $\mathbf{C}_N$, and the data term (assuming independence of the data points) is given by

$$p(\mathbf{t}_N|\mathbf{a}_N) = \prod_{n=1}^{N} \sigma(a_n)^{t_n}(1-\sigma(a_n))^{1-t_n} = \prod_{n=1}^{N} e^{a_n t_n}\sigma(-a_n). \tag{6.79}$$

We then obtain the Laplace approximation by Taylor expanding the logarithm of $p(\mathbf{a}_N|\mathbf{t}_N)$, which up to an additive normalization constant is given by the quantity

$$\begin{aligned}\Psi(\mathbf{a}_N) &= \ln p(\mathbf{a}_N) + \ln p(\mathbf{t}_N|\mathbf{a}_N) \\ &= -\frac{1}{2}\mathbf{a}_N^{\mathrm{T}}\mathbf{C}_N^{-1}\mathbf{a}_N - \frac{N}{2}\ln(2\pi) - \frac{1}{2}\ln|\mathbf{C}_N| + \mathbf{t}_N^{\mathrm{T}}\mathbf{a}_N \\ &\quad - \sum_{n=1}^{N}\ln(1+e^{a_n}) + \text{const}. \end{aligned} \tag{6.80}$$

First we need to find the mode of the posterior distribution, and this requires that we evaluate the gradient of $\Psi(\mathbf{a}_N)$, which is given by

$$\nabla\Psi(\mathbf{a}_N) = \mathbf{t}_N - \boldsymbol{\sigma}_N - \mathbf{C}_N^{-1}\mathbf{a}_N \tag{6.81}$$

where $\boldsymbol{\sigma}_N$ is a vector with elements $\sigma(a_n)$. We cannot simply find the mode by setting this gradient to zero, because $\boldsymbol{\sigma}_N$ depends nonlinearly on $\mathbf{a}_N$, and so we resort to an iterative scheme based on the Newton-Raphson method, which gives rise to an iterative reweighted least squares (IRLS) algorithm. This requires the second derivatives of $\Psi(\mathbf{a}_N)$, which we also require for the Laplace approximation anyway, and which are given by

Section 4.3.3

$$\nabla\nabla\Psi(\mathbf{a}_N) = -\mathbf{W}_N - \mathbf{C}_N^{-1} \tag{6.82}$$

where $\mathbf{W}_N$ is a diagonal matrix with elements $\sigma(a_n)(1-\sigma(a_n))$, and we have used the result (4.88) for the derivative of the logistic sigmoid function. Note that these diagonal elements lie in the range $(0, 1/4)$, and hence $\mathbf{W}_N$ is a positive definite matrix. Because $\mathbf{C}_N$ (and hence its inverse) is positive definite by construction, and because the sum of two positive definite matrices is also positive definite, we see that the Hessian matrix $\mathbf{A} = -\nabla\nabla\Psi(\mathbf{a}_N)$ is positive definite and so the posterior distribution $p(\mathbf{a}_N|\mathbf{t}_N)$ is log convex and therefore has a single mode that is the global

Exercise 6.24

maximum. The posterior distribution is not Gaussian, however, because the Hessian is a function of $\mathbf{a}_N$.

Exercise 6.25

Using the Newton-Raphson formula (4.92), the iterative update equation for $\mathbf{a}_N$ is given by

$$\mathbf{a}_N^{\text{new}} = \mathbf{C}_N(\mathbf{I} + \mathbf{W}_N\mathbf{C}_N)^{-1}\left\{\mathbf{t}_N - \boldsymbol{\sigma}_N + \mathbf{W}_N\mathbf{a}_N\right\}. \tag{6.83}$$

These equations are iterated until they converge to the mode which we denote by $\mathbf{a}_N^\star$. At the mode, the gradient $\nabla\Psi(\mathbf{a}_N)$ will vanish, and hence $\mathbf{a}_N^\star$ will satisfy

$$\mathbf{a}_N^\star = \mathbf{C}_N(\mathbf{t}_N - \boldsymbol{\sigma}_N). \tag{6.84}$$

Once we have found the mode $\mathbf{a}_N^\star$ of the posterior, we can evaluate the Hessian matrix given by

$$\mathbf{H} = -\nabla\nabla\Psi(\mathbf{a}_N) = \mathbf{W}_N + \mathbf{C}_N^{-1} \tag{6.85}$$

where the elements of $\mathbf{W}_N$ are evaluated using $\mathbf{a}_N^\star$. This defines our Gaussian approximation to the posterior distribution $p(\mathbf{a}_N|\mathbf{t}_N)$ given by

$$q(\mathbf{a}_N) = \mathcal{N}(\mathbf{a}_N|\mathbf{a}_N^\star, \mathbf{H}^{-1}). \tag{6.86}$$

Exercise 6.26

We can now combine this with (6.78) and hence evaluate the integral (6.77). Because this corresponds to a linear-Gaussian model, we can use the general result (2.115) to give

$$\mathbb{E}[a_{N+1}|\mathbf{t}_N] = \mathbf{k}^{\mathrm{T}}(\mathbf{t}_N - \boldsymbol{\sigma}_N) \tag{6.87}$$

$$\operatorname{var}[a_{N+1}|\mathbf{t}_N] = c - \mathbf{k}^{\mathrm{T}}(\mathbf{W}_N^{-1} + \mathbf{C}_N)^{-1}\mathbf{k}. \tag{6.88}$$

Now that we have a Gaussian distribution for $p(a_{N+1}|\mathbf{t}_N)$, we can approximate the integral (6.76) using the result (4.153). As with the Bayesian logistic regression model of Section 4.5, if we are only interested in the decision boundary corresponding to $p(t_{N+1}|\mathbf{t}_N) = 0.5$, then we need only consider the mean and we can ignore the effect of the variance.

We also need to determine the parameters $\boldsymbol{\theta}$ of the covariance function. One approach is to maximize the likelihood function given by $p(\mathbf{t}_N|\boldsymbol{\theta})$ for which we need expressions for the log likelihood and its gradient. If desired, suitable regularization terms can also be added, leading to a penalized maximum likelihood solution. The likelihood function is defined by

$$p(\mathbf{t}_N|\boldsymbol{\theta}) = \int p(\mathbf{t}_N|\mathbf{a}_N)p(\mathbf{a}_N|\boldsymbol{\theta})\,\mathrm{d}\mathbf{a}_N. \tag{6.89}$$

This integral is analytically intractable, so again we make use of the Laplace approximation. Using the result (4.135), we obtain the following approximation for the log of the likelihood function

$$\ln p(\mathbf{t}_N|\boldsymbol{\theta}) = \Psi(\mathbf{a}_N^\star) - \frac{1}{2}\ln|\mathbf{W}_N + \mathbf{C}_N^{-1}| + \frac{N}{2}\ln(2\pi) \tag{6.90}$$

where $\Psi(\mathbf{a}_N^\star) = \ln p(\mathbf{a}_N^\star|\boldsymbol{\theta}) + \ln p(\mathbf{t}_N|\mathbf{a}_N^\star)$. We also need to evaluate the gradient of $\ln p(\mathbf{t}_N|\boldsymbol{\theta})$ with respect to the parameter vector $\boldsymbol{\theta}$. Note that changes in $\boldsymbol{\theta}$ will cause changes in $\mathbf{a}_N^\star$, leading to additional terms in the gradient. Thus, when we differentiate (6.90) with respect to $\boldsymbol{\theta}$, we obtain two sets of terms, the first arising from the dependence of the covariance matrix $\mathbf{C}_N$ on $\boldsymbol{\theta}$, and the rest arising from dependence of $\mathbf{a}_N^\star$ on $\boldsymbol{\theta}$.

The terms arising from the explicit dependence on $\boldsymbol{\theta}$ can be found by using (6.80) together with the results (C.21) and (C.22), and are given by

$$\begin{aligned}\frac{\partial \ln p(\mathbf{t}_N|\boldsymbol{\theta})}{\partial \theta_j} &= \frac{1}{2}\mathbf{a}_N^{\star\mathrm{T}}\mathbf{C}_N^{-1}\frac{\partial \mathbf{C}_N}{\partial \theta_j}\mathbf{C}_N^{-1}\mathbf{a}_N^\star \\ &\quad -\frac{1}{2}\mathrm{Tr}\left[(\mathbf{I}+\mathbf{C}_N\mathbf{W}_N)^{-1}\mathbf{W}_N\frac{\partial \mathbf{C}_N}{\partial \theta_j}\right]. \end{aligned} \tag{6.91}$$

To compute the terms arising from the dependence of $\mathbf{a}_N^\star$ on $\boldsymbol{\theta}$, we note that the Laplace approximation has been constructed such that $\Psi(\mathbf{a}_N)$ has zero gradient at $\mathbf{a}_N = \mathbf{a}_N^\star$, and so $\Psi(\mathbf{a}_N^\star)$ gives no contribution to the gradient as a result of its dependence on $\mathbf{a}_N^\star$. This leaves the following contribution to the derivative with respect to a component θ_j of $\boldsymbol{\theta}$

$$\begin{aligned}&-\frac{1}{2}\sum_{n=1}^{N}\frac{\partial \ln|\mathbf{W}_N+\mathbf{C}_N^{-1}|}{\partial a_n^\star}\frac{\partial a_n^\star}{\partial \theta_j} \\ &\quad = -\frac{1}{2}\sum_{n=1}^{N}\left[(\mathbf{I}+\mathbf{C}_N\mathbf{W}_N)^{-1}\mathbf{C}_N\right]_{nn}\sigma_n^\star(1-\sigma_n^\star)(1-2\sigma_n^\star)\frac{\partial a_n^\star}{\partial \theta_j}\end{aligned} \tag{6.92}$$

where $\sigma_n^\star = \sigma(a_n^\star)$, and again we have used the result (C.22) together with the definition of $\mathbf{W}_N$. We can evaluate the derivative of $a_N^\star$ with respect to θ_j by differentiating the relation (6.84) with respect to θ_j to give

$$\frac{\partial a_n^\star}{\partial \theta_j} = \frac{\partial \mathbf{C}_N}{\partial \theta_j}(\mathbf{t}_N - \boldsymbol{\sigma}_N) - \mathbf{C}_N\mathbf{W}_N\frac{\partial a_n^\star}{\partial \theta_j}. \tag{6.93}$$

Rearranging then gives

$$\frac{\partial a_n^\star}{\partial \theta_j} = (\mathbf{I}+\mathbf{W}_N\mathbf{C}_N)^{-1}\frac{\partial \mathbf{C}_N}{\partial \theta_j}(\mathbf{t}_N - \boldsymbol{\sigma}_N). \tag{6.94}$$

Combining (6.91), (6.92), and (6.94), we can evaluate the gradient of the log likelihood function, which can be used with standard nonlinear optimization algorithms in order to determine a value for $\boldsymbol{\theta}$.

Appendix A

We can illustrate the application of the Laplace approximation for Gaussian processes using the synthetic two-class data set shown in Figure 6.12. Extension of the Laplace approximation to Gaussian processes involving $K > 2$ classes, using the softmax activation function, is straightforward (Williams and Barber, 1998).

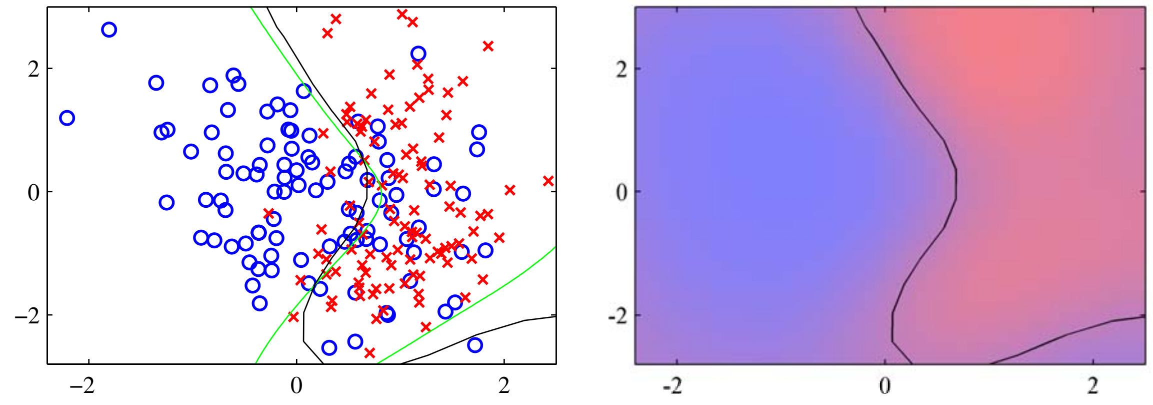

Figure 6.12 Illustration of the use of a Gaussian process for classification, showing the data on the left together with the optimal decision boundary from the true distribution in green, and the decision boundary from the Gaussian process classifier in black. On the right is the predicted posterior probability for the blue and red classes together with the Gaussian process decision boundary.

6.4.7 Connection to neural networks

We have seen that the range of functions which can be represented by a neural network is governed by the number M of hidden units, and that, for sufficiently large M, a two-layer network can approximate any given function with arbitrary accuracy. In the framework of maximum likelihood, the number of hidden units needs to be limited (to a level dependent on the size of the training set) in order to avoid over-fitting. However, from a Bayesian perspective it makes little sense to limit the number of parameters in the network according to the size of the training set.

In a Bayesian neural network, the prior distribution over the parameter vector $\mathbf{w}$, in conjunction with the network function $f(\mathbf{x}, \mathbf{w})$, produces a prior distribution over functions from $y(\mathbf{x})$ where $\mathbf{y}$ is the vector of network outputs. Neal (1996) has shown that, for a broad class of prior distributions over $\mathbf{w}$, the distribution of functions generated by a neural network will tend to a Gaussian process in the limit $M \to \infty$. It should be noted, however, that in this limit the output variables of the neural network become independent. One of the great merits of neural networks is that the outputs share the hidden units and so they can 'borrow statistical strength' from each other, that is, the weights associated with each hidden unit are influenced by all of the output variables not just by one of them. This property is therefore lost in the Gaussian process limit.

We have seen that a Gaussian process is determined by its covariance (kernel) function. Williams (1998) has given explicit forms for the covariance in the case of two specific choices for the hidden unit activation function (probit and Gaussian). These kernel functions $k(\mathbf{x}, \mathbf{x}')$ are nonstationary, i.e. they cannot be expressed as a function of the difference $\mathbf{x} - \mathbf{x}'$, as a consequence of the Gaussian weight prior being centred on zero which breaks translation invariance in weight space.

By working directly with the covariance function we have implicitly marginalized over the distribution of weights. If the weight prior is governed by hyperparameters, then their values will determine the length scales of the distribution over functions, as can be understood by studying the examples in Figure 5.11 for the case of a finite number of hidden units. Note that we cannot marginalize out the hyperparameters analytically, and must instead resort to techniques of the kind discussed in Section 6.4.

Exercises

6.1 ($\star\star$) **www** Consider the dual formulation of the least squares linear regression problem given in Section 6.1. Show that the solution for the components a_n of the vector $\mathbf{a}$ can be expressed as a linear combination of the elements of the vector $\boldsymbol{\phi}(\mathbf{x}_n)$. Denoting these coefficients by the vector $\mathbf{w}$, show that the dual of the dual formulation is given by the original representation in terms of the parameter vector $\mathbf{w}$.

6.2 ($\star\star$) In this exercise, we develop a dual formulation of the perceptron learning algorithm. Using the perceptron learning rule (4.55), show that the learned weight vector $\mathbf{w}$ can be written as a linear combination of the vectors $t_n\boldsymbol{\phi}(\mathbf{x}_n)$ where $t_n \in \{-1, +1\}$. Denote the coefficients of this linear combination by α_n and derive a formulation of the perceptron learning algorithm, and the predictive function for the perceptron, in terms of the α_n. Show that the feature vector $\boldsymbol{\phi}(\mathbf{x})$ enters only in the form of the kernel function $k(\mathbf{x}, \mathbf{x}') = \boldsymbol{\phi}(\mathbf{x})^{\mathrm{T}}\boldsymbol{\phi}(\mathbf{x}')$.

6.3 ($\star$) The nearest-neighbour classifier (Section 2.5.2) assigns a new input vector $\mathbf{x}$ to the same class as that of the nearest input vector $\mathbf{x}_n$ from the training set, where in the simplest case, the distance is defined by the Euclidean metric $\|\mathbf{x} - \mathbf{x}_n\|^2$. By expressing this rule in terms of scalar products and then making use of kernel substitution, formulate the nearest-neighbour classifier for a general nonlinear kernel.

6.4 ($\star$) In Appendix C, we give an example of a matrix that has positive elements but that has a negative eigenvalue and hence that is not positive definite. Find an example of the converse property, namely a 2×2 matrix with positive eigenvalues yet that has at least one negative element.

6.5 ($\star$) **www** Verify the results (6.13) and (6.14) for constructing valid kernels.

6.6 ($\star$) Verify the results (6.15) and (6.16) for constructing valid kernels.

6.7 ($\star$) **www** Verify the results (6.17) and (6.18) for constructing valid kernels.

6.8 ($\star$) Verify the results (6.19) and (6.20) for constructing valid kernels.

6.9 ($\star$) Verify the results (6.21) and (6.22) for constructing valid kernels.

6.10 ($\star$) Show that an excellent choice of kernel for learning a function $f(\mathbf{x})$ is given by $k(\mathbf{x}, \mathbf{x}') = f(\mathbf{x})f(\mathbf{x}')$ by showing that a linear learning machine based on this kernel will always find a solution proportional to $f(\mathbf{x})$.

6.11 ($\star$) By making use of the expansion (6.25), and then expanding the middle factor as a power series, show that the Gaussian kernel (6.23) can be expressed as the inner product of an infinite-dimensional feature vector.

6.12 ($\star\star$) **www** Consider the space of all possible subsets A of a given fixed set D. Show that the kernel function (6.27) corresponds to an inner product in a feature space of dimensionality $2^{|D|}$ defined by the mapping $\boldsymbol{\phi}(A)$ where A is a subset of D and the element $\phi_U(A)$, indexed by the subset U, is given by

$$\phi_U(A) = \begin{cases} 1, & \text{if } U \subseteq A; \\ 0, & \text{otherwise.} \end{cases} \tag{6.95}$$

Here $U \subseteq A$ denotes that U is either a subset of A or is equal to A.

6.13 ($\star$) Show that the Fisher kernel, defined by (6.33), remains invariant if we make a nonlinear transformation of the parameter vector $\boldsymbol{\theta} \rightarrow \boldsymbol{\psi}(\boldsymbol{\theta})$, where the function $\boldsymbol{\psi}(\cdot)$ is invertible and differentiable.

6.14 ($\star$) **www** Write down the form of the Fisher kernel, defined by (6.33), for the case of a distribution $p(\mathbf{x}|\boldsymbol{\mu}) = \mathcal{N}(\mathbf{x}|\boldsymbol{\mu}, \mathbf{S})$ that is Gaussian with mean $\boldsymbol{\mu}$ and fixed covariance $\mathbf{S}$.

6.15 ($\star$) By considering the determinant of a 2×2 Gram matrix, show that a positive-definite kernel function $k(x, x')$ satisfies the Cauchy-Schwartz inequality

$$k(x_1, x_2)^2 \leqslant k(x_1, x_1)k(x_2, x_2). \tag{6.96}$$

6.16 ($\star\star$) Consider a parametric model governed by the parameter vector $\mathbf{w}$ together with a data set of input values $\mathbf{x}_1, \ldots, \mathbf{x}_N$ and a nonlinear feature mapping $\boldsymbol{\phi}(\mathbf{x})$. Suppose that the dependence of the error function on $\mathbf{w}$ takes the form

$$J(\mathbf{w}) = f(\mathbf{w}^{\mathrm{T}}\boldsymbol{\phi}(\mathbf{x}_1), \ldots, \mathbf{w}^{\mathrm{T}}\boldsymbol{\phi}(\mathbf{x}_N)) + g(\mathbf{w}^{\mathrm{T}}\mathbf{w}) \tag{6.97}$$

where $g(\cdot)$ is a monotonically increasing function. By writing $\mathbf{w}$ in the form

$$\mathbf{w} = \sum_{n=1}^{N} \alpha_n \boldsymbol{\phi}(\mathbf{x}_n) + \mathbf{w}_{\perp} \tag{6.98}$$

show that the value of $\mathbf{w}$ that minimizes $J(\mathbf{w})$ takes the form of a linear combination of the basis functions $\boldsymbol{\phi}(\mathbf{x}_n)$ for $n = 1, \ldots, N$.

6.17 ($\star\star$) **www** Consider the sum-of-squares error function (6.39) for data having noisy inputs, where $\nu(\boldsymbol{\xi})$ is the distribution of the noise. Use the calculus of variations to minimize this error function with respect to the function $y(\mathbf{x})$, and hence show that the optimal solution is given by an expansion of the form (6.40) in which the basis functions are given by (6.41).

6.18 ($\star$) Consider a Nadaraya-Watson model with one input variable x and one target variable t having Gaussian components with isotropic covariances, so that the covariance matrix is given by $\sigma^2\mathbf{I}$ where $\mathbf{I}$ is the unit matrix. Write down expressions for the conditional density $p(t|x)$ and for the conditional mean $\mathbb{E}[t|x]$ and variance $\mathrm{var}[t|x]$, in terms of the kernel function $k(x, x_n)$.

6.19 ($\star\star$) Another viewpoint on kernel regression comes from a consideration of regression problems in which the input variables as well as the target variables are corrupted with additive noise. Suppose each target value t_n is generated as usual by taking a function $y(\mathbf{z}_n)$ evaluated at a point $\mathbf{z}_n$, and adding Gaussian noise. The value of $\mathbf{z}_n$ is not directly observed, however, but only a noise corrupted version $\mathbf{x}_n = \mathbf{z}_n + \boldsymbol{\xi}_n$ where the random variable $\boldsymbol{\xi}$ is governed by some distribution $g(\boldsymbol{\xi})$. Consider a set of observations $\{\mathbf{x}_n, t_n\}$, where $n = 1, \ldots, N$, together with a corresponding sum-of-squares error function defined by averaging over the distribution of input noise to give

$$E = \frac{1}{2}\sum_{n=1}^{N}\int \{y(\mathbf{x}_n - \boldsymbol{\xi}_n) - t_n\}^2 g(\boldsymbol{\xi}_n)\,\mathrm{d}\boldsymbol{\xi}_n. \tag{6.99}$$

By minimizing E with respect to the function $y(\mathbf{z})$ using the calculus of variations (Appendix D), show that optimal solution for $y(\mathbf{x})$ is given by a Nadaraya-Watson kernel regression solution of the form (6.45) with a kernel of the form (6.46).

6.20 ($\star\star$) **www** Verify the results (6.66) and (6.67).

6.21 ($\star\star$) **www** Consider a Gaussian process regression model in which the kernel function is defined in terms of a fixed set of nonlinear basis functions. Show that the predictive distribution is identical to the result (3.58) obtained in Section 3.3.2 for the Bayesian linear regression model. To do this, note that both models have Gaussian predictive distributions, and so it is only necessary to show that the conditional mean and variance are the same. For the mean, make use of the matrix identity (C.6), and for the variance, make use of the matrix identity (C.7).

6.22 ($\star\star$) Consider a regression problem with N training set input vectors $\mathbf{x}_1, \ldots, \mathbf{x}_N$ and L test set input vectors $\mathbf{x}_{N+1}, \ldots, \mathbf{x}_{N+L}$, and suppose we define a Gaussian process prior over functions $t(\mathbf{x})$. Derive an expression for the joint predictive distribution for $t(\mathbf{x}_{N+1}), \ldots, t(\mathbf{x}_{N+L})$, given the values of $t(\mathbf{x}_1), \ldots, t(\mathbf{x}_N)$. Show the marginal of this distribution for one of the test observations t_j where $N + 1 \leqslant j \leqslant N + L$ is given by the usual Gaussian process regression result (6.66) and (6.67).

6.23 ($\star\star$) **www** Consider a Gaussian process regression model in which the target variable $\mathbf{t}$ has dimensionality D. Write down the conditional distribution of $\mathbf{t}_{N+1}$ for a test input vector $\mathbf{x}_{N+1}$, given a training set of input vectors $\mathbf{x}_1, \ldots, \mathbf{x}_{N+1}$ and corresponding target observations $\mathbf{t}_1, \ldots, \mathbf{t}_N$.

6.24 ($\star$) Show that a diagonal matrix $\mathbf{W}$ whose elements satisfy $0 < W_{ii} < 1$ is positive definite. Show that the sum of two positive definite matrices is itself positive definite.

6.25 ($\star$) **www** Using the Newton-Raphson formula (4.92), derive the iterative update formula (6.83) for finding the mode $\mathbf{a}_N^\star$ of the posterior distribution in the Gaussian process classification model.

6.26 ($\star$) Using the result (2.115), derive the expressions (6.87) and (6.88) for the mean and variance of the posterior distribution $p(a_{N+1}|\mathbf{t}_N)$ in the Gaussian process classification model.

6.27 ($\star\star\star$) Derive the result (6.90) for the log likelihood function in the Laplace approximation framework for Gaussian process classification. Similarly, derive the results (6.91), (6.92), and (6.94) for the terms in the gradient of the log likelihood.

7 Sparse Kernel Machines

In the previous chapter, we explored a variety of learning algorithms based on non-linear kernels. One of the significant limitations of many such algorithms is that the kernel function $k(\mathbf{x}_n, \mathbf{x}_m)$ must be evaluated for all possible pairs $\mathbf{x}_n$ and $\mathbf{x}_m$ of training points, which can be computationally infeasible during training and can lead to excessive computation times when making predictions for new data points. In this chapter we shall look at kernel-based algorithms that have *sparse* solutions, so that predictions for new inputs depend only on the kernel function evaluated at a subset of the training data points.

We begin by looking in some detail at the *support vector machine* (SVM), which became popular in some years ago for solving problems in classification, regression, and novelty detection. An important property of support vector machines is that the determination of the model parameters corresponds to a convex optimization problem, and so any local solution is also a global optimum. Because the discussion of support vector machines makes extensive use of Lagrange multipliers, the reader is encouraged to review the key concepts covered in Appendix E. Additional information on support vector machines can be found in Vapnik (1995), Burges (1998), Cristianini and Shawe-Taylor (2000), Müller *et al.* (2001), Schölkopf and Smola (2002), and Herbrich (2002).

The SVM is a decision machine and so does not provide posterior probabilities. We have already discussed some of the benefits of determining probabilities in Section 1.5.4. An alternative sparse kernel technique, known as the *relevance vector machine* (RVM), is based on a Bayesian formulation and provides posterior probabilistic outputs, as well as having typically much sparser solutions than the SVM.

Section 7.2

7.1. Maximum Margin Classifiers

We begin our discussion of support vector machines by returning to the two-class classification problem using linear models of the form

$$y(\mathbf{x}) = \mathbf{w}^{\mathrm{T}}\boldsymbol{\phi}(\mathbf{x}) + b \tag{7.1}$$

where $\boldsymbol{\phi}(\mathbf{x})$ denotes a fixed feature-space transformation, and we have made the bias parameter b explicit. Note that we shall shortly introduce a dual representation expressed in terms of kernel functions, which avoids having to work explicitly in feature space. The training data set comprises N input vectors $\mathbf{x}_1, \ldots, \mathbf{x}_N$, with corresponding target values $t_1, \ldots, t_N$ where $t_n \in \{-1, 1\}$, and new data points $\mathbf{x}$ are classified according to the sign of $y(\mathbf{x})$.

We shall assume for the moment that the training data set is linearly separable in feature space, so that by definition there exists at least one choice of the parameters $\mathbf{w}$ and b such that a function of the form (7.1) satisfies $y(\mathbf{x}_n) > 0$ for points having $t_n = +1$ and $y(\mathbf{x}_n) < 0$ for points having $t_n = -1$, so that $t_n y(\mathbf{x}_n) > 0$ for all training data points.

There may of course exist many such solutions that separate the classes exactly. In Section 4.1.7, we described the perceptron algorithm that is guaranteed to find a solution in a finite number of steps. The solution that it finds, however, will be dependent on the (arbitrary) initial values chosen for $\mathbf{w}$ and b as well as on the order in which the data points are presented. If there are multiple solutions all of which classify the training data set exactly, then we should try to find the one that will give the smallest generalization error. The support vector machine approaches this problem through the concept of the *margin*, which is defined to be the smallest distance between the decision boundary and any of the samples, as illustrated in Figure 7.1.

In support vector machines the decision boundary is chosen to be the one for which the margin is maximized. The maximum margin solution can be motivated using *computational learning theory*, also known as *statistical learning theory*. However, a simple insight into the origins of maximum margin has been given by Tong and Koller (2000) who consider a framework for classification based on a hybrid of generative and discriminative approaches. They first model the distribution over input vectors $\mathbf{x}$ for each class using a Parzen density estimator with Gaussian kernels

Section 7.1.5

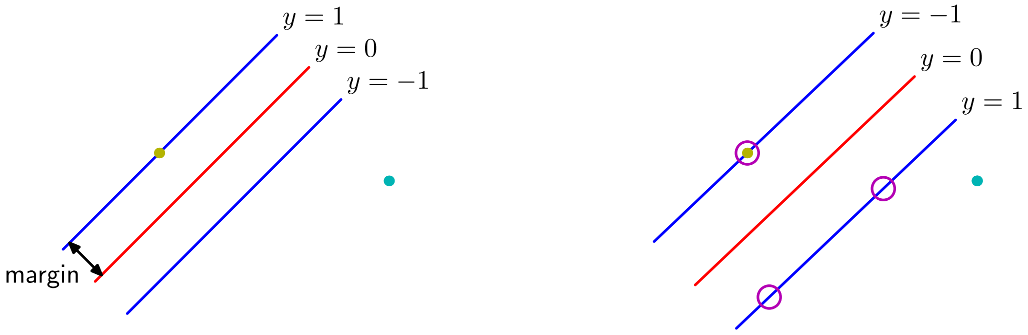

Figure 7.1 The margin is defined as the perpendicular distance between the decision boundary and the closest of the data points, as shown on the left figure. Maximizing the margin leads to a particular choice of decision boundary, as shown on the right. The location of this boundary is determined by a subset of the data points, known as support vectors, which are indicated by the circles.

having a common parameter σ^2. Together with the class priors, this defines an optimal misclassification-rate decision boundary. However, instead of using this optimal boundary, they determine the best hyperplane by minimizing the probability of error relative to the learned density model. In the limit $\sigma^2 \to 0$, the optimal hyperplane is shown to be the one having maximum margin. The intuition behind this result is that as σ^2 is reduced, the hyperplane is increasingly dominated by nearby data points relative to more distant ones. In the limit, the hyperplane becomes independent of data points that are not support vectors.

We shall see in Figure 10.13 that marginalization with respect to the prior distribution of the parameters in a Bayesian approach for a simple linearly separable data set leads to a decision boundary that lies in the middle of the region separating the data points. The large margin solution has similar behaviour.

Recall from Figure 4.1 that the perpendicular distance of a point $\mathbf{x}$ from a hyperplane defined by $y(\mathbf{x}) = 0$ where $y(\mathbf{x})$ takes the form (7.1) is given by $|y(\mathbf{x})|/\|\mathbf{w}\|$. Furthermore, we are only interested in solutions for which all data points are correctly classified, so that $t_n y(\mathbf{x}_n) > 0$ for all n. Thus the distance of a point $\mathbf{x}_n$ to the decision surface is given by

$$\frac{t_n y(\mathbf{x}_n)}{\|\mathbf{w}\|} = \frac{t_n(\mathbf{w}^{\mathrm{T}}\boldsymbol{\phi}(\mathbf{x}_n) + b)}{\|\mathbf{w}\|}. \tag{7.2}$$

The margin is given by the perpendicular distance to the closest point $\mathbf{x}_n$ from the data set, and we wish to optimize the parameters $\mathbf{w}$ and b in order to maximize this distance. Thus the maximum margin solution is found by solving

$$\underset{\mathbf{w},b}{\arg\max} \left\{ \frac{1}{\|\mathbf{w}\|} \min_n \left[t_n \left(\mathbf{w}^{\mathrm{T}}\boldsymbol{\phi}(\mathbf{x}_n) + b \right) \right] \right\} \tag{7.3}$$

where we have taken the factor $1/\|\mathbf{w}\|$ outside the optimization over n because $\mathbf{w}$

does not depend on n. Direct solution of this optimization problem would be very complex, and so we shall convert it into an equivalent problem that is much easier to solve. To do this we note that if we make the rescaling $\mathbf{w} \rightarrow \kappa\mathbf{w}$ and $b \rightarrow \kappa b$, then the distance from any point $\mathbf{x}_n$ to the decision surface, given by $t_n y(\mathbf{x}_n)/\|\mathbf{w}\|$, is unchanged. We can use this freedom to set

$$t_n \left(\mathbf{w}^{\mathrm{T}}\boldsymbol{\phi}(\mathbf{x}_n) + b\right) = 1 \tag{7.4}$$

for the point that is closest to the surface. In this case, all data points will satisfy the constraints

$$t_n \left(\mathbf{w}^{\mathrm{T}}\boldsymbol{\phi}(\mathbf{x}_n) + b\right) \geqslant 1, \qquad n = 1, \ldots, N. \tag{7.5}$$

This is known as the canonical representation of the decision hyperplane. In the case of data points for which the equality holds, the constraints are said to be *active*, whereas for the remainder they are said to be *inactive*. By definition, there will always be at least one active constraint, because there will always be a closest point, and once the margin has been maximized there will be at least two active constraints. The optimization problem then simply requires that we maximize $\|\mathbf{w}\|^{-1}$, which is equivalent to minimizing $\|\mathbf{w}\|^2$, and so we have to solve the optimization problem

$$\underset{\mathbf{w},b}{\arg\min}\,\frac{1}{2}\|\mathbf{w}\|^2 \tag{7.6}$$

subject to the constraints given by (7.5). The factor of $1/2$ in (7.6) is included for later convenience. This is an example of a *quadratic programming* problem in which we are trying to minimize a quadratic function subject to a set of linear inequality constraints. It appears that the bias parameter b has disappeared from the optimization. However, it is determined implicitly via the constraints, because these require that changes to $\|\mathbf{w}\|$ be compensated by changes to b. We shall see how this works shortly.

In order to solve this constrained optimization problem, we introduce Lagrange multipliers $a_n \geqslant 0$, with one multiplier a_n for each of the constraints in (7.5), giving the Lagrangian function

Appendix E

$$L(\mathbf{w}, b, \mathbf{a}) = \frac{1}{2}\|\mathbf{w}\|^2 - \sum_{n=1}^{N} a_n \left\{t_n(\mathbf{w}^{\mathrm{T}}\boldsymbol{\phi}(\mathbf{x}_n) + b) - 1\right\} \tag{7.7}$$

where $\mathbf{a} = (a_1, \ldots, a_N)^{\mathrm{T}}$. Note the minus sign in front of the Lagrange multiplier term, because we are minimizing with respect to $\mathbf{w}$ and b, and maximizing with respect to $\mathbf{a}$. Setting the derivatives of $L(\mathbf{w}, b, \mathbf{a})$ with respect to $\mathbf{w}$ and b equal to zero, we obtain the following two conditions

$$\mathbf{w} = \sum_{n=1}^{N} a_n t_n \boldsymbol{\phi}(\mathbf{x}_n) \tag{7.8}$$

$$0 = \sum_{n=1}^{N} a_n t_n. \tag{7.9}$$

Eliminating $\mathbf{w}$ and b from $L(\mathbf{w}, b, \mathbf{a})$ using these conditions then gives the *dual representation* of the maximum margin problem in which we maximize

$$\widetilde{L}(\mathbf{a}) = \sum_{n=1}^{N} a_n - \frac{1}{2} \sum_{n=1}^{N} \sum_{m=1}^{N} a_n a_m t_n t_m k(\mathbf{x}_n, \mathbf{x}_m) \tag{7.10}$$

with respect to $\mathbf{a}$ subject to the constraints

$$a_n \geqslant 0, \qquad n = 1, \ldots, N, \tag{7.11}$$

$$\sum_{n=1}^{N} a_n t_n = 0. \tag{7.12}$$

Here the kernel function is defined by $k(\mathbf{x}, \mathbf{x}') = \boldsymbol{\phi}(\mathbf{x})^{\mathrm{T}} \boldsymbol{\phi}(\mathbf{x}')$. Again, this takes the form of a quadratic programming problem in which we optimize a quadratic function of $\mathbf{a}$ subject to a set of inequality constraints. We shall discuss techniques for solving such quadratic programming problems in Section 7.1.1.

The solution to a quadratic programming problem in M variables in general has computational complexity that is $O(M^3)$. In going to the dual formulation we have turned the original optimization problem, which involved minimizing (7.6) over M variables, into the dual problem (7.10), which has N variables. For a fixed set of basis functions whose number M is smaller than the number N of data points, the move to the dual problem appears disadvantageous. However, it allows the model to be reformulated using kernels, and so the maximum margin classifier can be applied efficiently to feature spaces whose dimensionality exceeds the number of data points, including infinite feature spaces. The kernel formulation also makes clear the role of the constraint that the kernel function $k(\mathbf{x}, \mathbf{x}')$ be positive definite, because this ensures that the Lagrangian function $\widetilde{L}(\mathbf{a})$ is bounded below, giving rise to a well-defined optimization problem.

In order to classify new data points using the trained model, we evaluate the sign of $y(\mathbf{x})$ defined by (7.1). This can be expressed in terms of the parameters $\{a_n\}$ and the kernel function by substituting for $\mathbf{w}$ using (7.8) to give

$$y(\mathbf{x}) = \sum_{n=1}^{N} a_n t_n k(\mathbf{x}, \mathbf{x}_n) + b. \tag{7.13}$$

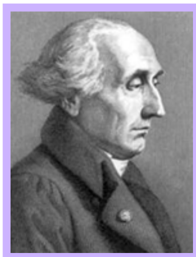

Joseph-Louis Lagrange
1736–1813

Although widely considered to be a French mathematician, Lagrange was born in Turin in Italy. By the age of nineteen, he had already made important contributions mathematics and had been appointed as Professor at the Royal Artillery School in Turin. For many years, Euler worked hard to persuade Lagrange to move to Berlin, which he eventually did in 1766 where he succeeded Euler as Director of Mathematics at the Berlin Academy. Later he moved to Paris, narrowly escaping with his life during the French revolution thanks to the personal intervention of Lavoisier (the French chemist who discovered oxygen) who himself was later executed at the guillotine. Lagrange made key contributions to the calculus of variations and the foundations of dynamics.

In Appendix E, we show that a constrained optimization of this form satisfies the *Karush-Kuhn-Tucker* (KKT) conditions, which in this case require that the following three properties hold

$$\begin{aligned} a_n &\geqslant 0 & (7.14)\\ t_n y(\mathbf{x}_n) - 1 &\geqslant 0 & (7.15)\\ a_n \{t_n y(\mathbf{x}_n) - 1\} &= 0. & (7.16)\end{aligned}$$

Thus for every data point, either $a_n = 0$ or $t_n y(\mathbf{x}_n) = 1$. Any data point for which $a_n = 0$ will not appear in the sum in (7.13) and hence plays no role in making predictions for new data points. The remaining data points are called *support vectors*, and because they satisfy $t_n y(\mathbf{x}_n) = 1$, they correspond to points that lie on the maximum margin hyperplanes in feature space, as illustrated in Figure 7.1. This property is central to the practical applicability of support vector machines. Once the model is trained, a significant proportion of the data points can be discarded and only the support vectors retained.

Having solved the quadratic programming problem and found a value for $\mathbf{a}$, we can then determine the value of the threshold parameter b by noting that any support vector $\mathbf{x}_n$ satisfies $t_n y(\mathbf{x}_n) = 1$. Using (7.13) this gives

$$t_n \left(\sum_{m \in \mathcal{S}} a_m t_m k(\mathbf{x}_n, \mathbf{x}_m) + b \right) = 1 \tag{7.17}$$

where $\mathcal{S}$ denotes the set of indices of the support vectors. Although we can solve this equation for b using an arbitrarily chosen support vector $\mathbf{x}_n$, a numerically more stable solution is obtained by first multiplying through by t_n, making use of $t_n^2 = 1$, and then averaging these equations over all support vectors and solving for b to give

$$b = \frac{1}{N_{\mathcal{S}}} \sum_{n \in \mathcal{S}} \left(t_n - \sum_{m \in \mathcal{S}} a_m t_m k(\mathbf{x}_n, \mathbf{x}_m) \right) \tag{7.18}$$

where $N_{\mathcal{S}}$ is the total number of support vectors.

For later comparison with alternative models, we can express the maximum-margin classifier in terms of the minimization of an error function, with a simple quadratic regularizer, in the form

$$\sum_{n=1}^{N} E_{\infty}(y(\mathbf{x}_n) t_n - 1) + \lambda \|\mathbf{w}\|^2 \tag{7.19}$$

where $E_{\infty}(z)$ is a function that is zero if $z \geqslant 0$ and ∞ otherwise and ensures that the constraints (7.5) are satisfied. Note that as long as the regularization parameter satisfies $\lambda > 0$, its precise value plays no role.

Figure 7.2 shows an example of the classification resulting from training a support vector machine on a simple synthetic data set using a Gaussian kernel of the

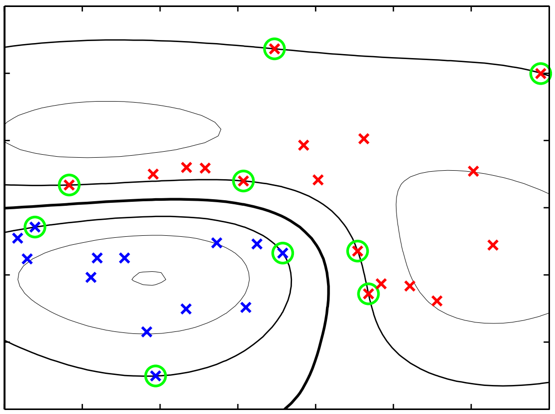
Figure 7.2 Example of synthetic data from two classes in two dimensions showing contours of constant $y(\mathbf{x})$ obtained from a support vector machine having a Gaussian kernel function. Also shown are the decision boundary, the margin boundaries, and the support vectors.

form (6.23). Although the data set is not linearly separable in the two-dimensional data space $\mathbf{x}$, it is linearly separable in the nonlinear feature space defined implicitly by the nonlinear kernel function. Thus the training data points are perfectly separated in the original data space.

This example also provides a geometrical insight into the origin of sparsity in the SVM. The maximum margin hyperplane is defined by the location of the support vectors. Other data points can be moved around freely (so long as they remain outside the margin region) without changing the decision boundary, and so the solution will be independent of such data points.

7.1.1 Overlapping class distributions

So far, we have assumed that the training data points are linearly separable in the feature space $\boldsymbol{\phi}(\mathbf{x})$. The resulting support vector machine will give exact separation of the training data in the original input space $\mathbf{x}$, although the corresponding decision boundary will be nonlinear. In practice, however, the class-conditional distributions may overlap, in which case exact separation of the training data can lead to poor generalization.

We therefore need a way to modify the support vector machine so as to allow some of the training points to be misclassified. From (7.19) we see that in the case of separable classes, we implicitly used an error function that gave infinite error if a data point was misclassified and zero error if it was classified correctly, and then optimized the model parameters to maximize the margin. We now modify this approach so that data points are allowed to be on the 'wrong side' of the margin boundary, but with a penalty that increases with the distance from that boundary. For the subsequent optimization problem, it is convenient to make this penalty a linear function of this distance. To do this, we introduce *slack variables*, $\xi_n \geqslant 0$ where $n = 1, \ldots, N$, with one slack variable for each training data point (Bennett, 1992; Cortes and Vapnik, 1995). These are defined by $\xi_n = 0$ for data points that are on or inside the correct margin boundary and $\xi_n = |t_n - y(\mathbf{x}_n)|$ for other points. Thus a data point that is on the decision boundary $y(\mathbf{x}_n) = 0$ will have $\xi_n = 1$, and points

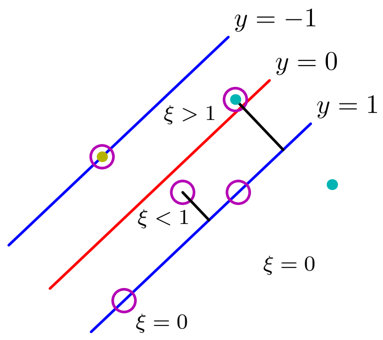

Figure 7.3 Illustration of the slack variables $\xi_n \geqslant 0$. Data points with circles around them are support vectors.

with $\xi_n > 1$ will be misclassified. The exact classification constraints (7.5) are then replaced with

$$t_n y(\mathbf{x}_n) \geqslant 1 - \xi_n, \qquad n = 1, \ldots, N \tag{7.20}$$

in which the slack variables are constrained to satisfy $\xi_n \geqslant 0$. Data points for which $\xi_n = 0$ are correctly classified and are either on the margin or on the correct side of the margin. Points for which $0 < \xi_n \leqslant 1$ lie inside the margin, but on the correct side of the decision boundary, and those data points for which $\xi_n > 1$ lie on the wrong side of the decision boundary and are misclassified, as illustrated in Figure 7.3. This is sometimes described as relaxing the hard margin constraint to give a *soft margin* and allows some of the training set data points to be misclassified. Note that while slack variables allow for overlapping class distributions, this framework is still sensitive to outliers because the penalty for misclassification increases linearly with ξ.

Our goal is now to maximize the margin while softly penalizing points that lie on the wrong side of the margin boundary. We therefore minimize

$$C \sum_{n=1}^{N} \xi_n + \frac{1}{2}\|\mathbf{w}\|^2 \tag{7.21}$$

where the parameter $C > 0$ controls the trade-off between the slack variable penalty and the margin. Because any point that is misclassified has $\xi_n > 1$, it follows that $\sum_n \xi_n$ is an upper bound on the number of misclassified points. The parameter C is therefore analogous to (the inverse of) a regularization coefficient because it controls the trade-off between minimizing training errors and controlling model complexity. In the limit $C \to \infty$, we will recover the earlier support vector machine for separable data.

We now wish to minimize (7.21) subject to the constraints (7.20) together with $\xi_n \geqslant 0$. The corresponding Lagrangian is given by

$$L(\mathbf{w}, b, \mathbf{a}) = \frac{1}{2}\|\mathbf{w}\|^2 + C\sum_{n=1}^{N} \xi_n - \sum_{n=1}^{N} a_n \{t_n y(\mathbf{x}_n) - 1 + \xi_n\} - \sum_{n=1}^{N} \mu_n \xi_n \tag{7.22}$$

Appendix E

where $\{a_n \geqslant 0\}$ and $\{\mu_n \geqslant 0\}$ are Lagrange multipliers. The corresponding set of KKT conditions are given by

$$\begin{aligned} a_n &\geqslant 0 && (7.23)\\ t_n y(\mathbf{x}_n) - 1 + \xi_n &\geqslant 0 && (7.24)\\ a_n\left(t_n y(\mathbf{x}_n) - 1 + \xi_n\right) &= 0 && (7.25)\\ \mu_n &\geqslant 0 && (7.26)\\ \xi_n &\geqslant 0 && (7.27)\\ \mu_n \xi_n &= 0 && (7.28) \end{aligned}$$

where $n = 1, \ldots, N$.

We now optimize out $\mathbf{w}$, b, and $\{\xi_n\}$ making use of the definition (7.1) of $y(\mathbf{x})$ to give

$$\frac{\partial L}{\partial \mathbf{w}} = 0 \quad \Rightarrow \quad \mathbf{w} = \sum_{n=1}^{N} a_n t_n \boldsymbol{\phi}(\mathbf{x}_n) \tag{7.29}$$

$$\frac{\partial L}{\partial b} = 0 \quad \Rightarrow \quad \sum_{n=1}^{N} a_n t_n = 0 \tag{7.30}$$

$$\frac{\partial L}{\partial \xi_n} = 0 \quad \Rightarrow \quad a_n = C - \mu_n. \tag{7.31}$$

Using these results to eliminate $\mathbf{w}$, b, and $\{\xi_n\}$ from the Lagrangian, we obtain the dual Lagrangian in the form

$$\widetilde{L}(\mathbf{a}) = \sum_{n=1}^{N} a_n - \frac{1}{2} \sum_{n=1}^{N} \sum_{m=1}^{N} a_n a_m t_n t_m k(\mathbf{x}_n, \mathbf{x}_m) \tag{7.32}$$

which is identical to the separable case, except that the constraints are somewhat different. To see what these constraints are, we note that $a_n \geqslant 0$ is required because these are Lagrange multipliers. Furthermore, (7.31) together with $\mu_n \geqslant 0$ implies $a_n \leqslant C$. We therefore have to minimize (7.32) with respect to the dual variables $\{a_n\}$ subject to

$$0 \leqslant a_n \leqslant C \tag{7.33}$$

$$\sum_{n=1}^{N} a_n t_n = 0 \tag{7.34}$$

for $n = 1, \ldots, N$, where (7.33) are known as *box constraints*. This again represents a quadratic programming problem. If we substitute (7.29) into (7.1), we see that predictions for new data points are again made by using (7.13).

We can now interpret the resulting solution. As before, a subset of the data points may have $a_n = 0$, in which case they do not contribute to the predictive model (7.13). The remaining data points constitute the support vectors. These have $a_n > 0$ and hence from (7.25) must satisfy

$$t_n y(\mathbf{x}_n) = 1 - \xi_n. \tag{7.35}$$

If $a_n < C$, then (7.31) implies that $\mu_n > 0$, which from (7.28) requires $\xi_n = 0$ and hence such points lie on the margin. Points with $a_n = C$ can lie inside the margin and can either be correctly classified if $\xi_n \leqslant 1$ or misclassified if $\xi_n > 1$.

To determine the parameter b in (7.1), we note that those support vectors for which $0 < a_n < C$ have $\xi_n = 0$ so that $t_n y(\mathbf{x}_n) = 1$ and hence will satisfy

$$t_n \left(\sum_{m \in \mathcal{S}} a_m t_m k(\mathbf{x}_n, \mathbf{x}_m) + b \right) = 1. \tag{7.36}$$

Again, a numerically stable solution is obtained by averaging to give

$$b = \frac{1}{N_{\mathcal{M}}} \sum_{n \in \mathcal{M}} \left(t_n - \sum_{m \in \mathcal{S}} a_m t_m k(\mathbf{x}_n, \mathbf{x}_m) \right) \tag{7.37}$$

where $\mathcal{M}$ denotes the set of indices of data points having $0 < a_n < C$.

An alternative, equivalent formulation of the support vector machine, known as the ν-*SVM*, has been proposed by Schölkopf *et al.* (2000). This involves maximizing

$$\widetilde{L}(\mathbf{a}) = -\frac{1}{2} \sum_{n=1}^{N} \sum_{m=1}^{N} a_n a_m t_n t_m k(\mathbf{x}_n, \mathbf{x}_m) \tag{7.38}$$

subject to the constraints

$$0 \leqslant a_n \leqslant 1/N \tag{7.39}$$

$$\sum_{n=1}^{N} a_n t_n = 0 \tag{7.40}$$

$$\sum_{n=1}^{N} a_n \geqslant \nu. \tag{7.41}$$

This approach has the advantage that the parameter ν, which replaces C, can be interpreted as both an upper bound on the fraction of *margin errors* (points for which $\xi_n > 0$ and hence which lie on the wrong side of the margin boundary and which may or may not be misclassified) and a lower bound on the fraction of support vectors. An example of the ν-SVM applied to a synthetic data set is shown in Figure 7.4. Here Gaussian kernels of the form $\exp\left(-\gamma \|\mathbf{x} - \mathbf{x}'\|^2\right)$ have been used, with $\gamma = 0.45$.

Although predictions for new inputs are made using only the support vectors, the training phase (i.e., the determination of the parameters $\mathbf{a}$ and b) makes use of the whole data set, and so it is important to have efficient algorithms for solving

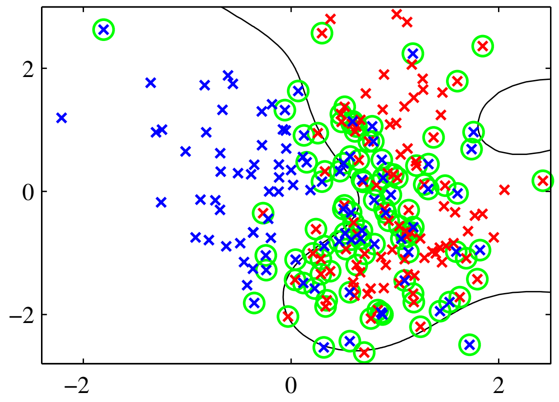

Figure 7.4 Illustration of the ν-SVM applied to a nonseparable data set in two dimensions. The support vectors are indicated by circles.

the quadratic programming problem. We first note that the objective function $\widetilde{L}(\mathbf{a})$ given by (7.10) or (7.32) is quadratic and so any local optimum will also be a global optimum provided the constraints define a convex region (which they do as a consequence of being linear). Direct solution of the quadratic programming problem using traditional techniques is often infeasible due to the demanding computation and memory requirements, and so more practical approaches need to be found. The technique of *chunking* (Vapnik, 1982) exploits the fact that the value of the Lagrangian is unchanged if we remove the rows and columns of the kernel matrix corresponding to Lagrange multipliers that have value zero. This allows the full quadratic programming problem to be broken down into a series of smaller ones, whose goal is eventually to identify all of the nonzero Lagrange multipliers and discard the others. Chunking can be implemented using *protected conjugate gradients* (Burges, 1998). Although chunking reduces the size of the matrix in the quadratic function from the number of data points squared to approximately the number of nonzero Lagrange multipliers squared, even this may be too big to fit in memory for large-scale applications. *Decomposition methods* (Osuna *et al.*, 1996) also solve a series of smaller quadratic programming problems but are designed so that each of these is of a fixed size, and so the technique can be applied to arbitrarily large data sets. However, it still involves numerical solution of quadratic programming subproblems and these can be problematic and expensive. One of the most popular approaches to training support vector machines is called *sequential minimal optimization*, or *SMO* (Platt, 1999). It takes the concept of chunking to the extreme limit and considers just two Lagrange multipliers at a time. In this case, the subproblem can be solved analytically, thereby avoiding numerical quadratic programming altogether. Heuristics are given for choosing the pair of Lagrange multipliers to be considered at each step. In practice, SMO is found to have a scaling with the number of data points that is somewhere between linear and quadratic depending on the particular application.

We have seen that kernel functions correspond to inner products in feature spaces that can have high, or even infinite, dimensionality. By working directly in terms of the kernel function, without introducing the feature space explicitly, it might therefore seem that support vector machines somehow manage to avoid the curse of di-

Section 1.4

mensionality. This is not the case, however, because there are constraints amongst the feature values that restrict the effective dimensionality of feature space. To see this consider a simple second-order polynomial kernel that we can expand in terms of its components

$$\begin{aligned} k(\mathbf{x},\mathbf{z}) &= \left(1+\mathbf{x}^{\mathrm{T}}\mathbf{z}\right)^2 = (1+x_1z_1+x_2z_2)^2 \\ &= 1+2x_1z_1+2x_2z_2+x_1^2z_1^2+2x_1z_1x_2z_2+x_2^2z_2^2 \\ &= (1,\sqrt{2}x_1,\sqrt{2}x_2,x_1^2,\sqrt{2}x_1x_2,x_2^2)(1,\sqrt{2}z_1,\sqrt{2}z_2,z_1^2,\sqrt{2}z_1z_2,z_2^2)^{\mathrm{T}} \\ &= \boldsymbol{\phi}(\mathbf{x})^{\mathrm{T}}\boldsymbol{\phi}(\mathbf{z}). \end{aligned} \tag{7.42}$$

This kernel function therefore represents an inner product in a feature space having six dimensions, in which the mapping from input space to feature space is described by the vector function $\boldsymbol{\phi}(\mathbf{x})$. However, the coefficients weighting these different features are constrained to have specific forms. Thus any set of points in the original two-dimensional space $\mathbf{x}$ would be constrained to lie exactly on a two-dimensional nonlinear manifold embedded in the six-dimensional feature space.

We have already highlighted the fact that the support vector machine does not provide probabilistic outputs but instead makes classification decisions for new input vectors. Veropoulos *et al.* (1999) discuss modifications to the SVM to allow the trade-off between false positive and false negative errors to be controlled. However, if we wish to use the SVM as a module in a larger probabilistic system, then probabilistic predictions of the class label t for new inputs $\mathbf{x}$ are required.

To address this issue, Platt (2000) has proposed fitting a logistic sigmoid to the outputs of a previously trained support vector machine. Specifically, the required conditional probability is assumed to be of the form

$$p(t=1|\mathbf{x}) = \sigma\left(Ay(\mathbf{x})+B\right) \tag{7.43}$$

where $y(\mathbf{x})$ is defined by (7.1). Values for the parameters A and B are found by minimizing the cross-entropy error function defined by a training set consisting of pairs of values $y(\mathbf{x}_n)$ and t_n. The data used to fit the sigmoid needs to be independent of that used to train the original SVM in order to avoid severe over-fitting. This two-stage approach is equivalent to assuming that the output $y(\mathbf{x})$ of the support vector machine represents the log-odds of $\mathbf{x}$ belonging to class $t=1$. Because the SVM training procedure is not specifically intended to encourage this, the SVM can give a poor approximation to the posterior probabilities (Tipping, 2001).

7.1.2 Relation to logistic regression

As with the separable case, we can re-cast the SVM for nonseparable distributions in terms of the minimization of a regularized error function. This will also allow us to highlight similarities, and differences, compared to the logistic regression model.

Section 4.3.2

We have seen that for data points that are on the correct side of the margin boundary, and which therefore satisfy $y_nt_n \geqslant 1$, we have $\xi_n = 0$, and for the

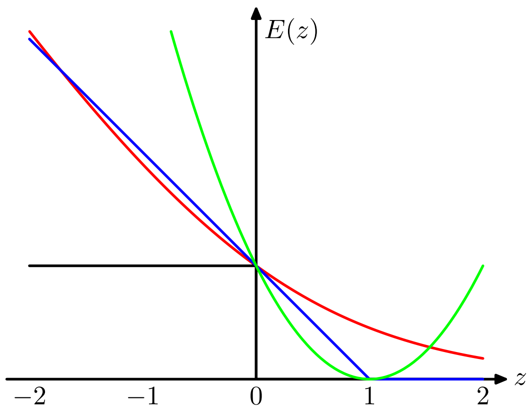

Figure 7.5 Plot of the 'hinge' error function used in support vector machines, shown in blue, along with the error function for logistic regression, rescaled by a factor of $1/\ln(2)$ so that it passes through the point $(0, 1)$, shown in red. Also shown are the misclassification error in black and the squared error in green.

remaining points we have $\xi_n = 1 - y_n t_n$. Thus the objective function (7.21) can be written (up to an overall multiplicative constant) in the form

$$\sum_{n=1}^{N} E_{\mathrm{SV}}(y_n t_n) + \lambda \|\mathbf{w}\|^2 \tag{7.44}$$

where $\lambda = (2C)^{-1}$, and $E_{\mathrm{SV}}(\cdot)$ is the *hinge* error function defined by

$$E_{\mathrm{SV}}(y_n t_n) = [1 - y_n t_n]_+ \tag{7.45}$$

where $[\,\cdot\,]_+$ denotes the positive part. The hinge error function, so-called because of its shape, is plotted in Figure 7.5. It can be viewed as an approximation to the misclassification error, i.e., the error function that ideally we would like to minimize, which is also shown in Figure 7.5.

When we considered the logistic regression model in Section 4.3.2, we found it convenient to work with target variable $t \in \{0, 1\}$. For comparison with the support vector machine, we first reformulate maximum likelihood logistic regression using the target variable $t \in \{-1, 1\}$. To do this, we note that $p(t = 1|y) = \sigma(y)$ where $y(\mathbf{x})$ is given by (7.1), and $\sigma(y)$ is the logistic sigmoid function defined by (4.59). It follows that $p(t = -1|y) = 1 - \sigma(y) = \sigma(-y)$, where we have used the properties of the logistic sigmoid function, and so we can write

$$p(t|y) = \sigma(yt). \tag{7.46}$$

Exercise 7.6

From this we can construct an error function by taking the negative logarithm of the likelihood function that, with a quadratic regularizer, takes the form

$$\sum_{n=1}^{N} E_{\mathrm{LR}}(y_n t_n) + \lambda \|\mathbf{w}\|^2. \tag{7.47}$$

where

$$E_{\mathrm{LR}}(yt) = \ln\left(1 + \exp(-yt)\right). \tag{7.48}$$

For comparison with other error functions, we can divide by $\ln(2)$ so that the error function passes through the point $(0, 1)$. This rescaled error function is also plotted in Figure 7.5 and we see that it has a similar form to the support vector error function. The key difference is that the flat region in $E_{\mathrm{SV}}(yt)$ leads to sparse solutions.

Both the logistic error and the hinge loss can be viewed as continuous approximations to the misclassification error. Another continuous error function that has sometimes been used to solve classification problems is the squared error, which is again plotted in Figure 7.5. It has the property, however, of placing increasing emphasis on data points that are correctly classified but that are a long way from the decision boundary on the correct side. Such points will be strongly weighted at the expense of misclassified points, and so if the objective is to minimize the misclassification rate, then a monotonically decreasing error function would be a better choice.

7.1.3 Multiclass SVMs

The support vector machine is fundamentally a two-class classifier. In practice, however, we often have to tackle problems involving $K > 2$ classes. Various methods have therefore been proposed for combining multiple two-class SVMs in order to build a multiclass classifier.

One commonly used approach (Vapnik, 1998) is to construct K separate SVMs, in which the k^{th} model $y_k(\mathbf{x})$ is trained using the data from class $\mathcal{C}_k$ as the positive examples and the data from the remaining $K - 1$ classes as the negative examples. This is known as the *one-versus-the-rest* approach. However, in Figure 4.2 we saw that using the decisions of the individual classifiers can lead to inconsistent results in which an input is assigned to multiple classes simultaneously. This problem is sometimes addressed by making predictions for new inputs $\mathbf{x}$ using

$$y(\mathbf{x}) = \max_k y_k(\mathbf{x}). \tag{7.49}$$

Unfortunately, this heuristic approach suffers from the problem that the different classifiers were trained on different tasks, and there is no guarantee that the real-valued quantities $y_k(\mathbf{x})$ for different classifiers will have appropriate scales.

Another problem with the one-versus-the-rest approach is that the training sets are imbalanced. For instance, if we have ten classes each with equal numbers of training data points, then the individual classifiers are trained on data sets comprising 90% negative examples and only 10% positive examples, and the symmetry of the original problem is lost. A variant of the one-versus-the-rest scheme was proposed by Lee *et al.* (2001) who modify the target values so that the positive class has target $+1$ and the negative class has target $-1/(K - 1)$.

Weston and Watkins (1999) define a single objective function for training all K SVMs simultaneously, based on maximizing the margin from each to remaining classes. However, this can result in much slower training because, instead of solving K separate optimization problems each over N data points with an overall cost of $O(KN^2)$, a single optimization problem of size $(K-1)N$ must be solved giving an overall cost of $O(K^2N^2)$.

Another approach is to train $K(K-1)/2$ different 2-class SVMs on all possible pairs of classes, and then to classify test points according to which class has the highest number of 'votes', an approach that is sometimes called *one-versus-one*. Again, we saw in Figure 4.2 that this can lead to ambiguities in the resulting classification. Also, for large K this approach requires significantly more training time than the one-versus-the-rest approach. Similarly, to evaluate test points, significantly more computation is required.

The latter problem can be alleviated by organizing the pairwise classifiers into a directed acyclic graph (not to be confused with a probabilistic graphical model) leading to the *DAGSVM* (Platt *et al.*, 2000). For K classes, the DAGSVM has a total of $K(K-1)/2$ classifiers, and to classify a new test point only $K-1$ pairwise classifiers need to be evaluated, with the particular classifiers used depending on which path through the graph is traversed.

A different approach to multiclass classification, based on error-correcting output codes, was developed by Dietterich and Bakiri (1995) and applied to support vector machines by Allwein *et al.* (2000). This can be viewed as a generalization of the voting scheme of the one-versus-one approach in which more general partitions of the classes are used to train the individual classifiers. The K classes themselves are represented as particular sets of responses from the two-class classifiers chosen, and together with a suitable decoding scheme, this gives robustness to errors and to ambiguity in the outputs of the individual classifiers. Although the application of SVMs to multiclass classification problems remains an open issue, in practice the one-versus-the-rest approach is the most widely used in spite of its ad-hoc formulation and its practical limitations.

There are also *single-class* support vector machines, which solve an unsupervised learning problem related to probability density estimation. Instead of modelling the density of data, however, these methods aim to find a smooth boundary enclosing a region of high density. The boundary is chosen to represent a quantile of the density, that is, the probability that a data point drawn from the distribution will land inside that region is given by a fixed number between 0 and 1 that is specified in advance. This is a more restricted problem than estimating the full density but may be sufficient in specific applications. Two approaches to this problem using support vector machines have been proposed. The algorithm of Schölkopf *et al.* (2001) tries to find a hyperplane that separates all but a fixed fraction ν of the training data from the origin while at the same time maximizing the distance (margin) of the hyperplane from the origin, while Tax and Duin (1999) look for the smallest sphere in feature space that contains all but a fraction ν of the data points. For kernels $k(\mathbf{x}, \mathbf{x}')$ that are functions only of $\mathbf{x} - \mathbf{x}'$, the two algorithms are equivalent.

7.1.4 SVMs for regression

Section 3.1.4

We now extend support vector machines to regression problems while at the same time preserving the property of sparseness. In simple linear regression, we

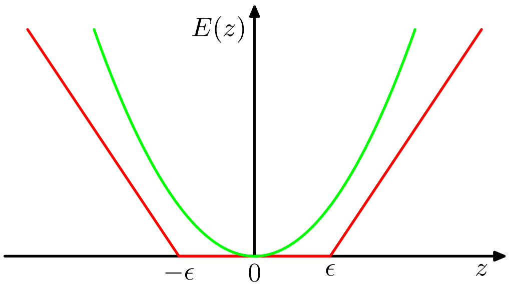

Figure 7.6 Plot of an ϵ-insensitive error function (in red) in which the error increases linearly with distance beyond the insensitive region. Also shown for comparison is the quadratic error function (in green).

minimize a regularized error function given by

$$\frac{1}{2}\sum_{n=1}^{N}\{y_n - t_n\}^2 + \frac{\lambda}{2}\|\mathbf{w}\|^2. \tag{7.50}$$

To obtain sparse solutions, the quadratic error function is replaced by an ϵ-*insensitive error function* (Vapnik, 1995), which gives zero error if the absolute difference between the prediction $y(\mathbf{x})$ and the target t is less than ϵ where $\epsilon > 0$. A simple example of an ϵ-insensitive error function, having a linear cost associated with errors outside the insensitive region, is given by

$$E_\epsilon(y(\mathbf{x}) - t) = \begin{cases} 0, & \text{if } |y(\mathbf{x}) - t| < \epsilon; \\ |y(\mathbf{x}) - t| - \epsilon, & \text{otherwise} \end{cases} \tag{7.51}$$

and is illustrated in Figure 7.6.

We therefore minimize a regularized error function given by

$$C\sum_{n=1}^{N} E_\epsilon(y(\mathbf{x}_n) - t_n) + \frac{1}{2}\|\mathbf{w}\|^2 \tag{7.52}$$

where $y(\mathbf{x})$ is given by (7.1). By convention the (inverse) regularization parameter, denoted C, appears in front of the error term.

As before, we can re-express the optimization problem by introducing slack variables. For each data point $\mathbf{x}_n$, we now need two slack variables $\xi_n \geqslant 0$ and $\widehat{\xi}_n \geqslant 0$, where $\xi_n > 0$ corresponds to a point for which $t_n > y(\mathbf{x}_n) + \epsilon$, and $\widehat{\xi}_n > 0$ corresponds to a point for which $t_n < y(\mathbf{x}_n) - \epsilon$, as illustrated in Figure 7.7.

The condition for a target point to lie inside the ϵ-tube is that $y_n - \epsilon \leqslant t_n \leqslant y_n + \epsilon$, where $y_n = y(\mathbf{x}_n)$. Introducing the slack variables allows points to lie outside the tube provided the slack variables are nonzero, and the corresponding conditions are

$$t_n \leqslant y(\mathbf{x}_n) + \epsilon + \xi_n \tag{7.53}$$

$$t_n \geqslant y(\mathbf{x}_n) - \epsilon - \widehat{\xi}_n. \tag{7.54}$$

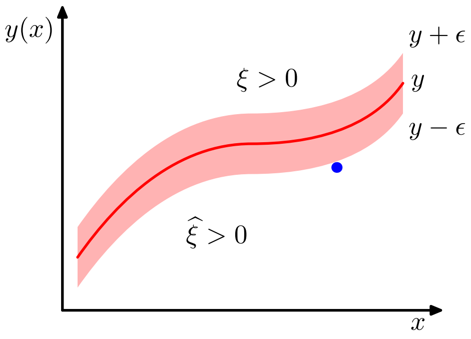

Figure 7.7 Illustration of SVM regression, showing the regression curve together with the ϵ-insensitive 'tube'. Also shown are examples of the slack variables ξ and $\widehat{\xi}$. Points above the ϵ-tube have $\xi > 0$ and $\widehat{\xi} = 0$, points below the ϵ-tube have $\xi = 0$ and $\widehat{\xi} > 0$, and points inside the ϵ-tube have $\xi = \widehat{\xi} = 0$.

The error function for support vector regression can then be written as

$$C\sum_{n=1}^{N}(\xi_n + \widehat{\xi}_n) + \frac{1}{2}\|\mathbf{w}\|^2 \tag{7.55}$$

which must be minimized subject to the constraints $\xi_n \geqslant 0$ and $\widehat{\xi}_n \geqslant 0$ as well as (7.53) and (7.54). This can be achieved by introducing Lagrange multipliers $a_n \geqslant 0$, $\widehat{a}_n \geqslant 0$, $\mu_n \geqslant 0$, and $\widehat{\mu}_n \geqslant 0$ and optimizing the Lagrangian

$$\begin{aligned} L &= C\sum_{n=1}^{N}(\xi_n + \widehat{\xi}_n) + \frac{1}{2}\|\mathbf{w}\|^2 - \sum_{n=1}^{N}(\mu_n\xi_n + \widehat{\mu}_n\widehat{\xi}_n) \\ &\quad - \sum_{n=1}^{N} a_n(\epsilon + \xi_n + y_n - t_n) - \sum_{n=1}^{N}\widehat{a}_n(\epsilon + \widehat{\xi}_n - y_n + t_n). \end{aligned} \tag{7.56}$$

We now substitute for $y(\mathbf{x})$ using (7.1) and then set the derivatives of the Lagrangian with respect to $\mathbf{w}$, b, ξ_n, and $\widehat{\xi}_n$ to zero, giving

$$\frac{\partial L}{\partial \mathbf{w}} = 0 \;\Rightarrow\; \mathbf{w} = \sum_{n=1}^{N}(a_n - \widehat{a}_n)\boldsymbol{\phi}(\mathbf{x}_n) \tag{7.57}$$

$$\frac{\partial L}{\partial b} = 0 \;\Rightarrow\; \sum_{n=1}^{N}(a_n - \widehat{a}_n) = 0 \tag{7.58}$$

$$\frac{\partial L}{\partial \xi_n} = 0 \;\Rightarrow\; a_n + \mu_n = C \tag{7.59}$$

$$\frac{\partial L}{\partial \widehat{\xi}_n} = 0 \;\Rightarrow\; \widehat{a}_n + \widehat{\mu}_n = C. \tag{7.60}$$

Using these results to eliminate the corresponding variables from the Lagrangian, we see that the dual problem involves maximizing *Exercise 7.7*

$$\begin{aligned}\widetilde{L}(\mathbf{a},\widehat{\mathbf{a}}) &= -\frac{1}{2}\sum_{n=1}^{N}\sum_{m=1}^{N}(a_n-\widehat{a}_n)(a_m-\widehat{a}_m)k(\mathbf{x}_n,\mathbf{x}_m) \\ &\quad -\epsilon\sum_{n=1}^{N}(a_n+\widehat{a}_n)+\sum_{n=1}^{N}(a_n-\widehat{a}_n)t_n \end{aligned} \tag{7.61}$$

with respect to $\{a_n\}$ and $\{\widehat{a}_n\}$, where we have introduced the kernel $k(\mathbf{x},\mathbf{x}') = \boldsymbol{\phi}(\mathbf{x})^{\mathrm{T}}\boldsymbol{\phi}(\mathbf{x}')$. Again, this is a constrained maximization, and to find the constraints we note that $a_n \geqslant 0$ and $\widehat{a}_n \geqslant 0$ are both required because these are Lagrange multipliers. Also $\mu_n \geqslant 0$ and $\widehat{\mu}_n \geqslant 0$ together with (7.59) and (7.60), require $a_n \leqslant C$ and $\widehat{a}_n \leqslant C$, and so again we have the box constraints

$$0 \leqslant a_n \leqslant C \tag{7.62}$$

$$0 \leqslant \widehat{a}_n \leqslant C \tag{7.63}$$

together with the condition (7.58).

Substituting (7.57) into (7.1), we see that predictions for new inputs can be made using

$$y(\mathbf{x}) = \sum_{n=1}^{N}(a_n-\widehat{a}_n)k(\mathbf{x},\mathbf{x}_n)+b \tag{7.64}$$

which is again expressed in terms of the kernel function.

The corresponding Karush-Kuhn-Tucker (KKT) conditions, which state that at the solution the product of the dual variables and the constraints must vanish, are given by

$$a_n(\epsilon+\xi_n+y_n-t_n) = 0 \tag{7.65}$$

$$\widehat{a}_n(\epsilon+\widehat{\xi}_n-y_n+t_n) = 0 \tag{7.66}$$

$$(C-a_n)\xi_n = 0 \tag{7.67}$$

$$(C-\widehat{a}_n)\widehat{\xi}_n = 0. \tag{7.68}$$

From these we can obtain several useful results. First of all, we note that a coefficient a_n can only be nonzero if $\epsilon+\xi_n+y_n-t_n=0$, which implies that the data point either lies on the upper boundary of the ϵ-tube ($\xi_n = 0$) or lies above the upper boundary ($\xi_n > 0$). Similarly, a nonzero value for $\widehat{a}_n$ implies $\epsilon+\widehat{\xi}_n-y_n+t_n=0$, and such points must lie either on or below the lower boundary of the ϵ-tube.

Furthermore, the two constraints $\epsilon+\xi_n+y_n-t_n=0$ and $\epsilon+\widehat{\xi}_n-y_n+t_n=0$ are incompatible, as is easily seen by adding them together and noting that ξ_n and $\widehat{\xi}_n$ are nonnegative while ϵ is strictly positive, and so for every data point $\mathbf{x}_n$, either a_n or $\widehat{a}_n$ (or both) must be zero.

The support vectors are those data points that contribute to predictions given by (7.64), in other words those for which either $a_n \neq 0$ or $\widehat{a}_n \neq 0$. These are points that lie on the boundary of the ϵ-tube or outside the tube. All points within the tube have

$a_n = \widehat{a}_n = 0$. We again have a sparse solution, and the only terms that have to be evaluated in the predictive model (7.64) are those that involve the support vectors.

The parameter b can be found by considering a data point for which $0 < a_n < C$, which from (7.67) must have $\xi_n = 0$, and from (7.65) must therefore satisfy $\epsilon + y_n - t_n = 0$. Using (7.1) and solving for b, we obtain

$$\begin{aligned} b &= t_n - \epsilon - \mathbf{w}^{\mathrm{T}}\boldsymbol{\phi}(\mathbf{x}_n) \\ &= t_n - \epsilon - \sum_{m=1}^{N}(a_m - \widehat{a}_m)k(\mathbf{x}_n, \mathbf{x}_m) \end{aligned} \tag{7.69}$$

where we have used (7.57). We can obtain an analogous result by considering a point for which $0 < \widehat{a}_n < C$. In practice, it is better to average over all such estimates of b.

As with the classification case, there is an alternative formulation of the SVM for regression in which the parameter governing complexity has a more intuitive interpretation (Schölkopf *et al.*, 2000). In particular, instead of fixing the width ϵ of the insensitive region, we fix instead a parameter ν that bounds the fraction of points lying outside the tube. This involves maximizing

$$\begin{aligned} \widetilde{L}(\mathbf{a}, \widehat{\mathbf{a}}) = & -\frac{1}{2}\sum_{n=1}^{N}\sum_{m=1}^{N}(a_n - \widehat{a}_n)(a_m - \widehat{a}_m)k(\mathbf{x}_n, \mathbf{x}_m) \\ & + \sum_{n=1}^{N}(a_n - \widehat{a}_n)t_n \end{aligned} \tag{7.70}$$

subject to the constraints

$$0 \leqslant a_n \leqslant C/N \tag{7.71}$$

$$0 \leqslant \widehat{a}_n \leqslant C/N \tag{7.72}$$

$$\sum_{n=1}^{N}(a_n - \widehat{a}_n) = 0 \tag{7.73}$$

$$\sum_{n=1}^{N}(a_n + \widehat{a}_n) \leqslant \nu C. \tag{7.74}$$

It can be shown that there are at most νN data points falling outside the insensitive tube, while at least νN data points are support vectors and so lie either on the tube or outside it.

Appendix A

The use of a support vector machine to solve a regression problem is illustrated using the sinusoidal data set in Figure 7.8. Here the parameters ν and C have been chosen by hand. In practice, their values would typically be determined by cross-validation.

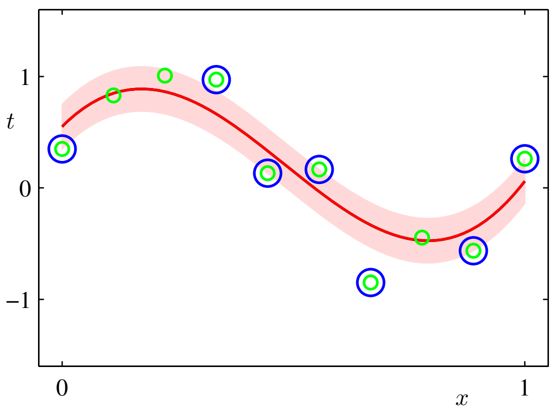

Figure 7.8 Illustration of the ν-SVM for regression applied to the sinusoidal synthetic data set using Gaussian kernels. The predicted regression curve is shown by the red line, and the ϵ-insensitive tube corresponds to the shaded region. Also, the data points are shown in green, and those with support vectors are indicated by blue circles.

7.1.5 Computational learning theory

Historically, support vector machines have largely been motivated and analysed using a theoretical framework known as *computational learning theory*, also sometimes called *statistical learning theory* (Anthony and Biggs, 1992; Kearns and Vazirani, 1994; Vapnik, 1995; Vapnik, 1998). This has its origins with Valiant (1984) who formulated the *probably approximately correct*, or PAC, learning framework. The goal of the PAC framework is to understand how large a data set needs to be in order to give good generalization. It also gives bounds for the computational cost of learning, although we do not consider these here.

Suppose that a data set $\mathcal{D}$ of size N is drawn from some joint distribution $p(\mathbf{x}, \mathbf{t})$ where $\mathbf{x}$ is the input variable and $\mathbf{t}$ represents the class label, and that we restrict attention to 'noise free' situations in which the class labels are determined by some (unknown) deterministic function $\mathbf{t} = \mathbf{g}(\mathbf{x})$. In PAC learning we say that a function $\mathbf{f}(\mathbf{x}; \mathcal{D})$, drawn from a space $\mathcal{F}$ of such functions on the basis of the training set $\mathcal{D}$, has good generalization if its expected error rate is below some pre-specified threshold ϵ, so that

$$\mathbb{E}_{\mathbf{x},\mathbf{t}} \left[I \left(\mathbf{f}(\mathbf{x}; \mathcal{D}) \neq \mathbf{t} \right) \right] < \epsilon \tag{7.75}$$

where $I(\cdot)$ is the indicator function, and the expectation is with respect to the distribution $p(\mathbf{x}, \mathbf{t})$. The quantity on the left-hand side is a random variable, because it depends on the training set $\mathcal{D}$, and the PAC framework requires that (7.75) holds, with probability greater than $1 - \delta$, for a data set $\mathcal{D}$ drawn randomly from $p(\mathbf{x}, \mathbf{t})$. Here δ is another pre-specified parameter, and the terminology 'probably approximately correct' comes from the requirement that with high probability (greater than $1 - \delta$), the error rate be small (less than ϵ). For a given choice of model space $\mathcal{F}$, and for given parameters ϵ and δ, PAC learning aims to provide bounds on the minimum size N of data set needed to meet this criterion. A key quantity in PAC learning is the *Vapnik-Chervonenkis dimension*, or VC dimension, which provides a measure of the complexity of a space of functions, and which allows the PAC framework to be extended to spaces containing an infinite number of functions.

The bounds derived within the PAC framework are often described as worstcase, because they apply to *any* choice for the distribution $p(\mathbf{x}, \mathbf{t})$, so long as both the training and the test examples are drawn (independently) from the same distribution, and for *any* choice for the function $\mathbf{f}(\mathbf{x})$ so long as it belongs to $\mathcal{F}$. In real-world applications of machine learning, we deal with distributions that have significant regularity, for example in which large regions of input space carry the same class label. As a consequence of the lack of any assumptions about the form of the distribution, the PAC bounds are very conservative, in other words they strongly over-estimate the size of data sets required to achieve a given generalization performance. For this reason, PAC bounds have found few, if any, practical applications.

One attempt to improve the tightness of the PAC bounds is the *PAC-Bayesian* framework (McAllester, 2003), which considers a distribution over the space $\mathcal{F}$ of functions, somewhat analogous to the prior in a Bayesian treatment. This still considers any possible choice for $p(\mathbf{x}, \mathbf{t})$, and so although the bounds are tighter, they are still very conservative.

7.2. Relevance Vector Machines

Support vector machines have been used in a variety of classification and regression applications. Nevertheless, they suffer from a number of limitations, several of which have been highlighted already in this chapter. In particular, the outputs of an SVM represent decisions rather than posterior probabilities. Also, the SVM was originally formulated for two classes, and the extension to $K > 2$ classes is problematic. There is a complexity parameter C, or ν (as well as a parameter ϵ in the case of regression), that must be found using a hold-out method such as cross-validation. Finally, predictions are expressed as linear combinations of kernel functions that are centred on training data points and that are required to be positive definite.

The *relevance vector machine* or RVM (Tipping, 2001) is a Bayesian sparse kernel technique for regression and classification that shares many of the characteristics of the SVM whilst avoiding its principal limitations. Additionally, it typically leads to much sparser models resulting in correspondingly faster performance on test data whilst maintaining comparable generalization error.

In contrast to the SVM we shall find it more convenient to introduce the regression form of the RVM first and then consider the extension to classification tasks.

7.2.1 RVM for regression

The relevance vector machine for regression is a linear model of the form studied in Chapter 3 but with a modified prior that results in sparse solutions. The model defines a conditional distribution for a real-valued target variable t, given an input vector $\mathbf{x}$, which takes the form

$$p(t|\mathbf{x}, \mathbf{w}, \beta) = \mathcal{N}(t|y(\mathbf{x}), \beta^{-1}) \tag{7.76}$$

where $\beta = \sigma^{-2}$ is the noise precision (inverse noise variance), and the mean is given by a linear model of the form

$$y(\mathbf{x}) = \sum_{i=1}^{M} w_i \phi_i(\mathbf{x}) = \mathbf{w}^{\mathrm{T}} \boldsymbol{\phi}(\mathbf{x}) \tag{7.77}$$

with fixed nonlinear basis functions $\phi_i(\mathbf{x})$, which will typically include a constant term so that the corresponding weight parameter represents a 'bias'.

The relevance vector machine is a specific instance of this model, which is intended to mirror the structure of the support vector machine. In particular, the basis functions are given by kernels, with one kernel associated with each of the data points from the training set. The general expression (7.77) then takes the SVM-like form

$$y(\mathbf{x}) = \sum_{n=1}^{N} w_n k(\mathbf{x}, \mathbf{x}_n) + b \tag{7.78}$$

where b is a bias parameter. The number of parameters in this case is $M = N + 1$, and $y(\mathbf{x})$ has the same form as the predictive model (7.64) for the SVM, except that the coefficients a_n are here denoted w_n. It should be emphasized that the subsequent analysis is valid for arbitrary choices of basis function, and for generality we shall work with the form (7.77). In contrast to the SVM, there is no restriction to positive-definite kernels, nor are the basis functions tied in either number or location to the training data points.

Suppose we are given a set of N observations of the input vector $\mathbf{x}$, which we denote collectively by a data matrix $\mathbf{X}$ whose n^{th} row is $\mathbf{x}_n^{\mathrm{T}}$ with $n = 1, \ldots, N$. The corresponding target values are given by $\mathbf{t} = (t_1, \ldots, t_N)^{\mathrm{T}}$. Thus, the likelihood function is given by

$$p(\mathbf{t}|\mathbf{X}, \mathbf{w}, \beta) = \prod_{n=1}^{N} p(t_n|\mathbf{x}_n, \mathbf{w}, \beta^{-1}). \tag{7.79}$$

Next we introduce a prior distribution over the parameter vector $\mathbf{w}$ and as in Chapter 3, we shall consider a zero-mean Gaussian prior. However, the key difference in the RVM is that we introduce a separate hyperparameter α_i for each of the weight parameters w_i instead of a single shared hyperparameter. Thus the weight prior takes the form

$$p(\mathbf{w}|\boldsymbol{\alpha}) = \prod_{i=1}^{M} \mathcal{N}(w_i|0, \alpha_i^{-1}) \tag{7.80}$$

where α_i represents the precision of the corresponding parameter w_i, and $\boldsymbol{\alpha}$ denotes $(\alpha_1, \ldots, \alpha_M)^{\mathrm{T}}$. We shall see that, when we maximize the evidence with respect to these hyperparameters, a significant proportion of them go to infinity, and the corresponding weight parameters have posterior distributions that are concentrated at zero. The basis functions associated with these parameters therefore play no role in the predictions made by the model and so are effectively pruned out, resulting in a sparse model.

Using the result (3.49) for linear regression models, we see that the posterior distribution for the weights is again Gaussian and takes the form

$$p(\mathbf{w}|\mathbf{t}, \mathbf{X}, \boldsymbol{\alpha}, \beta) = \mathcal{N}(\mathbf{w}|\mathbf{m}, \boldsymbol{\Sigma}) \tag{7.81}$$

where the mean and covariance are given by

$$\mathbf{m} = \beta\boldsymbol{\Sigma}\boldsymbol{\Phi}^{\mathrm{T}}\mathbf{t} \tag{7.82}$$

$$\boldsymbol{\Sigma} = \left(\mathbf{A} + \beta\boldsymbol{\Phi}^{\mathrm{T}}\boldsymbol{\Phi}\right)^{-1} \tag{7.83}$$

where $\boldsymbol{\Phi}$ is the $N \times M$ design matrix with elements $\Phi_{ni} = \phi_i(\mathbf{x}_n)$, and $\mathbf{A} = \mathrm{diag}(\alpha_i)$. Note that in the specific case of the model (7.78), we have $\boldsymbol{\Phi} = \mathbf{K}$, where $\mathbf{K}$ is the symmetric $(N+1) \times (N+1)$ kernel matrix with elements $k(\mathbf{x}_n, \mathbf{x}_m)$.

Section 3.5

The values of $\boldsymbol{\alpha}$ and β are determined using type-2 maximum likelihood, also known as the *evidence approximation*, in which we maximize the marginal likelihood function obtained by integrating out the weight parameters

$$p(\mathbf{t}|\mathbf{X}, \boldsymbol{\alpha}, \beta) = \int p(\mathbf{t}|\mathbf{X}, \mathbf{w}, \beta)p(\mathbf{w}|\boldsymbol{\alpha})\,\mathrm{d}\mathbf{w}. \tag{7.84}$$

Exercise 7.10

Because this represents the convolution of two Gaussians, it is readily evaluated to give the log marginal likelihood in the form

$$\begin{aligned}\ln p(\mathbf{t}|\mathbf{X}, \boldsymbol{\alpha}, \beta) &= \ln \mathcal{N}(\mathbf{t}|\mathbf{0}, \mathbf{C}) \\ &= -\frac{1}{2}\left\{N\ln(2\pi) + \ln|\mathbf{C}| + \mathbf{t}^{\mathrm{T}}\mathbf{C}^{-1}\mathbf{t}\right\}\end{aligned} \tag{7.85}$$

where $\mathbf{t} = (t_1, \ldots, t_N)^{\mathrm{T}}$, and we have defined the $N \times N$ matrix $\mathbf{C}$ given by

$$\mathbf{C} = \beta^{-1}\mathbf{I} + \boldsymbol{\Phi}\mathbf{A}^{-1}\boldsymbol{\Phi}^{\mathrm{T}}. \tag{7.86}$$

Our goal is now to maximize (7.85) with respect to the hyperparameters $\boldsymbol{\alpha}$ and β. This requires only a small modification to the results obtained in Section 3.5 for the evidence approximation in the linear regression model. Again, we can identify two approaches. In the first, we simply set the required derivatives of the marginal likelihood to zero and obtain the following re-estimation equations

Exercise 7.12

$$\alpha_i^{\mathrm{new}} = \frac{\gamma_i}{m_i^2} \tag{7.87}$$

$$(\beta^{\mathrm{new}})^{-1} = \frac{\|\mathbf{t} - \boldsymbol{\Phi}\mathbf{m}\|^2}{N - \sum_i \gamma_i} \tag{7.88}$$

where m_i is the i^{th} component of the posterior mean $\mathbf{m}$ defined by (7.82). The quantity γ_i measures how well the corresponding parameter w_i is determined by the data and is defined by

Section 3.5.3

$$\gamma_i = 1 - \alpha_i \Sigma_{ii} \tag{7.89}$$

in which Σ_{ii} is the i^{th} diagonal component of the posterior covariance $\boldsymbol{\Sigma}$ given by (7.83). Learning therefore proceeds by choosing initial values for $\boldsymbol{\alpha}$ and β, evaluating the mean and covariance of the posterior using (7.82) and (7.83), respectively, and then alternately re-estimating the hyperparameters, using (7.87) and (7.88), and re-estimating the posterior mean and covariance, using (7.82) and (7.83), until a suitable convergence criterion is satisfied.

The second approach is to use the EM algorithm, and is discussed in Section 9.3.4. These two approaches to finding the values of the hyperparameters that maximize the evidence are formally equivalent. Numerically, however, it is found that the direct optimization approach corresponding to (7.87) and (7.88) gives somewhat faster convergence (Tipping, 2001).

Exercise 9.23

As a result of the optimization, we find that a proportion of the hyperparameters $\{\alpha_i\}$ are driven to large (in principle infinite) values, and so the weight parameters w_i corresponding to these hyperparameters have posterior distributions with mean and variance both zero. Thus those parameters, and the corresponding basis functions $\phi_i(\mathbf{x})$, are removed from the model and play no role in making predictions for new inputs. In the case of models of the form (7.78), the inputs $\mathbf{x}_n$ corresponding to the remaining nonzero weights are called *relevance vectors*, because they are identified through the mechanism of automatic relevance determination, and are analogous to the support vectors of an SVM. It is worth emphasizing, however, that this mechanism for achieving sparsity in probabilistic models through automatic relevance determination is quite general and can be applied to any model expressed as an adaptive linear combination of basis functions.

Section 7.2.2

Having found values $\boldsymbol{\alpha}^\star$ and $\beta^\star$ for the hyperparameters that maximize the marginal likelihood, we can evaluate the predictive distribution over t for a new input $\mathbf{x}$. Using (7.76) and (7.81), this is given by

Exercise 7.14

$$\begin{aligned} p(t|\mathbf{x}, \mathbf{X}, \mathbf{t}, \boldsymbol{\alpha}^\star, \beta^\star) &= \int p(t|\mathbf{x}, \mathbf{w}, \beta^\star) p(\mathbf{w}|\mathbf{X}, \mathbf{t}, \boldsymbol{\alpha}^\star, \beta^\star)\, \mathrm{d}\mathbf{w} \\ &= \mathcal{N}\left(t|\mathbf{m}^{\mathrm{T}}\boldsymbol{\phi}(\mathbf{x}), \sigma^2(\mathbf{x})\right). \end{aligned} \tag{7.90}$$

Thus the predictive mean is given by (7.76) with $\mathbf{w}$ set equal to the posterior mean $\mathbf{m}$, and the variance of the predictive distribution is given by

$$\sigma^2(\mathbf{x}) = (\beta^\star)^{-1} + \boldsymbol{\phi}(\mathbf{x})^{\mathrm{T}} \boldsymbol{\Sigma} \boldsymbol{\phi}(\mathbf{x}) \tag{7.91}$$

where $\boldsymbol{\Sigma}$ is given by (7.83) in which $\boldsymbol{\alpha}$ and β are set to their optimized values $\boldsymbol{\alpha}^\star$ and $\beta^\star$. This is just the familiar result (3.59) obtained in the context of linear regression. Recall that for localized basis functions, the predictive variance for linear regression models becomes small in regions of input space where there are no basis functions. In the case of an RVM with the basis functions centred on data points, the model will therefore become increasingly certain of its predictions when extrapolating outside the domain of the data (Rasmussen and Quiñonero-Candela, 2005), which of course is undesirable. The predictive distribution in Gaussian process regression does not

Section 6.4.2

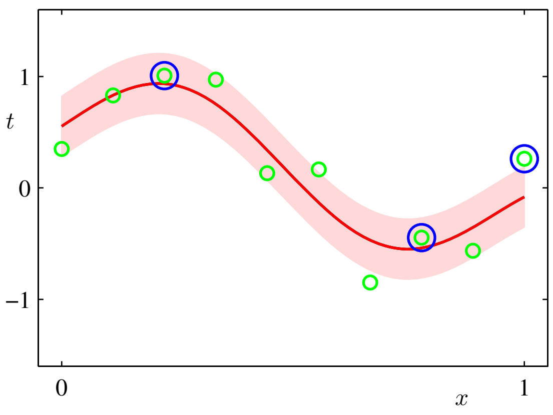

Figure 7.9 Illustration of RVM regression using the same data set, and the same Gaussian kernel functions, as used in Figure 7.8 for the ν-SVM regression model. The mean of the predictive distribution for the RVM is shown by the red line, and the one standard-deviation predictive distribution is shown by the shaded region. Also, the data points are shown in green, and the relevance vectors are indicated by blue circles. Note that there are only 3 relevance vectors compared to 7 support vectors for the ν-SVM in Figure 7.8.

suffer from this problem. However, the computational cost of making predictions with a Gaussian processes is typically much higher than with an RVM.

Figure 7.9 shows an example of the RVM applied to the sinusoidal regression data set. Here the noise precision parameter β is also determined through evidence maximization. We see that the number of relevance vectors in the RVM is significantly smaller than the number of support vectors used by the SVM. For a wide range of regression and classification tasks, the RVM is found to give models that are typically an order of magnitude more compact than the corresponding support vector machine, resulting in a significant improvement in the speed of processing on test data. Remarkably, this greater sparsity is achieved with little or no reduction in generalization error compared with the corresponding SVM.

The principal disadvantage of the RVM compared to the SVM is that training involves optimizing a nonconvex function, and training times can be longer than for a comparable SVM. For a model with M basis functions, the RVM requires inversion of a matrix of size $M \times M$, which in general requires $O(M^3)$ computation. In the specific case of the SVM-like model (7.78), we have $M = N+1$. As we have noted, there are techniques for training SVMs whose cost is roughly quadratic in N. Of course, in the case of the RVM we always have the option of starting with a smaller number of basis functions than $N + 1$. More significantly, in the relevance vector machine the parameters governing complexity and noise variance are determined automatically from a single training run, whereas in the support vector machine the parameters C and ϵ (or ν) are generally found using cross-validation, which involves multiple training runs. Furthermore, in the next section we shall derive an alternative procedure for training the relevance vector machine that improves training speed significantly.

7.2.2 Analysis of sparsity

We have noted earlier that the mechanism of *automatic relevance determination* causes a subset of parameters to be driven to zero. We now examine in more detail

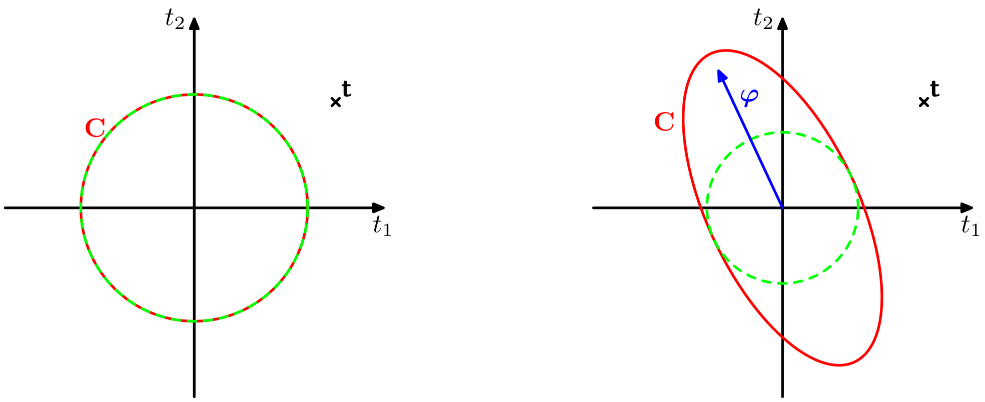

Figure 7.10 Illustration of the mechanism for sparsity in a Bayesian linear regression model, showing a training set vector of target values given by $\mathbf{t} = (t_1, t_2)^{\mathrm{T}}$, indicated by the cross, for a model with one basis vector $\boldsymbol{\varphi} = (\phi(\mathbf{x}_1), \phi(\mathbf{x}_2))^{\mathrm{T}}$, which is poorly aligned with the target data vector $\mathbf{t}$. On the left we see a model having only isotropic noise, so that $\mathbf{C} = \beta^{-1}\mathbf{I}$, corresponding to $\alpha = \infty$, with β set to its most probable value. On the right we see the same model but with a finite value of α. In each case the red ellipse corresponds to unit Mahalanobis distance, with $|\mathbf{C}|$ taking the same value for both plots, while the dashed green circle shows the contrition arising from the noise term β^{-1}. We see that any finite value of α reduces the probability of the observed data, and so for the most probable solution the basis vector is removed.

the mechanism of sparsity in the context of the relevance vector machine. In the process, we will arrive at a significantly faster procedure for optimizing the hyperparameters compared to the direct techniques given above.

Before proceeding with a mathematical analysis, we first give some informal insight into the origin of sparsity in Bayesian linear models. Consider a data set comprising $N = 2$ observations t_1 and t_2, together with a model having a single basis function $\phi(\mathbf{x})$, with hyperparameter α, along with isotropic noise having precision β. From (7.85), the marginal likelihood is given by $p(\mathbf{t}|\alpha, \beta) = \mathcal{N}(\mathbf{t}|\mathbf{0}, \mathbf{C})$ in which the covariance matrix takes the form

$$\mathbf{C} = \frac{1}{\beta}\mathbf{I} + \frac{1}{\alpha}\boldsymbol{\varphi}\boldsymbol{\varphi}^{\mathrm{T}} \tag{7.92}$$

where $\boldsymbol{\varphi}$ denotes the N-dimensional vector $(\phi(\mathbf{x}_1), \phi(\mathbf{x}_2))^{\mathrm{T}}$, and similarly $\mathbf{t} = (t_1, t_2)^{\mathrm{T}}$. Notice that this is just a zero-mean Gaussian process model over $\mathbf{t}$ with covariance $\mathbf{C}$. Given a particular observation for $\mathbf{t}$, our goal is to find $\alpha^\star$ and $\beta^\star$ by maximizing the marginal likelihood. We see from Figure 7.10 that, if there is a poor alignment between the direction of $\boldsymbol{\varphi}$ and that of the training data vector $\mathbf{t}$, then the corresponding hyperparameter α will be driven to ∞, and the basis vector will be pruned from the model. This arises because any finite value for α will always assign a lower probability to the data, thereby decreasing the value of the density at $\mathbf{t}$, provided that β is set to its optimal value. We see that any finite value for α would cause the distribution to be elongated in a direction away from the data, thereby increasing the probability mass in regions away from the observed data and hence reducing the value of the density at the target data vector itself. For the more general case of M

basis vectors $\boldsymbol{\varphi}_1, \ldots, \boldsymbol{\varphi}_M$ a similar intuition holds, namely that if a particular basis vector is poorly aligned with the data vector $\mathbf{t}$, then it is likely to be pruned from the model.

We now investigate the mechanism for sparsity from a more mathematical perspective, for a general case involving M basis functions. To motivate this analysis we first note that, in the result (7.87) for re-estimating the parameter α_i, the terms on the right-hand side are themselves also functions of α_i. These results therefore represent implicit solutions, and iteration would be required even to determine a single α_i with all other α_j for $j \neq i$ fixed.

This suggests a different approach to solving the optimization problem for the RVM, in which we make explicit all of the dependence of the marginal likelihood (7.85) on a particular α_i and then determine its stationary points explicitly (Faul and Tipping, 2002; Tipping and Faul, 2003). To do this, we first pull out the contribution from α_i in the matrix $\mathbf{C}$ defined by (7.86) to give

$$\begin{aligned} \mathbf{C} &= \beta^{-1}\mathbf{I} + \sum_{j \neq i} \alpha_j^{-1} \boldsymbol{\varphi}_j \boldsymbol{\varphi}_j^{\mathrm{T}} + \alpha_i^{-1} \boldsymbol{\varphi}_i \boldsymbol{\varphi}_i^{\mathrm{T}} \\ &= \mathbf{C}_{-i} + \alpha_i^{-1} \boldsymbol{\varphi}_i \boldsymbol{\varphi}_i^{\mathrm{T}} \end{aligned} \tag{7.93}$$

where $\boldsymbol{\varphi}_i$ denotes the i^{th} column of $\boldsymbol{\Phi}$, in other words the N-dimensional vector with elements $(\phi_i(\mathbf{x}_1), \ldots, \phi_i(\mathbf{x}_N))$, in contrast to $\boldsymbol{\phi}_n$, which denotes the n^{th} row of $\boldsymbol{\Phi}$. The matrix $\mathbf{C}_{-i}$ represents the matrix $\mathbf{C}$ with the contribution from basis function i removed. Using the matrix identities (C.7) and (C.15), the determinant and inverse of $\mathbf{C}$ can then be written

$$|\mathbf{C}| = |\mathbf{C}_{-i}||1 + \alpha_i^{-1} \boldsymbol{\varphi}_i^{\mathrm{T}} \mathbf{C}_{-i}^{-1} \boldsymbol{\varphi}_i| \tag{7.94}$$

$$\mathbf{C}^{-1} = \mathbf{C}_{-i}^{-1} - \frac{\mathbf{C}_{-i}^{-1} \boldsymbol{\varphi}_i \boldsymbol{\varphi}_i^{\mathrm{T}} \mathbf{C}_{-i}^{-1}}{\alpha_i + \boldsymbol{\varphi}_i^{\mathrm{T}} \mathbf{C}_{-i}^{-1} \boldsymbol{\varphi}_i}. \tag{7.95}$$

Exercise 7.15

Using these results, we can then write the log marginal likelihood function (7.85) in the form

$$L(\boldsymbol{\alpha}) = L(\boldsymbol{\alpha}_{-i}) + \lambda(\alpha_i) \tag{7.96}$$

where $L(\boldsymbol{\alpha}_{-i})$ is simply the log marginal likelihood with basis function $\boldsymbol{\varphi}_i$ omitted, and the quantity $\lambda(\alpha_i)$ is defined by

$$\lambda(\alpha_i) = \frac{1}{2}\left[\ln \alpha_i - \ln(\alpha_i + s_i) + \frac{q_i^2}{\alpha_i + s_i}\right] \tag{7.97}$$

and contains all of the dependence on α_i. Here we have introduced the two quantities

$$s_i = \boldsymbol{\varphi}_i^{\mathrm{T}} \mathbf{C}_{-i}^{-1} \boldsymbol{\varphi}_i \tag{7.98}$$

$$q_i = \boldsymbol{\varphi}_i^{\mathrm{T}} \mathbf{C}_{-i}^{-1} \mathbf{t}. \tag{7.99}$$

Here s_i is called the *sparsity* and q_i is known as the *quality* of $\boldsymbol{\varphi}_i$, and as we shall see, a large value of s_i relative to the value of q_i means that the basis function $\boldsymbol{\varphi}_i$

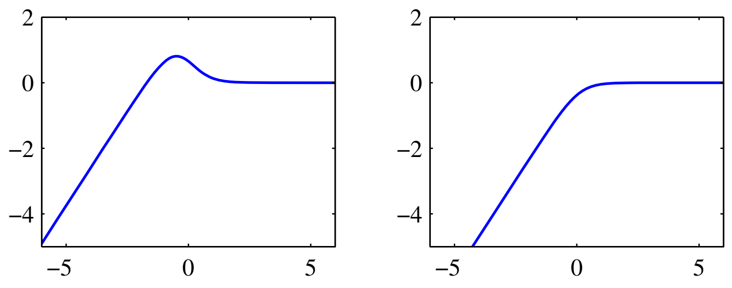

Figure 7.11 Plots of the log marginal likelihood $\lambda(\alpha_i)$ versus $\ln \alpha_i$ showing on the left, the single maximum at a finite α_i for $q_i^2 = 4$ and $s_i = 1$ (so that $q_i^2 > s_i$) and on the right, the maximum at $\alpha_i = \infty$ for $q_i^2 = 1$ and $s_i = 2$ (so that $q_i^2 < s_i$).

is more likely to be pruned from the model. The 'sparsity' measures the extent to which basis function $\boldsymbol{\varphi}_i$ overlaps with the other basis vectors in the model, and the 'quality' represents a measure of the alignment of the basis vector $\boldsymbol{\varphi}_n$ with the error between the training set values $\mathbf{t} = (t_1, \ldots, t_N)^{\mathrm{T}}$ and the vector $\mathbf{y}_{-i}$ of predictions that would result from the model with the vector $\boldsymbol{\varphi}_i$ excluded (Tipping and Faul, 2003).

The stationary points of the marginal likelihood with respect to α_i occur when the derivative

$$\frac{\mathrm{d}\lambda(\alpha_i)}{\mathrm{d}\alpha_i} = \frac{\alpha_i^{-1} s_i^2 - (q_i^2 - s_i)}{2(\alpha_i + s_i)^2} \tag{7.100}$$

is equal to zero. There are two possible forms for the solution. Recalling that $\alpha_i \geqslant 0$, we see that if $q_i^2 < s_i$, then $\alpha_i \to \infty$ provides a solution. Conversely, if $q_i^2 > s_i$, we can solve for α_i to obtain

$$\alpha_i = \frac{s_i^2}{q_i^2 - s_i}. \tag{7.101}$$

These two solutions are illustrated in Figure 7.11. We see that the relative size of the quality and sparsity terms determines whether a particular basis vector will be pruned from the model or not. A more complete analysis (Faul and Tipping, 2002), based on the second derivatives of the marginal likelihood, confirms these solutions are indeed the unique maxima of $\lambda(\alpha_i)$.

Exercise 7.16

Note that this approach has yielded a closed-form solution for α_i, for given values of the other hyperparameters. As well as providing insight into the origin of sparsity in the RVM, this analysis also leads to a practical algorithm for optimizing the hyperparameters that has significant speed advantages. This uses a fixed set of candidate basis vectors, and then cycles through them in turn to decide whether each vector should be included in the model or not. The resulting sequential sparse Bayesian learning algorithm is described below.

Sequential Sparse Bayesian Learning Algorithm

1. If solving a regression problem, initialize β.
2. Initialize using one basis function $\boldsymbol{\varphi}_1$, with hyperparameter α_1 set using (7.101), with the remaining hyperparameters α_j for $j \neq i$ initialized to infinity, so that only $\boldsymbol{\varphi}_1$ is included in the model.

3. Evaluate $\mathbf{\Sigma}$ and $\mathbf{m}$, along with q_i and s_i for all basis functions.
4. Select a candidate basis function $\boldsymbol{\varphi}_i$.
5. If $q_i^2 > s_i$, and $\alpha_i < \infty$, so that the basis vector $\boldsymbol{\varphi}_i$ is already included in the model, then update α_i using (7.101).
6. If $q_i^2 > s_i$, and $\alpha_i = \infty$, then add $\boldsymbol{\varphi}_i$ to the model, and evaluate hyperparameter α_i using (7.101).
7. If $q_i^2 \leqslant s_i$, and $\alpha_i < \infty$ then remove basis function $\boldsymbol{\varphi}_i$ from the model, and set $\alpha_i = \infty$.
8. If solving a regression problem, update β.
9. If converged terminate, otherwise go to 3.

Note that if $q_i^2 \leqslant s_i$ and $\alpha_i = \infty$, then the basis function $\boldsymbol{\varphi}_i$ is already excluded from the model and no action is required.

In practice, it is convenient to evaluate the quantities

$$Q_i = \boldsymbol{\varphi}_i^{\mathrm{T}}\mathbf{C}^{-1}\mathbf{t} \tag{7.102}$$

$$S_i = \boldsymbol{\varphi}_i^{\mathrm{T}}\mathbf{C}^{-1}\boldsymbol{\varphi}_i. \tag{7.103}$$

The quality and sparseness variables can then be expressed in the form

$$q_i = \frac{\alpha_i Q_i}{\alpha_i - S_i} \tag{7.104}$$

$$s_i = \frac{\alpha_i S_i}{\alpha_i - S_i}. \tag{7.105}$$

Exercise 7.17 Note that when $\alpha_i = \infty$, we have $q_i = Q_i$ and $s_i = S_i$. Using (C.7), we can write

$$Q_i = \beta\boldsymbol{\varphi}_i^{\mathrm{T}}\mathbf{t} - \beta^2\boldsymbol{\varphi}_i^{\mathrm{T}}\mathbf{\Phi}\mathbf{\Sigma}\mathbf{\Phi}^{\mathrm{T}}\mathbf{t} \tag{7.106}$$

$$S_i = \beta\boldsymbol{\varphi}_i^{\mathrm{T}}\boldsymbol{\varphi}_i - \beta^2\boldsymbol{\varphi}_i^{\mathrm{T}}\mathbf{\Phi}\mathbf{\Sigma}\mathbf{\Phi}^{\mathrm{T}}\boldsymbol{\varphi}_i \tag{7.107}$$

where $\mathbf{\Phi}$ and $\mathbf{\Sigma}$ involve only those basis vectors that correspond to finite hyperparameters α_i. At each stage the required computations therefore scale like $O(M^3)$, where M is the number of active basis vectors in the model and is typically much smaller than the number N of training patterns.

7.2.3 RVM for classification

We can extend the relevance vector machine framework to classification problems by applying the ARD prior over weights to a probabilistic linear classification model of the kind studied in Chapter 4. To start with, we consider two-class problems with a binary target variable $t \in \{0, 1\}$. The model now takes the form of a linear combination of basis functions transformed by a logistic sigmoid function

$$y(\mathbf{x}, \mathbf{w}) = \sigma\left(\mathbf{w}^{\mathrm{T}}\boldsymbol{\phi}(\mathbf{x})\right) \tag{7.108}$$

where $\sigma(\cdot)$ is the logistic sigmoid function defined by (4.59). If we introduce a Gaussian prior over the weight vector $\mathbf{w}$, then we obtain the model that has been considered already in Chapter 4. The difference here is that in the RVM, this model uses the ARD prior (7.80) in which there is a separate precision hyperparameter associated with each weight parameter.

In contrast to the regression model, we can no longer integrate analytically over the parameter vector $\mathbf{w}$. Here we follow Tipping (2001) and use the Laplace approximation, which was applied to the closely related problem of Bayesian logistic regression in Section 4.5.1.

Section 4.4

We begin by initializing the hyperparameter vector $\boldsymbol{\alpha}$. For this given value of $\boldsymbol{\alpha}$, we then build a Gaussian approximation to the posterior distribution and thereby obtain an approximation to the marginal likelihood. Maximization of this approximate marginal likelihood then leads to a re-estimated value for $\boldsymbol{\alpha}$, and the process is repeated until convergence.

Let us consider the Laplace approximation for this model in more detail. For a fixed value of $\boldsymbol{\alpha}$, the mode of the posterior distribution over $\mathbf{w}$ is obtained by maximizing

$$\begin{aligned}\ln p(\mathbf{w}|\mathsf{t},\boldsymbol{\alpha}) &= \ln\{p(\mathsf{t}|\mathbf{w})p(\mathbf{w}|\boldsymbol{\alpha})\} - \ln p(\mathsf{t}|\boldsymbol{\alpha}) \\ &= \sum_{n=1}^{N}\{t_n \ln y_n + (1-t_n)\ln(1-y_n)\} - \frac{1}{2}\mathbf{w}^{\mathrm{T}}\mathbf{A}\mathbf{w} + \text{const} \end{aligned} \tag{7.109}$$

where $\mathbf{A} = \operatorname{diag}(\alpha_i)$. This can be done using iterative reweighted least squares (IRLS) as discussed in Section 4.3.3. For this, we need the gradient vector and Hessian matrix of the log posterior distribution, which from (7.109) are given by

Exercise 7.18

$$\nabla \ln p(\mathbf{w}|\mathsf{t},\boldsymbol{\alpha}) = \boldsymbol{\Phi}^{\mathrm{T}}(\mathsf{t}-\mathsf{y}) - \mathbf{A}\mathbf{w} \tag{7.110}$$

$$\nabla\nabla \ln p(\mathbf{w}|\mathsf{t},\boldsymbol{\alpha}) = -\left(\boldsymbol{\Phi}^{\mathrm{T}}\mathbf{B}\boldsymbol{\Phi} + \mathbf{A}\right) \tag{7.111}$$

where $\mathbf{B}$ is an $N \times N$ diagonal matrix with elements $b_n = y_n(1-y_n)$, the vector $\mathsf{y} = (y_1, \ldots, y_N)^{\mathrm{T}}$, and $\boldsymbol{\Phi}$ is the design matrix with elements $\Phi_{ni} = \phi_i(\mathbf{x}_n)$. Here we have used the property (4.88) for the derivative of the logistic sigmoid function. At convergence of the IRLS algorithm, the negative Hessian represents the inverse covariance matrix for the Gaussian approximation to the posterior distribution.

The mode of the resulting approximation to the posterior distribution, corresponding to the mean of the Gaussian approximation, is obtained setting (7.110) to zero, giving the mean and covariance of the Laplace approximation in the form

$$\mathbf{w}^{\star} = \mathbf{A}^{-1}\boldsymbol{\Phi}^{\mathrm{T}}(\mathsf{t}-\mathsf{y}) \tag{7.112}$$

$$\boldsymbol{\Sigma} = \left(\boldsymbol{\Phi}^{\mathrm{T}}\mathbf{B}\boldsymbol{\Phi} + \mathbf{A}\right)^{-1}. \tag{7.113}$$

We can now use this Laplace approximation to evaluate the marginal likelihood. Using the general result (4.135) for an integral evaluated using the Laplace approximation, we have

$$\begin{aligned} p(\mathbf{t}|\boldsymbol{\alpha}) &= \int p(\mathbf{t}|\mathbf{w})p(\mathbf{w}|\boldsymbol{\alpha})\,\mathrm{d}\mathbf{w} \\ &\simeq p(\mathbf{t}|\mathbf{w}^{\star})p(\mathbf{w}^{\star}|\boldsymbol{\alpha})(2\pi)^{M/2}|\boldsymbol{\Sigma}|^{1/2}. \end{aligned} \tag{7.114}$$

Exercise 7.19

If we substitute for $p(\mathbf{t}|\mathbf{w}^{\star})$ and $p(\mathbf{w}^{\star}|\boldsymbol{\alpha})$ and then set the derivative of the marginal likelihood with respect to α_i equal to zero, we obtain

$$-\frac{1}{2}(w_i^{\star})^2 + \frac{1}{2\alpha_i} - \frac{1}{2}\Sigma_{ii} = 0. \tag{7.115}$$

Defining $\gamma_i = 1 - \alpha_i \Sigma_{ii}$ and rearranging then gives

$$\alpha_i^{\text{new}} = \frac{\gamma_i}{(w_i^{\star})^2} \tag{7.116}$$

which is identical to the re-estimation formula (7.87) obtained for the regression RVM.

If we define

$$\widehat{\mathbf{t}} = \boldsymbol{\Phi}\mathbf{w}^{\star} + \mathbf{B}^{-1}(\mathbf{t} - \mathbf{y}) \tag{7.117}$$

we can write the approximate log marginal likelihood in the form

$$\ln p(\mathbf{t}|\boldsymbol{\alpha}, \beta) = -\frac{1}{2}\left\{N\ln(2\pi) + \ln|\mathbf{C}| + (\widehat{\mathbf{t}})^{\mathrm{T}}\mathbf{C}^{-1}\widehat{\mathbf{t}}\right\} \tag{7.118}$$

where

$$\mathbf{C} = \mathbf{B} + \boldsymbol{\Phi}\mathbf{A}\boldsymbol{\Phi}^{\mathrm{T}}. \tag{7.119}$$

This takes the same form as (7.85) in the regression case, and so we can apply the same analysis of sparsity and obtain the same fast learning algorithm in which we fully optimize a single hyperparameter α_i at each step.

Appendix A

Figure 7.12 shows the relevance vector machine applied to a synthetic classification data set. We see that the relevance vectors tend not to lie in the region of the decision boundary, in contrast to the support vector machine. This is consistent with our earlier discussion of sparsity in the RVM, because a basis function $\phi_i(\mathbf{x})$ centred on a data point near the boundary will have a vector $\boldsymbol{\varphi}_i$ that is poorly aligned with the training data vector $\mathbf{t}$.

One of the potential advantages of the relevance vector machine compared with the SVM is that it makes probabilistic predictions. For example, this allows the RVM to be used to help construct an emission density in a nonlinear extension of the linear dynamical system for tracking faces in video sequences (Williams *et al.*, 2005).

Section 13.3

So far, we have considered the RVM for binary classification problems. For $K > 2$ classes, we again make use of the probabilistic approach in Section 4.3.4 in which there are K linear models of the form

$$a_k = \mathbf{w}_k^{\mathrm{T}}\mathbf{x} \tag{7.120}$$

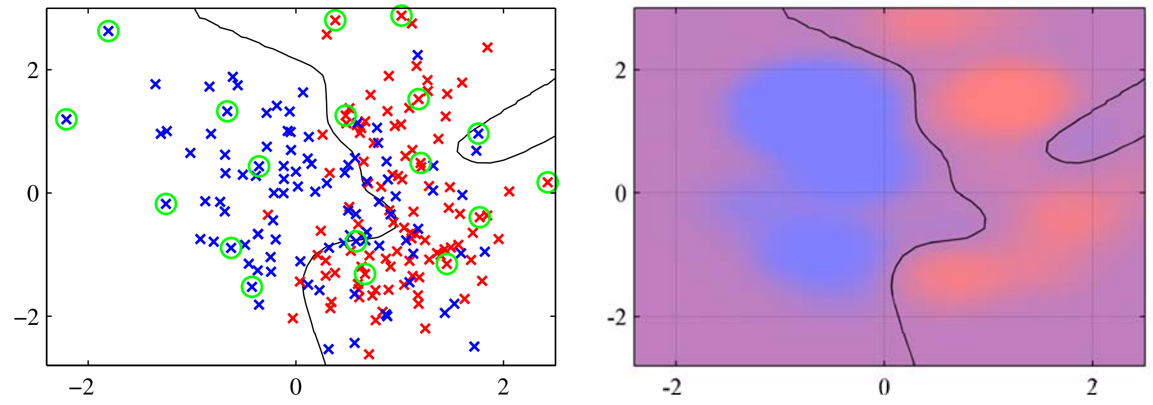

Figure 7.12 Example of the relevance vector machine applied to a synthetic data set, in which the left-hand plot shows the decision boundary and the data points, with the relevance vectors indicated by circles. Comparison with the results shown in Figure 7.4 for the corresponding support vector machine shows that the RVM gives a much sparser model. The right-hand plot shows the posterior probability given by the RVM output in which the proportion of red (blue) ink indicates the probability of that point belonging to the red (blue) class.

which are combined using a softmax function to give outputs

$$y_k(\mathbf{x}) = \frac{\exp(a_k)}{\sum_j \exp(a_j)}. \tag{7.121}$$

The log likelihood function is then given by

$$\ln p(\mathbf{T}|\mathbf{w}_1, \ldots, \mathbf{w}_K) = \prod_{n=1}^{N} \prod_{k=1}^{K} y_{nk}^{t_{nk}} \tag{7.122}$$

where the target values t_{nk} have a 1-of-K coding for each data point n, and $\mathbf{T}$ is a matrix with elements t_{nk}. Again, the Laplace approximation can be used to optimize the hyperparameters (Tipping, 2001), in which the model and its Hessian are found using IRLS. This gives a more principled approach to multiclass classification than the pairwise method used in the support vector machine and also provides probabilistic predictions for new data points. The principal disadvantage is that the Hessian matrix has size $MK \times MK$, where M is the number of active basis functions, which gives an additional factor of K^3 in the computational cost of training compared with the two-class RVM.

The principal disadvantage of the relevance vector machine is the relatively long training times compared with the SVM. This is offset, however, by the avoidance of cross-validation runs to set the model complexity parameters. Furthermore, because it yields sparser models, the computation time on test points, which is usually the more important consideration in practice, is typically much less.